8-17-2015 12:00 AM

Coinage Metal Silylphosphido Complexes Stabilized by N-Heterocyclic Carbene Ligands

Bahareh Khalili Najafabadi
The University of Western Ontario

Supervisor
John F. Corrigan
The University of Western Ontario

Graduate Program in Chemistry
A thesis submitted in partial fulfillment of the requirements for the degree in Doctor of Philosophy

COINAGE METAL SILYLPHOSPHIDO COMPLEXES STABILIZED BY N-HETEROCYCLIC CARBENE LIGANDS

(Thesis format: Integrated Article)

by

Bahareh Khalili Najafabadi

Graduate Program in Chemistry

A thesis submitted in partial fulfillment
of the requirements for the degree of
Doctor of Philosophy

The School of Graduate and Postdoctoral Studies
The University of Western Ontario
London, Ontario, Canada

Abstract

N-Heterocyclic carbenes (NHCs) are strong σ-donating ligands and thus, promising candidates for decorating and stabilizing metal-phosphide nanoclusters. While much research has been focused on the coordination of NHC ligands to different coinage metal centers in order to synthesize mononuclear organometallic complexes, their application in nanocluster chemistry has been relatively unexplored. The work described in this thesis involves employment of NHC ligands for stabilizing coinage metal t-butylthiolate and silylphosphido complexes. These complexes are promising molecular precursors for formation of larger NHC-stabilized nanoclusters.

In particular, the ligation of NHCs to [CuS^{t}Bu] and [AgS^{t}Bu] was developed as an alternative to PR_3 ligands as solubilizing reagents for these coordination polymers in order to form polynuclear copper and silver t-butylthiolate clusters. 1,3-Di-isopropylbenzimidazol-2-ylidene (^{i}Pr$_2$-bimy) and 1,3-di-isopropyl-4,5-dimethylimidazol-2-ylidene (^{i}Pr$_2$-mimy) were ligated to [CuS^{t}Bu] and [AgS^{t}Bu] forming [Cu$_4$(S^{t}Bu)$_4$(^{i}Pr$_2$-bimy)$_2$] (**1**), [Cu$_4$(S^{t}Bu)$_4$(^{i}Pr$_2$-mimy)$_2$] (**2**), [Ag$_4$(S^{t}Bu)$_4$(^{i}Pr$_2$-bimy)$_2$] (**5**) and [Ag$_5$(S^{t}Bu)$_6$][Ag(^{i}Pr$_2$-mimy)$_2$] (**6**). For comparison, the trialkyl phosphines P^{n}Pr$_3$ and P^{i}Pr$_3$ were also used to solubilize [AgS^{t}Bu] and [CuS^{t}Bu] to form copper and silver t-butylthiolate clusters. [Cu$_4$(S^{t}Bu)$_4$(P^{n}Pr$_3$)$_2$] (**3**), [Cu$_4$(S^{t}Bu)$_4$(P^{i}Pr$_3$)$_2$] (**4**), [Ag$_4$(S^{t}Bu)$_4$(P^{n}Pr$_3$)$_2$] (**7**), and [Ag$_6$(S^{t}Bu)$_6$(P^{i}Pr$_3$)$_2$] (**8**) were thus formed upon reaction with [CuS^{t}Bu] and [AgS^{t}Bu]. The synthesized complexes have been characterized via spectroscopic and crystallographic methods. The molecular structures of the clusters, which can vary according to the ligand type, are described.

Moreover, the facile preparation and structural characterization of [M$_6${P(SiMe$_3$)$_2$}$_6$] (M = Ag, Cu) is reported. These complexes show limited stability towards solvent loss at ambient temperature; however, NHC ligands were used to synthesize more thermally stable metal-silylphosphido compounds. ^{i}Pr$_2$-bimy and 1,3-bis(2,6-diisopropylphenyl)imidazol-2-ylidene (IPr) are found to be excellent ligands to stabilize silylphosphido-copper compounds that show higher stability when compared to [Cu$_6${P(SiMe$_3$)$_2$}$_6$] (**9**).

Furthermore, ^{i}Pr$_2$-bimy is found to be an excellent ligand for the stabilization of silver–phosphorus polynuclear complexes. The straightforward preparation and characterization of the clusters [Ag$_{12}$(PSiMe$_3$)$_6$(^{i}Pr$_2$-bimy)$_6$] (**13**) and [Ag$_{26}$P$_2$(PSiMe$_3$)$_{10}$(^{i}Pr$_2$-bimy)$_8$] (**14**)

are described, representing the first examples of such structurally characterized, higher nuclearity complexes obtained using this class of ligands.

Lastly, $^{i}Pr_2$-bimy and IPr were successfully utilized in the facile preparation of four gold silylphosphido complexes: [IPrAuP(Ph)$SiMe_3$] (**15**), [IPrAuP($SiMe_3$)$_2$] (**16**), [($^{i}Pr_2$-bimy)AuP(Ph)$SiMe_3$] (**17**), and [($^{i}Pr_2$-bimy)AuP($SiMe_3$)$_2$] (**18**). Furthermore, reactivity of the P−Si bond in **15** and **17** was explored via the addition of PhC(O)Cl. The product of such reactions was the formation of [(IPrAu)$_2$PPhC(O)Ph][$AuCl_2$] (**19**) and PPh(C(O)Ph)$_2$ (**20**), respectively, as well as the elimination of $ClSiMe_3$.

Keywords:

N-heterocyclic carbene, silylphosphido, copper, silver, gold, nanocluster, X-ray crystallography, t-butylthiolate, silver phosphide

Acknowledgments

First and foremost, I would like to express my sincere appreciation to my supervisor Prof. John F. Corrigan for letting me to join his research group, and for all of his patience, positive energy and support throughout my Ph.D. studies. John, you have been a tremendous mentor for me and I cannot thank you enough for allowing me to grow as a research scientist.

I would like to thank all the past and present members of the Corrigan group that I have had the pleasure to work with or alongside of. The group has been a source of friendships as well as good advice and collaboration.

Dr. Paul Boyle is greatly acknowledged for a lot of crystallography advices he generously offered me during the past few years. I benefited extremely from his knowledge and expertise in the area of X-ray crystallography. We had lots of fruitful discussions regarding scientific and even non-scientific subjects.

My time at Western was made enjoyable in large part due to the many great friends that became part of my life. I am especially grateful for the times spent with my Persian friends during our coffee breaks, potluck gatherings, game nights, camping trips, and many other events. And yes, food was always a big part of our memories either when we baked together for our charity bake sales or enjoyed great international cuisines in different food festivals or restaurants together.

Lastly, I would like to thank my parents, who although physically thousand of kilometers far from me, their unconditional love and support carried me through. And above all, my loving, supportive, encouraging, and patient better half, Amin, who took this journey along my side. I could never ask for a better life partner.

تقدیم به پدر و مادر عزیزم

به پاس قلبهای بزرگشان

Table of Contents

List of Figures

List of Schemes

List of Tables

List of Abbreviations

$\{^1H\}$	proton decoupled
°C	degree Celcius
6-MesDAC	N-mesityl-substituted diamidocarbene
Anal	elemental analysis
Au UNPs	ultra-small gold nanoparticles
AuNPs	gold nanoperticles
br	broad
$C_{18}H_{37}$-MIM	1-methyl-3-octadecyl-imidazolium
$C_{18}H_{37}$-NHC	1-methyl-3-octadecyl-imidazol-2-ylidene
Calcd	calculated
CB	conduction band
d	doublet
d-dots	doped quantum dots
DCM	dichloromethane
dd	doublet of doublet
DDT	dodecanethiol
dec.	decomposition
e.g.	*exempli gratia* (for example)
EDX	energy dispersive X-ray
E_g	band gap energy
et al.	*et alii* (and others)
eV	electron volt
g	gram
h	hour
HOMO	highest occupied molecular orbital
HRMS	high-resolution mass spectrometry
Hz	Hertz
in vacuo	in a vacuum
IPr	1,3-bis(2,6-diisopropylphenyl)imidazol-2-ylidene

$^{i}Pr_2$-bimy	1,3-diisopropylbenzimidazol-2-ylidene
$^{i}Pr_2$-mimy	1,3-diisopropyl-4,5-dimethylimidazol-2-ylidene
IR	infrared
J	*coupling constant*
LUMO	lowest unoccupied molecular orbital
m	multiplet
m.p.	melting point
min	minute
ml	millilitre
mol	mole
NHC	N-heterocyclic carbene
nm	nanometre
NMR	nuclear magnetic resonance
NP	nanoparticle
NSHC	N,S-heterocyclic carbenes
P-C_{NHC}-P	N,N'-diphosphanylimidazol-2-ylidene
Ph	phenyl
Ph′	2,6-*i*$Pr_2C_6H_3$
PL	photoluminescence
ppm	part per million
PXRD	powder X-ray diffraction
q-dots	quantum dots
r.t.	room temperature
s	singlet
SEM	scanning electron microscopy
sep	septet
t	triplet
^{t}Bu	tert-butyl
TEP	Tolman's electronic parameter
THF	tetrahydrofuran
tht	tetrahydothiophene

VB	valence band
V_{bur}	buried volume
δ	chemical shift

NHC Ligands Used in This Thesis

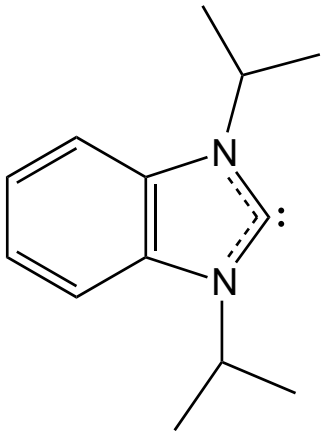

$^{i}Pr_2$-bimy

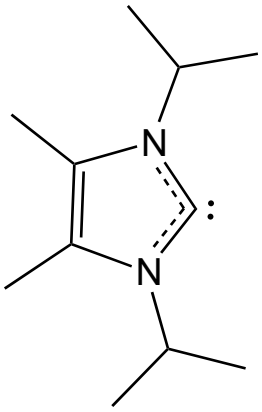

$^{i}Pr_2$-mimy

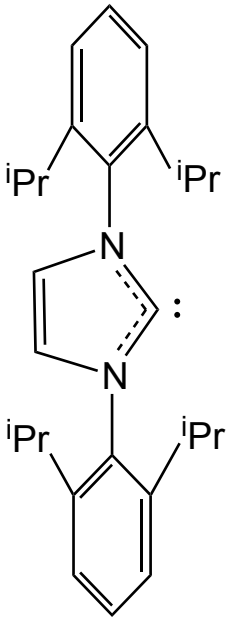

IPr

Chapter 1

NHCs as Stabilizing Ligands for Coinage Metal Clusters

1.1 Introduction

N-heterocyclic carbenes (NHC) have been the subject of explosive interest in the past decades due to their surprisingly high stability.[1] An NHC is defined as a divalent carbon with an electron sextet that is incorporated in a nitrogen-containing heterocycle.[2, 3] In 1968, Wanzlick *et al*.[4] and Öfele[5], separately reported two different metal complexes of NHCs for the first time, and since then, numerous metal-NHC compounds have been synthesized[6] and employed as catalyst in various organic and inorganic reactions.[7] The first successful isolation of a free N-heterocyclic carbene in 1991[8] gave the research of this class of chemistry great momentum. Due to the presence of an electron-rich carbon center, NHCs are very good σ-donating ligands that form stronger bonds with metal atoms, compared to the tertiary phosphines.[9]

Coinage metal-NHC complexes have been widely studied.[10-14] In particular, Ag(I)–NHC complexes[15, 16] have attracted great attention due to their facile preparation and application in synthesis of other metal-NHCs through transmetalation reactions.[17] However, unlike mononuclear compounds, multinuclear complexes and clusters of coinage metals coordinated with NHC ligands have been less explored. In this chapter, NHC-stabilized

multinuclear complexes of group-11 metals with three or more metal centers are reviewed.

1.2 Structure and Properties of NHCs

As mentioned above, N-heterocyclic carbenes refer to heterocyclic species that contain a divalent carbon with six electrons in its valance shell as well as at least one nitrogen atom in the ring structure.[2, 3] Despite their incomplete electron octet and coordination unsaturation, NHCs can exhibit remarkable stability that is a result of the combination of electronic and steric effects of the nitrogen substituents.[1] Bulky substituents on nitrogen (R groups), adjacent to the carbene carbon, can sterically shield the carbene centre and avoid dimerization reactions. More importantly, NHCs are electronically stabilized by σ-electron-withdrawing and π-electron-donating nitrogen atoms (Figure 1-1). NHCs contain a carbene carbon atom whose bonding can be described as consisting of three sp^2 (σ) and one p (p_π) orbitals. The two nonbonding electrons on the sextet carbon atom can occupy two empty orbitals with parallel spins ($\sigma^1 p_\pi^1$), which leads to a triplet ground state. Alternatively, those electrons may fill the σ orbital with antiparallel spins ($\sigma^2 p_\pi^0$), leaving the p_π orbital empty, which leads to a singlet ground state. σ-electron-withdrawing nitrogen atoms lower the energy of the nonbonding σ orbital on the carbene centre and hence favor the more stable singlet ground state.[1, 18] Nitrogen atoms also stabilize NHCs mesomerically by donating electron density to the empty p_π orbitals on the sextet carbon atom.[19, 20]

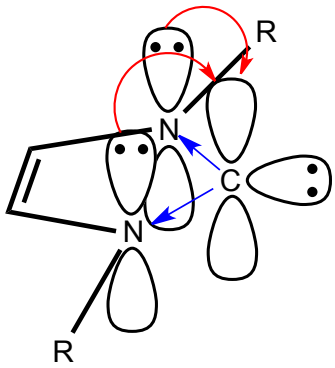

Figure 1-1 σ-withdrawing (blue arrows) and π-donating (red arrows) effects of the nitrogen heteroatoms to stabilize the singlet carbene structure in NHCs.[1]

The cyclic structure of the heterocycle forces the carbene carbon atom to a bent geometry (sp^2 hybridization) and therefore favors a singlet ground state. The backbone of the heterocycle can also affect the stability of the NHC by being a part of the conjugated system or by means of substituents that impose electronic effects on the carbene centre. Due to the presence of a NHC's stabilized lone pair in the plane of the heterocycle (sp^2 orbital), they are nucleophilic species that act as a σ-donor when bound to metallic or non-metallic moieties. Hence N-heterocyclic carbenes compete with phosphines as ligands in the area of organometallic chemistry and in general are more electron-donating than the latter.[1] It is more effective to describe steric and electronic properties of these ligands by the means of quantitative measurements.

1.3 Quantitative Measures of Steric and Electronic Properties

The steric demand of different NHCs can be quantified by the 'buried volume' method that has been developed and refined by Nolan, Cavallo, and co-workers.[21, 22] The buried volume ($\%V_{bur}$) represents the percentage of a sphere that is occupied by the atoms of the ligand upon coordination to the metal at the center of the sphere (Figure 1-2) with fixed metal to ligand bond length (*e.g.* d = 2.0 Å) and radius for the sphere (*e.g.* r = 3.0 or 3.5 Å). The $\%V_{bur}$ value can be derived from crystallographic or quantum chemically calculated data. The more sterically demanding the ligand of interest, the larger the $\%V_{bur}$ value. This method is not limited to a certain class of ligands and can also be used to compare steric properties between different classes of ligands such as NHCs and phosphines. [23]

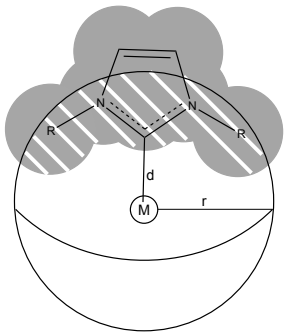

Figure 1-2 Graphical illustration of the buried volume ($\%V_{bur}$) parameter.[23]

There are different methods to describe the electronic characteristics of ligands[21, 24-26] but the most established one is monitoring the A_1 stretching frequency of CO ligands in tetrahedral [$Ni(CO)_3(L)$] complexes. This frequency that is known as Tolman's electronic parameter (TEP) was originally developed by Tolman for phosphine ligands.[27] Later, less toxic *cis*-[$IrCl(CO)_2(NHC)$] and *cis*-[$RhCl(CO)_2(NHC)$] complexes were investigated by Crabtree[28] and Nolan[29] to determine TEP values for NHC ligands. It is possible to correlate the values obtained from the iridium or rhodium complexes to the nickel-based TEP values through the use of simple equations[29]:

Ir to Ni: TEP [cm^{-1}] = $0.8475\nu_{CO}^{av/Ir}$ [cm^{-1}] + 336.2 [cm^{-1}]

Rh to Ni: TEP [cm^{-1}] = $0.8001\nu_{CO}^{av/Rh}$ [cm^{-1}] + 420.0 [cm^{-1}]

The more electron-donating the NHC ligand of interest, the lower the infrared stretching frequency of CO ligands (TEP). TEP values that are obtained for NHC ligands illustrate that most of them are significantly more electron rich than phosphines.[23]

1.4 Polydentate NHC Ligands

NHCs with several sites of coordination enhance the possibility of the formation of polynuclear complexes, since they can interact with different metal centers and gather them together. There are several examples of multinuclear coinage metal-NHC complexes reported in the literature that gain advantage from the multiple coordination sites of the ligands but do not show any significant metal-metal interactions.[30-33] Although these compounds are very interesting and show different applications such as in catalysis, clusters with more condensed cores will be focused on here.

N-phosphanyl-functionalized NHC ligands have P and C coordination sites and have been utilized for the preparation of polynuclear complexes.[34] Hofmann and coworkers have synthesized dinuclear and tetranuclear copper complexes using this class of ligand.[35] A tetranuclear copper bromide complex has been formed as a result of treating the $^{Mes}NHCP^{tBu}$ ligand with [$CuBr\{S(CH_3)_2\}$]. This complex exhibits a nearly planar centrosymmetric Cu_4 square cluster, which, with two μ_4-bridging bromido ligands forms an octahedral substructure (Figure 1-3).

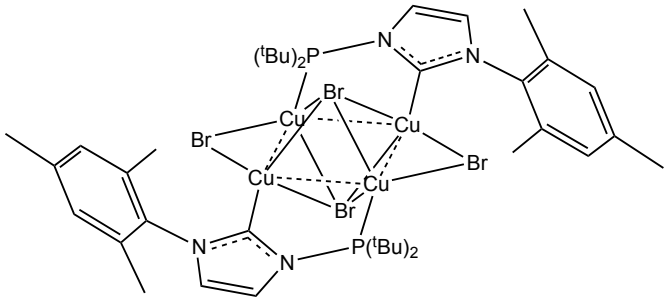

Figure 1-3 Molecular structure of $[Cu_4\{\mu\text{-}(^{Mes}NHCP^{tBu})\text{-}\varkappa^2C,P\}_2(\mu_4\text{-}Br)_2(\mu_2\text{-}Br)_2]$.[35]

Furthermore, tri-dentate P–C_{NHC}–P donor ligands have been investigated for the preparation of polynuclear coinage metal clusters. Recently Ai and coworkers reported the successful synthesis of linear M_3 (M = Cu, Ag, Au)[36] using the rigid N,N'-diphosphanylimidazol-2-ylidene (P–C_{NHC}–P) ligand. Cyclic penta- and hexanuclear gold complexes[37] with metallophilic interactions were also prepared. They found that the nature of the gold(I) precursor had dramatic effect on the final product, and in the case of [AuCl(tht)] (tht = tetrahydothiophene) novel cyclic hexanuclear gold(I) complex was formed after the cleavage of one $(^tBu)_2$–P–N_{imid} group of the P–C–P ligand. The authors have been also able to isolate a cationic Au_{11} cluster from the reaction of a P–C–Li precursor with two equivalents of [AuCl(tht)]. This complex contains two $[Au_5(\mu_3\text{-}P\text{–}C\text{-}\varkappa P,\varkappa C,\varkappa N)]^+$ cations that display d^{10}–d^{10} interactions with a central $[AuCl_2]^-$ anion. This Au_{11} monocation is charge balanced by another $[AuCl_2]^-$ anion. Some short distances between the gold centers in the latter two clusters cannot be solely due to the short-bite effect of the ligand and are described as peripheral Au…Au interactions by the authors.

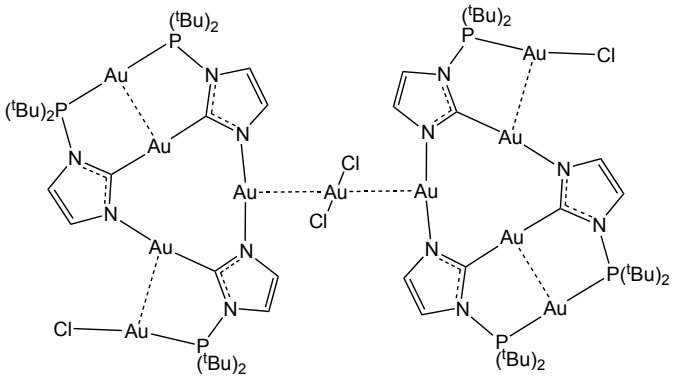

Figure 1-4 molecular structure of $[Au_5(\mu_3\text{-}P\text{–}C\text{-}\varkappa P,\varkappa C,\varkappa N)]_2[AuCl_2]^+$.[37]

Bis-imidazolylidene ligands bridged by a N-heteroarene are tetradentate ligands that offer a great tool for design and synthesis of polynuclear metal complexes. From the reaction of phenanthroline-bridged diimidazolium salts with copper powder at room temperature, Liu and coworkers have synthesized di-, tri-, and tetranuclear copper(I)-NHC complexes.[38] The structure of these clusters depends on the N-substituents as well as the counterions. The phenanthroline dicarbene ligands with less bulky N-substituents such as allyl and benzyl groups favor Cu_3 and Cu_4 chain complexes, compared to more sterically hindered groups that tend to form cyclic Cu_3 clusters as is shown in Figure 1-5. Several triangular Cu_3 complexes ligated by NHC ligands have been reported that all show Cu–Cu distances among 2.4–2.9 Å[39-45], as well as similar triangular Ag_3 clusters.[40]

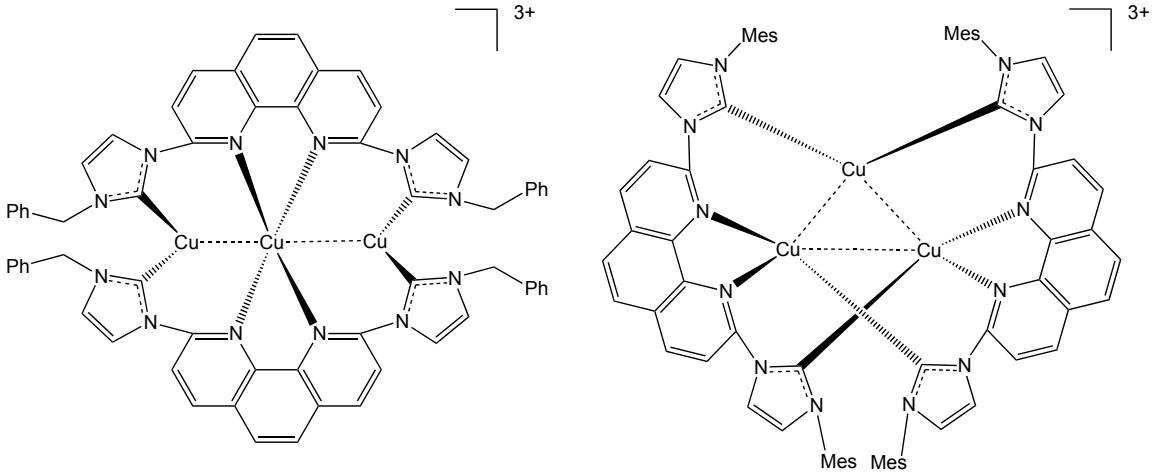

Figure 1-5 Examples of chain (left) and cyclic (right) Cu_3 complexes ligated by phenanthroline linked dicarbene ligands.[38]

Another example from this category of complexes is the light and air stable $[Ag_6L_2](PF_6)_4$ cluster (L = 3,5-bis(N-picolylimidazolylidenylmethyl)pyrazolate) that is formed from treating the corresponding imidazolium salt with Ag_2O in acetonitrile.[46] The core of this cluster consists of two symmetrically related trisilver units that form a triangular ring (bolded in figure) due to the Ag–Ag interactions. Six silver atoms arranged themselves into a chair-like ring structure, although the two triangles are largely separated (dashed lines in figure) and don't exhibit any metal-metal interactions (Figure 1-6). This cluster has been further used to synthesize di- and tetranuclear copper(II) hydroxide complexes ligated with the corresponding NHC that are efficient catalysts for N-arylation of imidazoles and aromatic amines under very mild conditions.

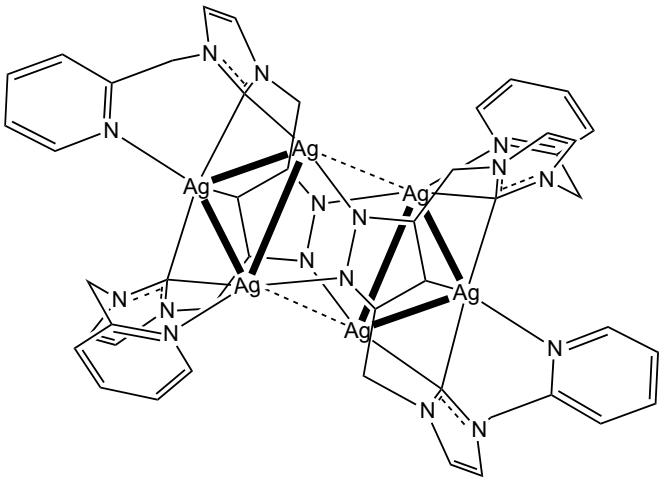

Figure 1-6 molecular structure of $[Ag_6L_2]^{4+}$ (L = 3,5-bis(N-picolylimidazolylidenylmethyl)pyrazolate).[46]

The first series of tetra-NHC-Ag(I)-halide cubane-type clusters were synthesized by Clark and coworkers from the addition of bis-imidazolium dihalide salts to Ag_2O. Although Ag–Ag distances vary significantly in the formed clusters, there are several short Ag–Ag distances that are evidence for argentophilic interactions between silver centers. In each of the five reported clusters in this series, the silver-halide core exhibits a distorted cubic structure that is stabilized by phenyl bridged bis-N-heterocyclic carbene ligands (for example see Figure 1-7).[47]

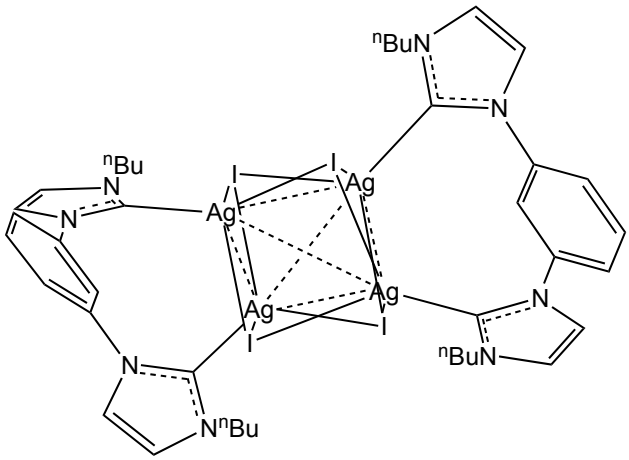

Figure 1-7 Molecular structure of bis(μ-1,3-bis(3′-butylimidazol-2′-ylidene)benzene-κ-C)tetra-μ_3-iodotetrasilver(I).[47]

1.5 Monodentate NHC Ligands

It has been shown that NHCs are excellent ligands to stabilize clusters that are otherwise difficult to isolate with other type of ligands, such as an octahedral neutral Ga_6 cluster that exhibits five-coordinate gallium centers.[48] N,S-heterocyclic carbenes (NSHC) have recently been utilized to stabilize multinuclear Cu(I) complexes that show significant range of stoichiometry-dependent coordination geometries. Di- and tetra-nuclear compounds were formed via aggregation of copper atoms through bridging and capping halides.[49]

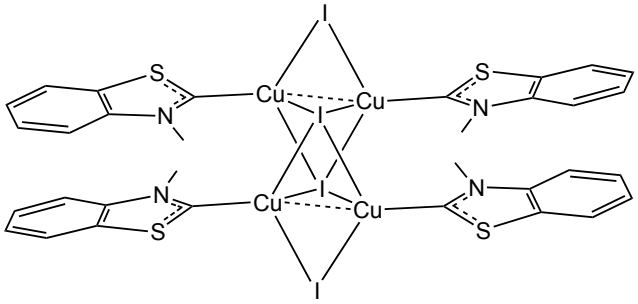

Figure 1-8 Molecular structure of a Cu_4I_4 core stabilized by four NSHC ligands.[49]

Monodentate NHC ligands have been further explored for the synthesis of multinuclear copper and silver ring clusters.[50] Di-, tri-, and tetra nuclear Cu–Cl cyclic complexes were formed from the reaction of N-mesityl-substituted diamidocarbene (6-MesDAC) ligand with different ratios of CuCl (Figure 1-9). Utilizing either the isolated free or in situ generated carbene has influence on the formulation of the final product.[50]

Copper- and silver-phenylchalcogenolate ring clusters were similarly prepared from the reaction of $[CuCl(^{i}Pr_2\text{-bimy})]_2$ and $[Ag(OAc)(^{i}Pr_2\text{-bimy})]$ with $E(Ph)SiMe_3$ (E = S, Se).[51] Tri-nuclear $[Cu_3(\mu\text{-}EPh)_3(^{i}Pr_2\text{-bimy})_3]$ and tetra-nuclear $[Ag_4(\mu\text{-}EPh)_4(^{i}Pr_2\text{-bimy})_4]$ ring clusters were formed, in which all of the metal centers are coordinated by NHCs, compared to the above examples where some of the metal centers are not ligated by NHC ligands.[50]

These recent examples of polynuclear clusters show that N-heterocyclic carbenes are excellent candidates to substitute tertiary phosphine ligands in the synthesis of larger condensed group 11 clusters.[52] Group 11 phosphide nanoclusters stabilized by phosphine ligands are specifically rare, with only a few structurally characterized examples

reported.[53-55]

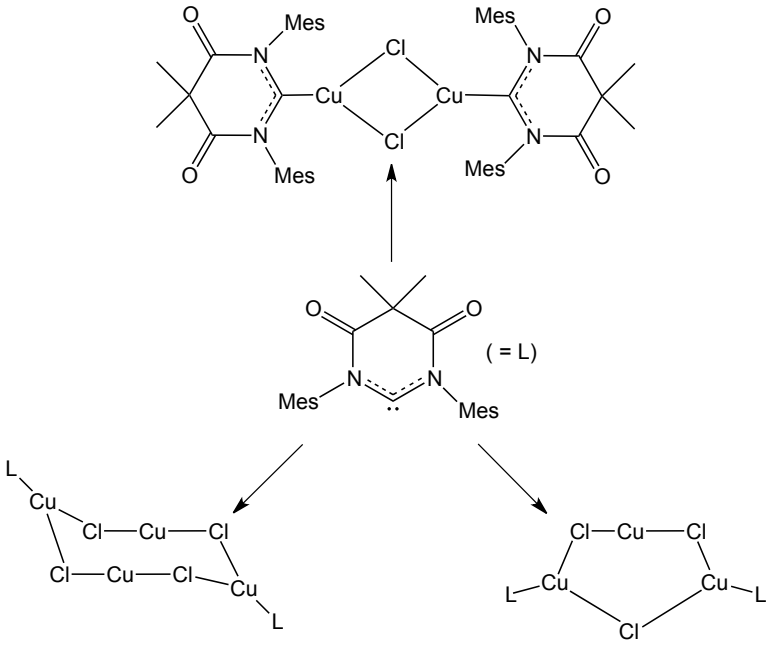

Figure 1-9 NHC ligated cyclic Cu–Cl complexes.[50]

1.6 NHC-stabilized Nanoparticles

N-heterocyclic carbenes have been used as capping ligands for Ru,[56, 57] Pd,[58, 59] and Ir[60] nanoparticles. Due to the strong σ-donating properties of NHCs, one would expect NHC-stabilized nanoparticles to be resistant to degradation and show catalytic properties similar to previously prepared nanoparticles. The first attempt on the preparation of NHC-protected gold nanoparticles was done by Hurst and coworkers via a ligand exchange reaction.[61] Bis-tert-butylimidazol-2-ylidene was reacted with the Au nanoparticles protected by a thioether (Figure 1-10). Characterization methods confirmed that the ligand exchange was complete after 12 h and nearly spherical NHC-coated Au nanoparticles with an average diameter of 2.6 ± 0.5 nm were formed. Although the synthesized nanoparticles were stable at –4 °C in the solid state, they exhibit limited stability in solution and released lower nuclearity NHC–Au complexes.

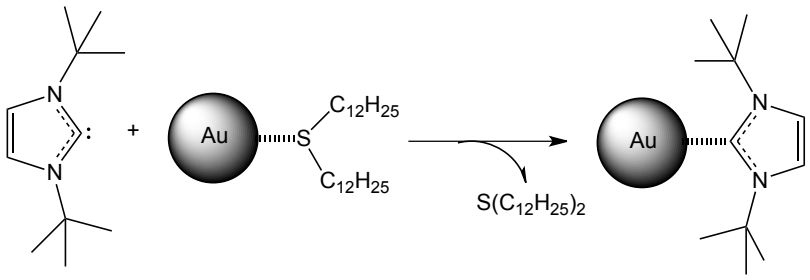

Figure 1-10 Ligand exchange reaction on the Au nanoparticles.[61]

In a one phase synthesis method, AuNPs were also prepared via the reduction of NHC–AuCl complexes which lead to their self-assembly into nanoparticles with markedly different sizes. The nature of the N substituent on the NHC ligands had remarkable influence on the size of the formed AuNPs to the point where reduction of the very bulky [IPrAuCl] (IPr = 1,3-bis(2,6-diisopropylphenyl)imidazol-2-ylidene) complex did not lead to the formation of nanoparticles. On the other hand, [AuCl($^{i}Pr_2$Im)] formed AuNPs with a diameter of ~2 nm via reduction, while a long linear chain substituent ($C_{14}H_{29}$) on NHC resulted in the formation of ~6–7 nm AuNPs.[62] Hence, the size of the N-substituent in the NHC ligand is another tool to control the size of the nanoparticles beside ligand-to-metal ratio in general NP preparation methods.

Recently a solvent free thermolysis method was reported for the synthesis of ultra-small gold nanoparticles (Au UNPs: 1 to 2 nm in size). In this method two types of Au(I)–C_6F_5 complexes, [$C_{18}H_{37}$-MIM][Au(C_6F_5)$_2$] ($C_{18}H_{37}$-MIM = 1-methyl-3-octadecyl-imidazolium) and [Au(C_6F_5)-($C_{18}H_{37}$-NHC)] ($C_{18}H_{37}$-NHC = 1-methyl-3-octadecyl-imidazol-2-ylidene) were heated separately at optimized temperatures and time to form the nanoparticles. After the thermolysis of [$C_{18}H_{37}$-MIM][Au(C_6F_5)$_2$], a mixture of Au UNPs with diameter of 1.5 nm and larger nanocrystals (> 50 nm) were formed while the thermolysis of [Au(C_6F_5)-($C_{18}H_{37}$-NHC)] lead to the isolation of 1.0 nm Au UNPs. These nanoparticles display stability in solution for several weeks and characterization techniques confirm the presence of the NHC ligands on their surface.[63]

Taking a different synthetic approach, Serpell and co-workers have recently reported the preparation of Pd and Au nanoparticles from the reduction of the metallate imidazolium ionic liquids. Au- and Pd-containing imidazolium salts were first deprotonated with NaH and then reduction by $NaBH_4$ resulted NHC-coated nanoparticles. These gold

nanoparticles were large and polydisperse at 16.6 nm ± 6.5. Although theses NPs were stable enough to be characterized, the authors comment that the "NHCs are comparatively poor pacifying agents for metal NPs".[64]

A comparative study has been done on the formation of Au and Ag nanocrystals when NHC–M–Cl (M = Au, Ag) complexes with different NHC ligands were used as precursors and dodecanethiol (DDT) was added as stabilizer. In all of the cases, metal nanocrystals were prepared from optimizing the reducing reagents. Ag–NHC precursors reacted with a thiol and lead to the formation of silver thiolates while Au–NHCs remained unchanged and lead to the formation of well-defined nanocrystals of narrow size distribution (4.6–6.7%). The steric hindrance of the NHC ligands did not have any effect in the case of silver derivatives while it becomes important for the gold nanocrystals when a very bulky NHC is used. This study showed that different reaction pathways and species are involved in the formation of silver and gold nanocrystals from NHC–M–Cl precursors.[65]

Recently, a NHC polymer-supported silver nanoparticle catalyst has been prepared from the reaction of poly-imidazolium with $AgNO_3$ in hot dimethyl sulfoxide. This system is a dispersion of silver nanoparticles (3–5 nm) in the poly-NHC polymer material, which exhibits very high activity, stability and reusability in the carboxylation of terminal alkynes with CO_2 at ambient conditions.[66] It has also been reported that Ag(I)–NHC complexes with long N-alkyl chains formed Ag nanoparticles upon reduction by $NaBH_4$. The prepared silver nanoparticles show spherical and rectangular morphologies and are probably capped with imidazolium moieties.[67]

1.7 Metal-Phosphide Chemistry

Transition-metal phosphides, in the form of nanoparticles and nanoclusters, are in a class of compounds for which few synthetic methods have been explored. Since these materials can adopt a wide range of stoichiometries and structures, their controlled synthesis has been a challenge for chemists. The high reactivity of phosphide sources used in accessing these materials is often a difficulty in this field. Despite these challenges, these materials attract interest due to the novel properties shown in the corresponding bulk transition-metal phosphides, and the potential of unique, size-tunable properties in nanoscale

phases.[68] In addition, transition-metal phosphides show high catalytic reactivity for hydroprocessing[69] and their magnetic properties can vary from antiferromagnetic to paramagnetic, leading to great scientific interest in materials science and chemistry.[68]

Our interest lies in the semiconductor properties of metal-phosphides. For example, the group 12-15 semiconductors, with narrow band gaps, are very interesting materials that have applications in infrared detectors, lasers and solar cell materials.[70] The electronic characteristics of metal phosphides vary from displaying metallic to large band gap semiconductor properties. There are thus metallic phosphides (*e.g.* FeP) reported as well as semiconductors with very low (*e.g.* MnP_4 with $E_g = 0.14$ eV), medium (*e.g.* Zn_3P_2 with $E_g = 1.32$ eV) and higher band gap energies (*e.g.* AlP with $E_g = 2.50$ eV).[71]

1.8 Semiconductor Nanomaterials and the Quantum Confinement Effect

Materials that have at least one dimension in the range of 1–100 nm are often called "nanomaterials" which can be further classified in different subgroups such as nanoparticles, nanoclusters and nanowires.[72, 73] Semiconductors exhibit unique, size-dependent optical and electronic properties in the transition from bulk material to molecular solid. The properties result from the quantum confinement effect. By transition from bulk semiconductor to nanoparticle and then molecular material, the size of the band gap increases. The quantization of levels of energy within the bands also occurs when the size of the particles is decreased (Figure 1-11).[74]

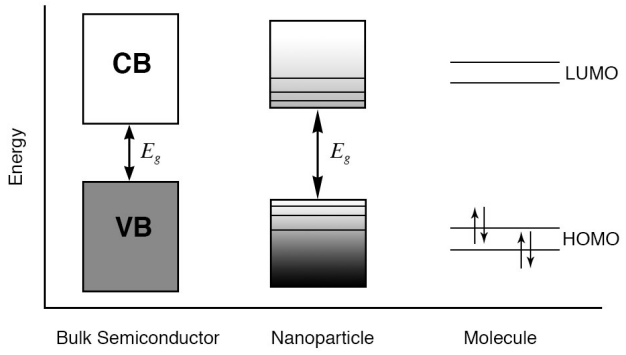

Figure 1-11 Schematic representation of the electronic structure of bulk semiconductors, nanoparticles, and molecules. VB = valence band, CB = conduction band, E_g = band gap energy.

Phosphide semiconductors display these quantum-confined features. For example, it has been reported that InP nanoparticles with an average size of 7.2 nm have a band gap of 1.92 eV, which is larger than the corresponding band gap (1.27 eV) of the bulk material.[75] It has been shown that 12–15 semiconductors, such as Cd_3P_2 nanoparticles, exhibit very pronounced quantum confinement effects, such that with a small change in the size of the particle the band gap changes significantly with a distinct effect on the optical spectra of these materials.[76, 77] Figure 1-12 shows the effect of size and core composition of InP and Cu-doped InP nanocrystals on their PL spectra.[78]

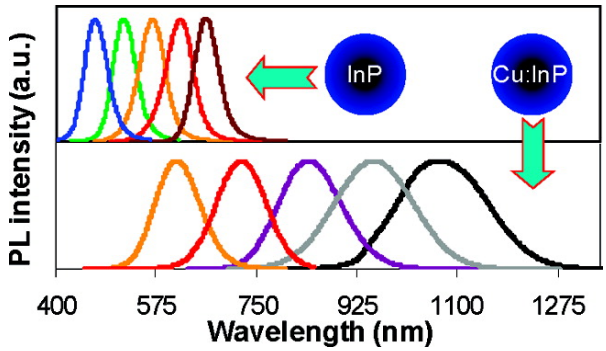

Figure 1-12 PL spectra of differently sized InP q-dots and Cu:InP d-dots*

1.9 Synthesis of Metal Phosphide Clusters, Nanoclusters and Nanoparticles

Scientists have pursued different approaches to prepare a wide variety of phosphide complexes. In this vein, different sources of phosphorus (such as P_4, PH_3, Na_3P and $P(SiMe_3)_3$) have been reacted with a variety of main group and transition metal salts and complexes under different conditions. Following is described some of these approaches and examples of phosphides that are synthesized using these methods.

Solvothermal synthesis is one of the methods which has been reported for the preparation of nanocrystalline phosphides. This process is done at a temperature higher than the normal boiling point of the solvent and under high pressure. FeP, CoP, Co_2P and Ni_2P

* Reprinted with permission from R. Xie and X. Peng, *J. Am. Chem. Soc.*, 2009, **131**, 10645-10651. © American Chemical Society 2009

nanoparticles are some of the examples that have been prepared using a solvothermal approach. Reactive phosphide sources (Na_3P or P_4) have been used for these syntheses. In most of the solvothermal syntheses, the prepared crystalline particles show a large polydispersity. Since the first report by Qian and co-workers in 1997 using this methodology for metal-phosphide nanoparticle preparation, different mechanisms have been postulated for their formation, but it is still not well-understood how to particularly control the particle phase and size.[68]

It is generally difficult to classify P_4 reactions as proceeding via electrophilic, nucleophilic or redox activation as each of these is possible. Figure 1-13 displays the general reactivity pattern of P_4 phosphorus showing electrophilic and nucleophilic reactivity as well as radical bond breaking.[79]

Main group elements and compounds activate P_4 to form cage phosphides by degradation of the tetrahedral structure. For example Roesky *et al*. used bulky nacnac Al(I) species $[HC(CMeN\ Ph')_2Al]$ (Ph′ = 2,6-*i*$Pr_2C_6H_3$) and inserted them into two opposite P–P bonds of the P_4 tetrahedron (Figure 1-14).[80] $Ga_4[C(SiMe_3)_3]_4$ also reacts with P_4 phosphorus and the addition of monovalent Ga unit into P–P bonds to give a nortricyclane-like molecule, as shown in Figure 1-15.[81]

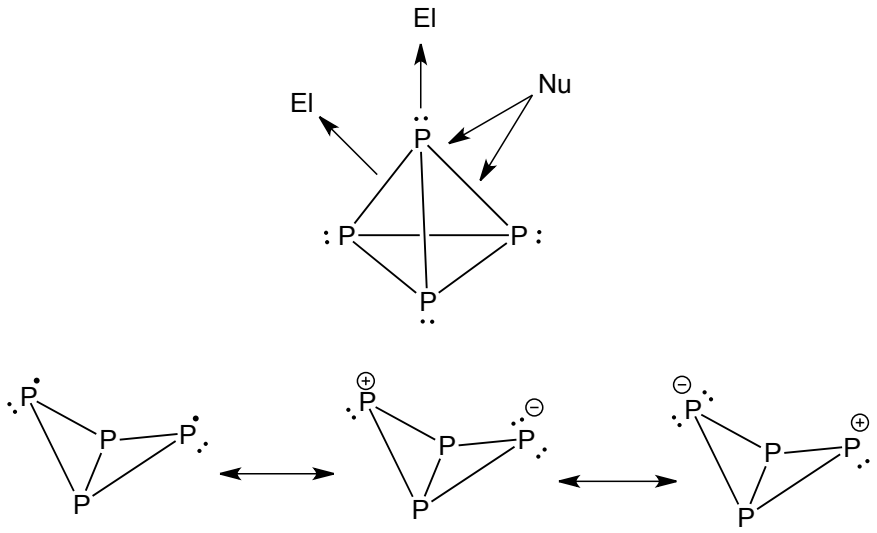

Figure 1-13 General reactivity of P_4.[79]

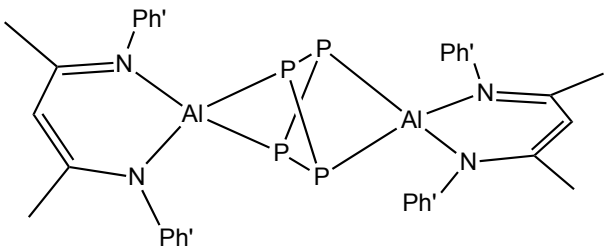

Figure 1-14 Molecular structure of $P_4[HC(CMeNPh')_2Al]_2$.[80]

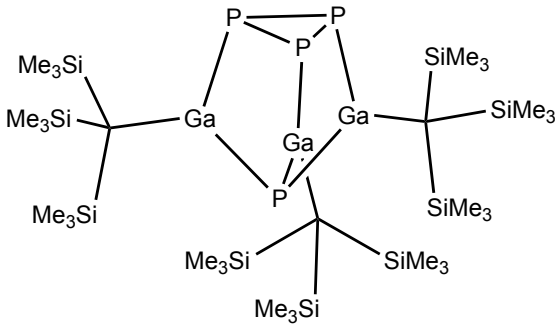

Figure 1-15 Molecular structure of $P_4[GaC(SiMe_3)_3]_3$.[81]

Although activation of P_4 has been done using different elements and compounds and numerous complexes have been synthesized, usually they stay in the molecular size regime and thus, this method is not very powerful to prepare larger systems such as nanoclusters.[79] By taking advantage of the coordinative flexibility of *cyclo*-phosphorus species (such as P_5, P_4S and P_2S_3 units), it has been possible to synthesize supramolecular systems.[82-84] For example, Scheer and co-workers have used the *cyclo*-P_5 ligand complex $[(\eta^5\text{-}C_5Me_5)Fe(\eta^5\text{-}P_5)]$ as linking units between copper(I) halides to form fullerene-like supramolecular aggregates (Figure 1-16). By variation of solvents and stoichiometry they have been able to control the size and shape of their resultant complexes.[84]

The chemistry of molecular compounds containing Si–P bonds has been developed since the middle of the 19th century. Since then, these materials have played an important role in the synthesis of different compounds. Common reaction proceeds by cleavage of the Si–P bond.[85] Reaction of tris(trimethylsilyl)phosphine with metal salts or complexes in the presence of a coordinating solvent gives metal phosphide particles. By coordinating to the surface of the growing particles, coordinating solvents prevent aggregation of metal-phosphide particles into the bulk solid phases.

$$MX_3 + P(SiMe_3)_3 \longrightarrow MP + 3XSiMe_3$$

This method has been used to synthesize main-group-metal-phosphides (InP, GaP)[86-88] as well as transition-metal-phosphides (FeP, MnP, Zn_3P_2).[89-91] In the formation of some of these particles, co-surfactants have been needed in addition to fine temperature and time control. The result is that the formed nanoparticles show more solubility and lower polydispersity compared to those prepared using other methods such as solvothermal synthesis.[68]

Despite these recent successes, there is still little structural information on the formation of these nanoscopic assemblies. This is in stark contrast to 11-16, 12-16, and related systems for which the transition molecule ⇨cluster ⇨ nanocluster ⇨ nanoparticle has been well developed.[92-95] To the best of our knowledge, there are only a few condensed group 11-phosphide clusters that have been prepared and characterized crystallographically.[53-55]

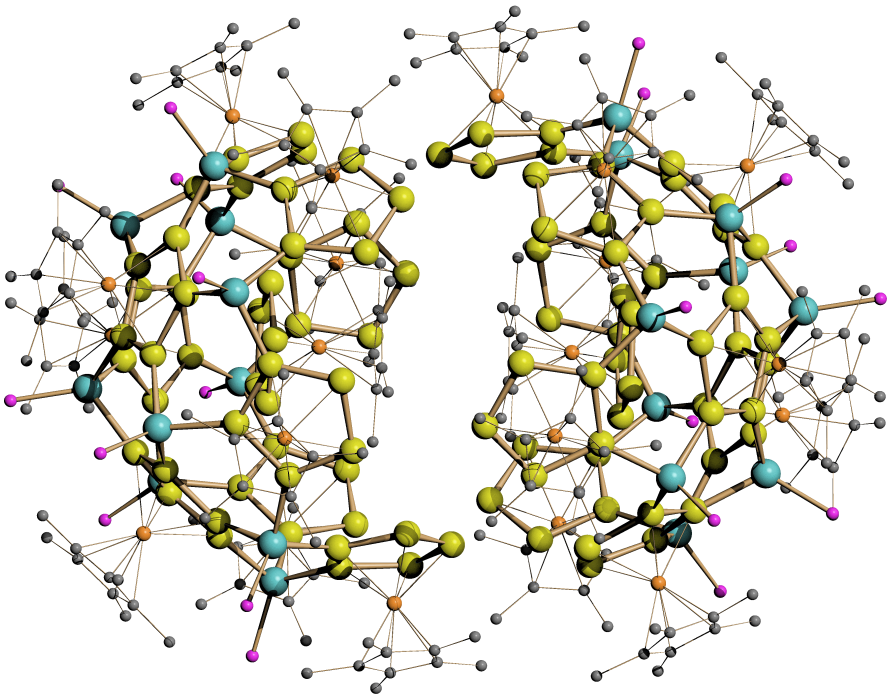

Figure 1-16 Molecular structure of nanometer-sized capsule consisting of *cyclo*-P_5 units and Cu(I) ions. ($[Cp^*Fe(\eta^5\text{-}P_5)]_2$@$[\{CuCl\}_{10}\{Cp^*Fe(\eta^5\text{:}\eta^1\text{:}\eta^1\text{:}\eta^1\text{:}\eta^1\text{-}P_5)\}_3\{Cp^*Fe(\eta^5\text{:}\eta^1\text{:}\eta^1\text{:}\eta^1\text{-}P_5)\}_3\{Cp^*Fe(\eta^5\text{:}\eta^1\text{:}\eta^1\text{-}P_5)\}_3]_2$, $Cp^* = \eta^5\text{-}C_5Me_5$). Cu: teal, P: yellow, Fe: orange, Cl: purple, C: grey.[84]

1.10 Scope of the Thesis

The demonstrated ability of N-heterocyclic carbenes to stabilize polynuclear group 11 clusters and nanoparticles prompted us to synthesize silylated NHC-metal precursors for the preparation of metal-phosphide nanoclusters that have been difficult to stabilize using more classical (phosphine) ligands. As discussed earlier, nanoscale metal-phosphide semiconductors promise to show unique properties that lie between those of the bulk material and molecular units. In addition, these properties should be tunable by differing the surface or the core composition. This area of research is virtually unexplored, unlike other nanomaterial semiconductors such as metal chalcogenides. The focus of this research was to target silylated group 11 phosphido compounds ligated with NHC ligands for nanocluster assemblies. Metal phosphido complexes as precursors can be reacted with a different metal source to synthesize new ternary metal-phosphide clusters.

Chapter 2 of this thesis reports the ligation of N-heterocyclic carbenes to [CuS^tBu] and [AgS^tBu] as an alternative to PR_3 ligands as solubilizing reagents for these coordination polymers in order to form copper and silver t-butylthiolate clusters. 1,3-Di-isopropylbenzimidazol-2-ylidene ($^iPr_2$-bimy) and 1,3-di-isopropyl-4,5-dimethylimidazol-2-ylidene ($^iPr_2$-mimy) were ligated to [CuS^tBu] and [AgS^tBu] forming four polynuclear copper and silver clusters. For comparison, the trialkyl phosphines P^nPr_3 and P^iPr_3 were also used to solubilize [AgS^tBu] and [CuS^tBu] to form copper and silver t-butylthiolate clusters.

Chapter 3 describes the facile preparation of $[M_6\{P(SiMe_3)_2\}_6]$ (M = Ag, Cu) as well as their structural characterization. Since these complexes show limited stability towards solvent loss and ambient temperature, N-heterocyclic carbene ligands were used to synthesize more stable silylphosphido compounds. 1,3-Di-isopropylbenzimidazole-2-ylidene ($^iPr_2$-bimy) and 1,3-bis(2,6-diisopropylphenyl)imidazol-2-ylidene (IPr) are found to be excellent ligands to stabilize silylphosphido-copper compounds that show higher stability when compared to $[Cu_6\{P(SiMe_3)_2\}_6]$. The $^iPr_2$-bimy is found to be also an excellent ligand for the stabilization of silver–phosphorus polynuclear complexes. The straightforward preparation and characterization of the clusters $[Ag_{12}(PSiMe_3)_6(^iPr_2\text{-bimy})_6]$ and $[Ag_{26}P_2(PSiMe_3)_{10}(^iPr_2\text{-bimy})_8]$ are described in Chapter 4, representing the

first examples of such structurally characterized, higher nuclearity complexes obtained using this class of ligand.

NHC-gold complexes have been studied extensively but there is only one NHC–Au–PR_2 compound known to date.[96] In Chapter 5 the synthesis and characterization of four new NHC–Au–PR_2 complexes, that contain $SiMe_3$ groups attached to the phosphorus center, are described. These silylphosphido gold complexes are good candidates for the preparation of larger gold-phosphide clusters. The reactivity of these complexes towards the addition of PhC(O)Cl are also described.

The final chapter (Chapter 6) summarizes the results obtained and provides thoughts on the use of the synthesized molecular precursors and suggestions for future research in this area that could be pursued.

1.11 References

1. M. N. Hopkinson, C. Richter, M. Schedler and F. Glorius, *Nature*, 2014, **510**, 485-496.
2. D. Bourissou, O. Guerret, F. P. Gabbaï and G. Bertrand, *Chem. Rev.*, 2000, **100**, 39-91.
3. G. Bertrand, *Carbene chemistry: from fleeting intermediates to powerful reagents*, Marcel Dekker and FontisMedia, New York; Lausanne, Switzerland, 2002.
4. H. W. Wanzlick and H. J. Schönher, *Angew. Chem. Int. Ed.*, 1968, **7**, 141-142.
5. K. Öfele, *J. Organomet. Chem.*, 1968, **12**, 42-43.
6. S. Díez-González, *N-heterocyclic carbenes: from laboratory curiosities to efficient synthetic tools*, Royal Society of Chemistry, Cambridge, 2011.
7. F. Glorius, *N-heterocyclic carbenes in transition metal catalysis*, Springer, Berlin, 2007.
8. A. J. Arduengo, R. L. Harlow and M. Kline, *J. Am. Chem. Soc.*, 1991, **113**, 361-363.
9. S. P. Nolan, *N-Heterocyclic carbenes in synthesis*, Wiley-VCH; John Wiley distributor, Weinheim, Chichester, 2006.
10. S. P. Nolan, *Acc. Chem. Res.*, 2011, **44**, 91-100.
11. J. C. Y. Lin, R. T. W. Huang, C. S. Lee, A. Bhattacharyya, W. S. Hwang and I. J.

B. Lin, *Chem. Rev.*, 2009, **109**, 3561-3598.

12. S. Díez-González and S. P. Nolan, *Aldrichimica Acta*, 2008, **41**, 43-51.
13. P. de Fremont, N. M. Scott, E. D. Stevens and S. P. Nolan, *Organometallics*, 2005, **24**, 2411-2418.
14. A. Kascatan-Nebioglu, M. J. Panzner, C. A. Tessier, C. L. Cannon and W. J. Youngs, *Coord. Chem. Rev.*, 2007, **251**, 884-895.
15. I. J. B. Lin and C. S. Vasam, *Comments Inorg. Chem.*, 2004, **25**, 75-129.
16. I. J. B. Lin and C. S. Vasam, *Coord. Chem. Rev.*, 2007, **251**, 642-670.
17. J. C. Garrison and W. J. Youngs, *Chem. Rev.*, 2005, **105**, 3978-4008.
18. F. E. Hahn and M. C. Jahnke, *Angew. Chem. Int. Ed.*, 2008, **47**, 3122-3172.
19. R. Hoffmann, G. D. Zeiss and G. W. Vandine, *J. Am. Chem. Soc.*, 1968, **90**, 1485-1498.
20. N. C. Baird and K. F. Taylor, *J. Am. Chem. Soc.*, 1978, **100**, 1333-1338.
21. A. C. Hillier, W. J. Sommer, B. S. Yong, J. L. Petersen, L. Cavallo and S. P. Nolan, *Organometallics*, 2003, **22**, 4322-4326.
22. H. Clavier and S. P. Nolan, *Chem. Commun.*, 2010, **46**, 841-861.
23. T. Droege and F. Glorius, *Angew. Chem. Int. Ed.*, 2010, **49**, 6940-6952.
24. A. B. P. Lever, *Inorg. Chem.*, 1990, **29**, 1271-1285.
25. S. S. Fielder, M. C. Osborne, A. B. P. Lever and W. J. Pietro, *J. Am. Chem. Soc.*, 1995, **117**, 6990-6993.
26. A. B. P. Lever, *Inorg. Chem.*, 1991, **30**, 1980-1985.
27. C. A. Tolman, *Chem. Rev.*, 1977, **77**, 313-348.
28. A. R. Chianese, X. W. Li, M. C. Janzen, J. W. Faller and R. H. Crabtree, *Organometallics*, 2003, **22**, 1663-1667.
29. R. A. Kelly, H. Clavier, S. Giudice, N. M. Scott, E. D. Stevens, J. Bordner, I. Samardjiev, C. D. Hoff, L. Cavallo and S. P. Nolan, *Organometallics*, 2008, **27**, 202-210.
30. X. L. Hu, I. Castro-Rodriguez and K. Meyer, *J. Am. Chem. Soc.*, 2003, **125**, 12237-12245.
31. X. L. Hu, I. Castro-Rodriguez, K. Olsen and K. Meyer, *Organometallics*, 2004, **23**, 755-764.

32. A. Rit, T. Pape, A. Hepp and F. E. Hahn, *Organometallics*, 2011, **30**, 334-347.
33. A. Biffis, C. Tubaro, E. Scattolin, M. Basato, G. Papini, C. Santini, E. Alvarez and S. Conejero, *Dalton Trans*., 2009, 7223-7229.
34. S. Gaillard and J. L. Renaud, *Dalton Trans*., 2013, **42**, 7255-7270.
35. E. Kuhnel, I. V. Shishkov, F. Rominger, T. Oeser and P. Hofmann, *Organometallics*, 2012, **31**, 8000-8011.
36. P. F. Ai, A. A. Danopoulos, P. Braunstein and K. Y. Monakhovc, *Chem. Commun*., 2014, **50**, 103-105.
37. P. Ai, A. A. Danopoulos and P. Braunstein, *Inorg. Chem*., 2015, **54**, 3722-3724.
38. B. Liu, S. F. Pan, B. Liu and W. Z. Chen, *Inorg. Chem*., 2014, **53**, 10485-10497.
39. B. Liu, Q. Q. Xia and W. Z. Chen, *Angew. Chem. Int. Ed*., 2009, **48**, 5513-5516.
40. V. J. Catalano, L. B. Munro, C. E. Strasser and A. F. Samin, *Inorg. Chem*., 2011, **50**, 8465-8476.
41. C. E. Ellul, G. Reed, M. F. Mahon, S. I. Pascu and M. K. Whittlesey, *Organometallics*, 2010, **29**, 4097-4104.
42. C. Chen, H. Qiu and W. Chen, *J. Organomet. Chem*., 2012, **696**, 4166-4172.
43. M. Nonmenmacher, D. Kunz and F. Rominger, *Organometallics*, 2008, **27**, 1561-1568.
44. J. A. Aitken, V. Ganzha-Hazen and S. L. Brock, *J. Solid State Chem*., 2005, **178**, 970-975.
45. B. Liu, Y. Zhang, D. Xu and W. Chen, *Chem. Commun*., 2011, **47**, 2883-2885.
46. B. Liu, B. Liu, Y. Zhou and W. Chen, *Organometallics*, 2010, **29**, 1457-1464.
47. W. D. Clark, G. E. Tyson, T. K. Hollis, H. U. Valle, E. J. Valente, A. G. Oliver and M. P. Dukes, *Dalton Trans*., 2013, **42**, 7338-7344.
48. B. Quillian, P. Wei, C. S. Wannere, P. v. R. Schleyer and G. H. Robinson, *J. Am. Chem. Soc*., 2009, **131**, 3168-3169.
49. X. Han, Z. Weng, D. J. Young, G. Jin and T. S. Andy Hor, *Dalton Trans*., 2014, **43**, 1305-1312.
50. L. R. Collins, J. P. Lowe, M. F. Mahon, R. C. Poulten and M. K. Whittlesey, *Inorg. Chem*., 2014, **53**, 2699-2707.
51. W. J. Humenny, S. Mitzinger, C. B. Khadka, B. Khalili Najafabadi, I. Vieira and

J. F. Corrigan, *Dalton Trans*., 2012, **41**, 4413-4422.

52. A. Eychmüller, U. Banin, S. Dehnen, A. Eichhöfer, J. F. Corrigan and D. Fenske, in *Nanoparticles*, Wiley-VCH Verlag GmbH & Co. KGaA, 2005.
53. D. Fenske and W. Holstein, *Angew. Chem. Int. Ed*., 1994, **33**, 1290-1292.
54. D. Fenske and F. Simon, *Angew. Chem. Int. Ed*., 1997, **36**, 230-233.
55. P. Sevillano, O. Fuhr, O. Hampe, S. Lebedkin, E. Matern, D. Fenske and M. M. Kappes, *Inorg. Chem*., 2007, **46**, 7294-7298.
56. P. Lara, O. Rivada-Wheelaghan, S. Conejero, R. Poteau, K. Philippot and B. Chaudret, *Angew. Chem. Int. Ed*., 2011, **50**, 12080-12084.
57. D. Gonzalez-Galvez, P. Lara, O. Rivada-Wheelaghan, S. Conejero, B. Chaudret, K. Philippot and P. W. N. M. van Leeuwen, *Catal. Sci. Tech*., 2013, **3**, 99-105.
58. K. V. S. Ranganath, J. Kloesges, A. H. Schafer and F. Glorius, *Angew. Chem. Int. Ed*., 2010, **49**, 7786-7789.
59. C. Richter, K. Schaepe, F. Glorius and B. J. Ravoo, *Chem. Commun*., 2014, **50**, 3204-3207.
60. J. D. Scholten, G. Ebeling and J. Dupont, *Dalton Trans*., 2007, 5554-5560.
61. E. C. Hurst, K. Wilson, I. J. S. Fairlamb and V. Chechik, *New J. Chem*., 2009, **33**, 1837-1840.
62. J. Vignolle and T. D. Tilley, *Chem. Commun*., 2009, 7230-7232.
63. J. Crespo, Y. Guari, A. Ibarra, J. Larionova, T. Lasanta, D. Laurencin, J. M. Lopez-de-Luzuriaga, M. Monge, M. E. Olmos and S. Richeter, *Dalton Trans*., 2014, **43**, 15713-15718.
64. C. J. Serpell, J. Cookson, A. L. Thompson, C. M. Brown and P. D. Beer, *Dalton Trans*., 2013, **42**, 1385-1393.
65. X. Ling, N. Schaeffer, S. Roland and M. P. Pileni, *Langmuir*, 2013, **29**, 12647-12656.
66. D. Y. Yu, M. X. Tan and Y. G. Zhang, *Adv. Synth. Catal*., 2012, **354**, 969-974.
67. C. K. Lee, C. S. Vasam, T. W. Huang, H. M. J. Wang, R. Y. Yang, C. S. Lee and I. J. B. Lin, *Organometallics*, 2006, **25**, 3768-3775.
68. S. L. Brock, S. C. Perera and K. L. Stamm, *Chem. Eur. J*., 2004, **10**, 3364-3371.
69. S. T. Oyama, *J. Catal*., 2003, **216**, 343-352.

70. G. Shen and D. Chen, *Nanoscale Res. Lett.*, 2009, **4**, 779-788.
71. M. Sharon and G. Tamizhmani, *J. Mater. Sci.*, 1986, **21**, 2193-2201.
72. C. N. R. Rao, G. U. Kulkarni, P. J. Thomas and P. P. Edwards, *Chem. Eur. J.*, 2002, **8**, 29-35.
73. C. N. R. Rao, A. Müller and A. K. Cheetham, *The chemistry of nanomaterials: synthesis, properties and applications*, Wiley-VCH, Weinheim, 2004.
74. T. J. Meyer, *Comprehensive coordination chemistry II: from biology to nanotechnology*, Elsevier Pergamon, Amsterdam ; Boston, 2004.
75. N. L. Pickett and P. O'Brien, *Chem. Rec.*, 2001, **1**, 467-479.
76. M. Green and P. O'Brien, *J. Mater. Chem.*, 1999, **9**, 243-247.
77. P. K. Khanna, N. Singh and P. More, *Curr. Appl. Phys.*, 2010, **10**, 84-88.
78. R. Xie and X. Peng, *J. Am. Chem. Soc.*, 2009, **131**, 10645-10651.
79. M. Scheer, G. Balazs and A. Seitz, *Chem. Rev.*, 2010, **110**, 4236-4256.
80. Y. Peng, H. J. Fan, H. P. Zhu, H. W. Roesky, J. Magull and C. E. Hughes, *Angew. Chem. Int. Ed.*, 2004, **43**, 3443-3445.
81. W. Uhl and M. Benter, *Chem. Commun.*, 1999, 771-772.
82. C. Groeger, H. R. Kalbitzer, W. Meier, M. Pronold, M. Scheer, J. Wachter and M. Zabel, *Inorg. Chim. Acta*, 2011, **370**, 191-197.
83. M. Scheer, A. Schindler, J. Bai, B. P. Johnson, R. Merkle, R. Winter, A. V. Virovets, E. V. Peresypkina, V. A. Blatov, M. Sierka and H. Eckert, *Chem. Eur. J.*, 2010, **16**, 2092-2107.
84. S. Welsch, C. Groeger, M. Sierka and M. Scheer, *Angew. Chem. Int. Ed.*, 2011, **50**, 1435-1438.
85. G. Fritz and P. Scheer, *Chem. Rev.*, 2000, **100**, 3341-3402.
86. D. Battaglia and X. G. Peng, *Nano Lett.*, 2002, **2**, 1027-1030.
87. Y. H. Kim, Y. W. Jun, B. H. Jun, S. M. Lee and J. W. Cheon, *J. Am. Chem. Soc.*, 2002, **124**, 13656-13657.
88. H. Yu, J. B. Li, R. A. Loomis, L. W. Wang and W. E. Buhro, *Nat. Mater.*, 2003, **2**, 517-520.
89. S. C. Perera, P. S. Fodor, G. M. Tsoi, L. E. Wenger and S. L. Brock, *Chem. Mater.*, 2003, **15**, 4034-4038.

90. S. C. Perera, G. Tsoi, L. E. Wenger and S. L. Brock, *J. Am. Chem. Soc.*, 2003, **125**, 13960-13961.
91. M. H. Mobarok, E. J. Luber, G. M. Bernard, L. Peng, R. E. Wasylishen and J. M. Buriak, *Chem. Mater.*, 2014, **26**, 1925-1935.
92. C. E. Anson, A. Eichhöfer, I. Issac, D. Fenske, O. Fuhr, P. Sevillano, C. Persau, D. Stalke and J. Zhang, *Angew. Chem. Int. Ed.*, 2008, **47**, 1326-1331.
93. M. Fu, I. Issac, D. Fenske and O. Fuhr, *Angew. Chem. Int. Ed.*, 2010, **49**, 6899-6903.
94. R. Langer, B. Breitung, L. Wuensche, D. Fenske and O. Fuhr, *Z. Anorg. Allg. Chem.*, 2011, **637**, 995-1006.
95. M. N. Sokolov and P. A. Abramov, *Coord. Chem. Rev.*, 2012, **256**, 1972-1991.
96. M. W. Johnson, S. L. Shevick, F. D. Toste and R. G. Bergman, *Chem. Sci.*, 2013, **4**, 1023-1027.

Chapter 2

N-Heterocyclic Carbenes as Effective Ligands for the Preparation of Stabilized Copper- and Silver-t-Butylthiolate Clusters†

2.1 Introduction

Copper-thiolates have received much attention due to their interesting photochemical properties,[1,2] their presence in biological systems (cysteine-rich copper (I) proteins)[3-5] and their use in synthetic[6] and materials chemistry, such as in the preparation of organocuprate reagents[7], as precursors for copper sulfide thin films[8,9] or as p-type charge carriers.[10] In addition, homoleptic silver(I)-thiolates [AgSR] have demonstrated use as precursors for the synthesis of silver-chalcogenide nanoclusters via the addition of the chalcogenide sources ($S(SiMe_3)_2$ and $Se(SiMe_3)_2$),[11,12] as well as well defined coordination polymers and biological sensors.[13] Since [CuSR] and [AgSR] are generally insoluble in common solvents and have poor crystal habit, their crystal structures are not typically well-known; however, they are generally considered to be coordination polymers.[14] Dance predicted a chain structure consisting of $M_4(SR)_4$ cycles for [CuSR] and [AgSR] compounds[15] and powder X-ray diffraction refinements have illustrated chain[16] structures, although lamellar

† **B. Khalili Najafabadi**, J. F. Corrigan, *Dalton Trans*., **2014**, 43, 2104-2111. Reproduced by permission of The Royal Society of Chemistry.

structures have also been proposed depending on the organic substituent on sulfur.[17-19] In order to solubilize the tert-butylthiolates [CuS^tBu] and [AgS^tBu], different phosphines have been used and in most cases cyclic, molecular clusters are obtained.[7,9,13,14] Such [CuS^tBu]/[AgS^tBu]:phosphine adducts are the key components in the synthesis of the nanoclusters, nanoparticles and thin films that were described above.

N-heterocyclic carbenes (NHCs), divalent species with an electron sextet carbon, contain a carbene carbon incorporated in a nitrogen-containing heterocycle.[20] Their importance is reflected in the ever growing number of review articles concerning the preparative chemistry and properties of metal-NHC complexes,[21-26] including those of silver and copper.[27-36] Compared with phosphines, NHCs can form stronger bonds with most metals due to their excellent σ-donating properties.[27,37] Recently we have shown that the NHC 1,3-di-isopropylbenzimidazol-2-ylidene ($^iPr_2$-bimy) can be used to stabilize polynuclear Cu(I) and Ag(I) phenylchalcogenolate clusters prepared from phenylchalcogentrimethylsilanes, which are the first examples of using this class of ligand in the preparation of such metal-chalcogen cluster complexes.[38] Since copper-thiolate ring complexes prepared from the reaction of [CuS^tBu] with phosphines are reported to have limited stability in ambient light,[8,9,14] we were interested in probing the stability of this class of clusters using NHCs instead of phosphines as ancillary ligand. In the present work it is shown that N-heterocyclic carbenes can be used as ligands to solubilize [CuS^tBu] and [AgS^tBu] polymers to form copper and silver cyclic cluster structures. Two different NHCs ($^iPr_2$-bimy and $^iPr_2$-mimy) are used to solubilize [CuS^tBu] and [AgS^tBu] polymers in order to form polynuclear copper and silver t-butylthiolate clusters. We have also performed the same experiments with two phosphines of approximately similar size (P^nPr_3 and P^iPr_3) for comparison.

Nolan, Cavallo and co-workers have developed and refined the "buried volume" method to quantify the steric demand of different NHCs and phosphines.[39,40] The percent buried volume ($\%V_{bur}$) represents the percent of the total volume of a sphere around the metal atom, which is occupied by a specific ligand. More sterically demanding ligands have larger $\%V_{bur}$. $^iPr_2$-bimy and $^iPr_2$-mimy that were chosen for this work, show different $\%V_{bur}$ values, hence introducing the potential for the formation of different structures upon their reaction with [CuS^tBu] and [AgS^tBu] due to differing steric demands. P^nPr_3 and

P^iPr_3 were selected since they have similar $\%V_{bur}$ values close to $^iPr_2$-bimy and $^iPr_2$-mimy, respectively.[41]

2.2 Experimental

All synthetic and handling procedures were carried out under an inert atmosphere of high purity dried nitrogen using Schlenk line techniques and inert atmosphere glove boxes. Non-chlorinated solvents were dried using an MBraun MB-SP Series Solvent Purification system with tandem activated alumina (THF) or activated alumina-activated copper redox catalyst (pentane). Chloroform-d and dichloromethane were dried and distilled over P_2O_5. Benzene-d was dried and distilled over Na/K alloy. [AgS^tBu] and [CuS^tBu] were prepared according to literature procedures.[8,42] 1,3-Diisopropyl-4,5-dimethylimidazol-2-ylidene ($^iPr_2$-mimy) was synthesized by reduction of corresponding imidazole-2(3H)-thione.[43] 1,3-Di-isopropylbenzimidazole-2-ylidene ($^iPr_2$-bimy)[44] was prepared from 1,3-di-isopropylbenzimidazoliumiodide[45] with a minor modification of a literature procedure. NMR spectra [^{1}H (399.763 MHz), $^{13}C\{^1H\}$ (100.522 MHz)] were recorded on a Varian Mercury 400 NMR spectrometer. ^{1}H and ^{13}C chemical shifts are referenced to $SiMe_4$ (δ = 0 ppm) using the solvent peaks as a secondary reference. $^{31}P\{^1H\}$ (161.827 MHz) NMR spectra were recorded on the same spectrometer and are referenced to 85% H_3PO_4 (δ = 0 ppm). Elemental analysis was performed by Laboratoire d'Analyse Élementaire de l'Université de Montréal, Canada. Residual lattice solvents were included in the formulae according to the ^{1}H NMR spectra of dried samples (see Supporting Information for Chapter 2).

Single crystal X-ray diffraction measurements were performed on a Bruker APEXII or a Nonius KappaCCD diffractometer, with the molecular structures determined via direct methods using the SHELX suite of crystallographic programs.[46] Cluster **4** was refined as a 2-component twin (HKLF 5), with a twin component of 0.3771(3). Complex **6** was satisfactorily refined as an inversion twin (twin component 0.31(5)). Residual electron density in the difference Fourier map for **6** indicated additional (disordered) solvent in the lattice; a suitable model was not able to be refined.

2.2.1 $[Cu_4(S^tBu)_4(^iPr_2\text{-bimy})_2]$ (1)

$^iPr_2$-bimy (0.06 g, 0.33 mmol) was dissolved in 10 ml of THF together with [CuS^tBu] (0.10 g, 0.66 mmol). The solid dissolved after a few seconds to yield a clear yellow solution. It was mixed with 8 ml of hexanes and kept at –40 °C for 3–4 days to form colourless crystals. The crystals were washed with hexanes and dried under vacuum. Reactions were also performed in CH_2Cl_2 with similar yields. Yield: 0.070 g, 0.069 mmol (42%)

NMR ^{1}H (C_6D_6, 293K) δ = 7.16 (m, 4H, overlapping with the solvent peak), 6.93 (m, 4H), 5.66 (br, 4H), 1.73 (s, 36H), 1.59 (d, 24H, $^3J_{HH}$ = 6.64 Hz); ^{13}C{^{1}H} (C_6D_6, 293K) δ = 134.04, 121.99, 112.91, 53.81, 38.38, 21.80. Anal. Calcd: C, 49.67; H, 7.15; N, 5.52; S, 12.60. Anal. Calcd **1**.$(CH_2Cl_2)_2$: C, 44.58; H, 6.47; N, 4.73; S, 10.82. Found: C, 44.22; H, 6.62; N, 4.64; S, 11.24.

2.2.2 $[Cu_4(S^tBu)_4(^iPr_2\text{-mimy})_2]$ (2)

Compound **2** was prepared analogously to **1** except that $^iPr_2$-mimy was used as the carbene. Yield: 0.075 g, 0.077 mmol (47%)

NMR ^{1}H ($CDCl_3$, 293K) δ = 4.61 (br, 4H), 2.15 (s, 12H), 1.63 (d, 24H, $^3J_{HH}$ = 6.6 Hz) 1.54 (s, 36H); NMR ^{13}C ($CDCl_3$, 293K) δ = 123.8, 50.5, 38.4, 30.6, 24.4, 21.2, 9.4. Anal. Calcd: C, 46.98; H, 7.89; N, 5.77; S, 13.18. Found: C, 46.91; H, 7.89; N, 5.72; S, 13.29.

2.2.3 $[Cu_4(S^tBu)_4(P^nPr_3)_2]$ (3)

[CuS^tBu] (0.050 g, 0.33 mmol) was suspended in 10 ml of THF. P^nPr_3 (0.03 ml, 0.16 mmol) was then added to the suspension, which caused the solid to dissolve to yield a clear light yellow solution. The volume of the solution was reduced to ~5 ml *in vacuo* and 5 ml of hexanes was added. This mixture was kept at –40 °C for crystallization. Colorless single crystals were formed after 3–4 days. The liquid was removed with a pipette and the crystals were washed with hexanes and dried under vacuum. Reactions were also performed in CH_2Cl_2 with similar yields. Yield: 0.055 g, 0.059 mmol (72%)

NMR ^{1}H (C_6D_6, 293K) δ = 1.76 (s, 36H), 1.52 (m, 24H), 0.98 (t, 18H, $^3J_{HH}$ = 6.8 Hz); ^{13}C{^{1}H}(C_6D_6, 293K) δ = 44.48, 38.45, 28.11 (d, $^1J_{PC}$ = 13.04 Hz), 18.19 (d, $^2J_{PC}$ = 3.83 Hz), 16.48 (d, $^3J_{PC}$ = 13.04 Hz). ^{31}P{^{1}H}($CDCl_3$, 293K) δ = –22.9. Anal. Calcd: C, 43.84; H, 8.45; S, 13.74. Anal. Calcd **3**.$(CH_2Cl_2)_{0.3}$: C, 43.05; H, 8.32; S, 13.34. Found: C, 42.71; H, 8.86; S, 12.97.

2.2.4 $[Cu_4(S^tBu)_4(P^iPr_3)_2]$ (4)

Complex **4** was synthesized via the same method used for **3**, using P^iPr_3 instead of P^nPr_3. Yield: 0.051 g, 0.055 mmol (67%)

NMR ^1H (C_6D_6, 293K) δ = 1.91 (m, 6H), 1.79 (s, 36H), 1.19 (dd, 36H, $^3J_{HP}$ = 13.29 Hz, $^3J_{HH}$ = 7.03 Hz); $^{13}C\{^1H\}$ ($CDCl_3$, 293K) δ = 38.25, 30.56, 20.40, 16.61 (d, J = 3.07Hz); $^{31}P\{^1H\}$ (C_6D_6, 293K) δ = 21.14. Anal. Calcd: C, 43.84; H, 8.45; S, 13.74. Found: C, 43.72; H, 8.44; S, 13.72.

2.2.5 $[Ag_4(S^tBu)_4(^iPr_2\text{-bimy})_2]$ (5)

Complex **5** was prepared analogously to **1** but [AgS^tBu] was used instead of [CuS^tBu]. Product was dissolved in ~5ml of toluene and cooled to –40 °C for crystallization. Yield: 0.10 g, 0.084 mmol (51%)

NMR ^1H (C_6D_6, 293K) δ = 7.07 (m, 4H), 6.93 (m, 4H), 5.29 (br, 4H), 1.84 (s, 36H), 1.52 (d, 24H, $^3J_{HH}$ = 7.03 Hz); $^{13}C\{^1H\}$ (C_6D_6, 293K) δ = 133.93, 122.52, 112.95, 54.39, 42.76, 39.88, 22.05. Anal. Calcd: C, 42.28; H, 6.09; N, 4.70; S, 10.73. Anal. Calcd. **5**.$(THF)_{0.4}$ C, 42.87; H, 6.20; N, 4.59; S, 10.50. Found: C, 43.05; H, 6.34; N, 4.29; S, 11.08.

2.2.6 $[Ag_5(S^tBu)_6][Ag(^iPr_2\text{-mimy})_2]$ (6)

Compound **6** was synthesized via the same method as complex **1** except that [AgS^tBu] was reacted with $^iPr_2$-mimy. Yield: 0.093 g, 0.060 mmol (55%)

NMR ^1H (CD_3CN, 293K) δ = 4.61 (sep, 4H, $^3J_{HH}$ = 6.84 Hz), 2.18 (s, 12H), 1.56 (d, 24H, $^3J_{HH}$ = 7.03 Hz) 1.42 (s, 54H); $^{13}C\{^1H\}$ (CD_3CN, 293K) δ = 39.99, 24.95, 9.98. Anal. Calcd: C, 35.80; H, 6.14; N, 3.63;S, 12.44. Anal. Calcd. **6**.$(THF)_{0.9}$ C, 37.05; H, 6.34; N, 3.48;S, 11.97. Found: C, 37.58; H, 6.44; N, 3.47; S, 12.72.

2.2.7 $[Ag_4(S^tBu)_4(P^nPr_3)_2]$ (7)

Complex **7** was prepared in the same way as **3** except that [AgS^tBu] was used as the starting material. Yield: 0.064 g, 0.058 mmol (70%)

NMR ^1H ($CDCl_3$, 293K) δ = 1.58 (m, 24H), 1.51 (s, 36H), 1.02 (t, 18H, $^3J_{HH}$ = 6.84 Hz); $^{13}C\{^1H\}$ ($CDCl_3$, 293K) δ = 43.85, 39.28, 28.11 (d, $^1J_{PC}$ = 10.74 Hz), 19.08 (d, $^2J_{PC}$ = 6.13 Hz), 16.13 (d, $^3J_{PC}$ = 13.8 Hz); $^{31}P\{^1H\}$ ($CDCl_3$, 293K) δ = –12.63. Anal. Calcd: C, 36.83; H, 7.10; S, 11.54. Found: C, 36.77; H, 7.23; S, 11.49.

2.2.8 $[Ag_6(S^tBu)_6(P^iPr_3)_2]$ (8)

8 was synthesized using the same method that was used for the preparation of **3** except that $[AgS^tBu]$ was reacted with P^iPr_3. Yield: 0.090 g, 0.060 mmol (73%)

NMR ^1H ($CDCl_3$, 293K) δ = 2.15 (m, 6H), 1.54 (s, 54H), 1.28 (dd, 36H, $^3J_{HP}$ = 14.65 Hz, $^3J_{HH}$ = 7.23 Hz); $^{13}C\{^1H\}$ ($CDCl_3$, 293K) δ = 44.53, 39.43, 22.74 (d, $^1J_{PC}$ = 11.5 Hz), 20.75 (d, $^2J_{PC}$ = 5.37 Hz); $^{31}P\{^1H\}$ ($CDCl_3$, 293K) δ = 40.91. Anal. Calcd: C, 33.56; H, 6.44; S, 12.77. Found: C, 33.66; H, 6.48; S, 12.77.

2.3 Results and Discussion

$[CuS^tBu]$ and $[AgS^tBu]$ have a polymeric chain structure and are insoluble in most organic solvents.[15] One of the approaches to solve the problem of insolubility is to treat these coordination polymers with good Lewis bases such as phosphines in order to break up the bridging thiolate interactions and thus the chain. A few phosphines have been used for this purpose previously.[9, 14] In this work, N-heterocyclic carbenes have been used as alternative solubilizing ligands which, due to their strong Lewis basicity, form stable clusters with both $[CuS^tBu]$ and $[AgS^tBu]$.

Two NHC ligands, $^iPr_2$-bimy and $^iPr_2$-mimy, were chosen due to their ease of preparation and optimum steric effect such that ^{i}Pr groups have been shown to avoid dimerization of these carbenes[23, 37, 41, 47] while they are still small enough to allow the formation of μ-SR.[38] Polynuclear complexes $[Cu_4(S^tBu)_4(^iPr_2\text{-bimy})_2]$ **1**, $[Cu_4(S^tBu)_4(^iPr_2\text{-mimy})_2]$ **2**, $[Cu_4(S^tBu)_4(P^nPr_3)_2]$ **3** and $[Cu_4(S^tBu)_4(P^iPr_3)_2]$ **4** were synthesized via ligation of the corresponding ligands to $[CuS^tBu]$ at room temperature in 1:2 ratio, breaking the chain structure of the polymer (Scheme 2-1). All of the reactions with phosphines were performed in subdued light. Obtaining a clear solution from the starting suspension is a simple means of indicating the completion of the reactions. Complexes **3** and **4** were crystallized and kept in subdued light since a color change from colorless to brown was observed upon leaving the reaction solutions in ambient conditions; which has been reported previously for the complexes formed from the reaction of $[CuS^tBu]$ with other phosphines.[8, 9, 14] Of note is that evidence for this decomposition was not observed for complexes **1** and **2** with NHC ligands attached to the copper atoms. Because of the lone pair donation from the nitrogen atoms to the divalent carbon atom in NHCs, they are electron

rich nucleophilic compounds that are better σ-donors compared to phosphines[27] and would bind the metal atoms more strongly. Presumably, this strong coordination avoids the dissociation of the NHC ligands, hence photo activated decomposition is not observed. It was found that solutions of **1** and **2** could be kept under ambient conditions after their formation without any discoloration observed. Ultimately, however, isolated yields were higher for the phosphine-ligated clusters synthesized compared to those with ancillary NHC ligands. Solution ^{1}H NMR spectra of clusters **1**-**4** show a singlet peak at ~1.7 ppm for the hydrogen atoms of S^{t}Bu groups together with the characteristic peaks of the ancillary ligand used, the ^{t}Bu rendered equivalent on the NMR timescale in solution. Integration values versus the methyl resonance of the S^{t}Bu groups confirm the 1:2 ligand to metal ratio for the synthesized complexes. These NMR spectra also indicate that the solid-state structures are stable in the solution with no evidence of ligand exchange or contractions.

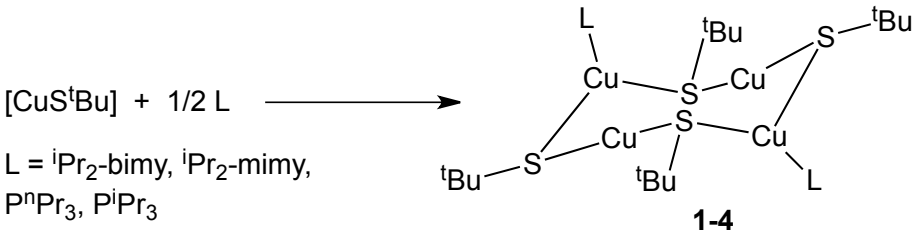

Scheme 2-1 Preparation of **1**-**4**

The silver-thiolate clusters [Ag$_4$(S^{t}Bu)$_4$(^{i}Pr$_2$-bimy)$_2$] **5**, [Ag$_5$(S^{t}Bu)$_6$][Ag(^{i}Pr$_2$-mimy)$_2$] **6**, [Ag$_4$(S^{t}Bu)$_4$(P^{n}Pr$_3$)$_2$] **7** and [Ag$_6$(S^{t}Bu)$_6$(P^{i}Pr$_3$)$_2$] **8** were similarly prepared by reacting the [AgS^{t}Bu] polymer with the corresponding carbene or phosphine ligands in a 1:2 ratio (Scheme 2-2). The syntheses were done at room temperature and in subdued light. Isolated crystalline yields for the silver thiolate clusters were generally higher than those for copper thiolate clusters when using the same ancillary ligand. Complexes **5** and **7** show the same 8-membered ring structure as for the copper clusters but for **6** and **8** different structures were obtained (*vide infra*). NMR data for solutions of these clusters confirm the ratio of ^{t}Bu groups to the ancillary ligands via integration of the phosphine/NHC ligands versus the methyl resonance of the S^{t}Bu groups, which appear as a singlet at ~1.5 ppm. The observed S^{t}Bu to ligand ratio for **5** and **7** is 2:1 and for **6** and **8** it is 3:1.

The formation of these clusters clearly demonstrates that N-heterocyclic carbenes can be

effectively used to enhance the solubility of insoluble [AgS^{t}Bu] and [CuS^{t}Bu] polymers. One advantage of using NHCs as stabilizing ligands is that the formed clusters are more stable than similar complexes prepared using phosphine ligands.

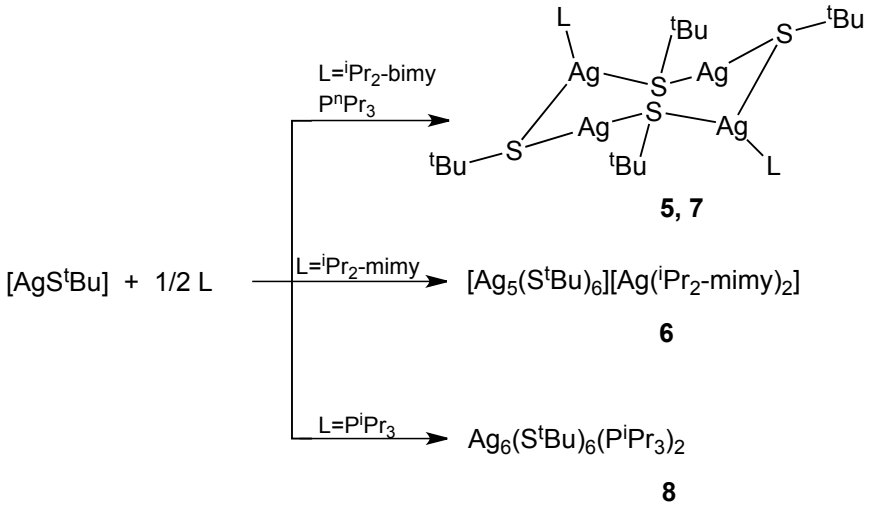

Scheme 2-2 Preparation of **5**-**8**

Table 2-1 Crystallographic data for **1**–**4**

	1·$(CH_2Cl_2)_2$	**2**·$(CH_2Cl_2)_2$	**3**	**4**
Formula	$C_{44}H_{76}Cl_4Cu_4N_4S_4$	$C_{40}H_{80}Cl_4Cu_4N_4S_4$	$C_{34}H_{78}Cu_4P_2S_4$	$C_{34}H_{78}Cu_4P_2S_4$
Formula Weight	1185.28	1141.28	931.30	931.30
Crystal System	Monoclinic	Monoclinic	Triclinic	Monoclinic
Space Group	$P2_1/c$	$P2_1/c$	$P\bar{1}$	$P2_1/c$
Temperature, K	110(2)	110(2)	150(2)	110(2)
a, Å	10.315(2)	10.363(2)	9.468(3)	10.2300(14)
b, Å	24.927(7)	23.568(6)	10.869(4)	13.023(2)
c, Å	11.256(2)	11.579(3)	12.157(5)	18.533(3)
α,°	90.00	90.00	68.774(14)	90.00
β,°	104.654(10)	106.670(4)	78.351(10)	114.317(4)
γ,°	90.00	90.00	82.542(12)	90.00
V, Å^3	2800.0(12)	2709.0(12)	1139.9(7)	2250.0(6)
Z	2	2	1	2
F(000)	1232	1192	492	984
ρ (g/cm^3)	1.406	1.399	1.357	1.375
μ (mm^{-1})	1.871	1.930	2.115	2.143
Reflections measured	118869	126773	25671	19802
Unique reflections	15872	10352	8769	19802
R_1 ($I > 2s(I)$)	0.0315	0.0288	0.0368	0.0298
wR_2 ($I > 2s(I)$)	0.0680	0.0702	0.0735	0.0592

Complexes **1**–**8** were isolated as single crystals and their molecular structures in the solid state were determined using single crystal X-ray diffraction. A summary of the crystallographic data is provided in Table 2-1 and Table 2-2. In the solid state these clusters are

stable at room temperature and could be exposed to air without any noticeable discoloration or decomposition. With a constant ratio of [MS^{t}Bu] to ligand of 2:1, the structure of the formed cluster depends on the steric demands of the ligand as well as the size of the metal centers. The selected NHC and phosphine ligands in this study form a similar Cu_4S_4 structure (**1**–**4**) upon reaction with [CuS^{t}Bu]; the metal centers accommodate this geometry with the ligands even though the latter have different steric requirements (Table 2-3). $\%V_{bur}$ values shown in Table 2-3 are determined from the crystal structures of the (NHC)AuCl complexes and, in the case of trialklyphosphines, a calculated R_3P–M model based on the crystal structure of the phosphines (P^nPr_3 and P^iPr_3).[41] For the silver-thiolate clusters three different structures are observed. ^{i}Pr$_2$-bimy and P^nPr_3 have smaller $\%V_{bur}$ values and coordinate silver atoms in a manner to form an Ag_4S_4 cluster core structure (**5** and **7**) while ^{i}Pr$_2$-mimy and P^iPr_3, with larger $\%V_{bur}$ values, force the complexes to adopt more complicated structures (**6** and **8**).

Table 2-2 Crystallographic data for **5**–**8**

	5·(C_7H_8)	**6**·(C_4H_8O)$_{0.34}$	**7**	**8**
Formula	$C_{98}H_{160}Ag_8N_8S_8$	$C_{47.38}H_{96.75}Ag_6N_4O_{0.34}S_6$	$C_{34}H_{78}Ag_4P_2S_4$	$C_{42}H_{96}Ag_6P_2S_6$
Formula Weight	2569.77	1567.61	1108.62	1502.70
Crystal System	Triclinic	Monoclinic	Triclinic	Orthorhombic
Space Group	$P\bar{1}$	$C2$	$P\bar{1}$	*Pnna*
Temperature, K	110(2)	150(2)	110(2)	110(2)
a, Å	9.990(3)	29.293(11)	9.538(4)	24.641(9)
b, Å	12.648(4)	12.976(5)	10.919(3)	15.066(5)
c, Å	23.429(9)	19.198(8)	12.288(4)	16.081(5)
α,°	78.597(13)	90	69.848(19)	90
β,°	78.069(9)	98.423(7)	78.879(13)	90
γ,°	80.553(12)	90	83.194(9)	90
V, Å^3	2815.7(17)	7219(5)	1177.0(7)	5970(4)
Z	1	4	1	4
F(000)	1308	3159	564	3024
ρ (g/cm^3)	1.516	1.442	1.564	1.672
μ (mm^{-1})	1.553	1.798	1.905	2.219
Reflections measured	52327	101010	26384	83082
Unique reflections	13901	18753	8855	5693
R_1 ($I > 2s(I)$)	0.0455	0.0522	0.0191	0.0398
wR_2 ($I > 2s(I)$)	0.1038	0.1461	0.0374	0.0834

The clusters exhibit similarities in the atom connectivity and local geometry, although compounds **6** and **8** have different structures compared to the 8-membered rings for the other complexes. Clusters **1**–**5** and **7** have a cyclic, molecular structure that consists of a M_4S_4 ring (M = Ag, Cu). This cyclic structure has been observed for different copper

thiolates.[7, 51] Due to the presence of two linear –SMS– segments, the overall structure simulates that of a six-membered ring; in **1**–**5** and **7**, this manifests itself in the rings displaying a chair conformation. Unlike some of the previously reported ring clusters formed from [CuS^{t}Bu], all of these compounds show a symmetric structure. According to how Dance describes this class of molecule,[14] in the M_4S_4 ring, there are two types of metal atoms that are linked together with sulfur atoms, linear digonal metal centers (M1) and trigonal metal atoms (M2) with one ligand (L = NHC or phosphine) attached to them (Figure 2-1). Since the structure of the ring can be described similarly to that of a chair conformation for a six-membered ring, there are corresponding axial and equatorial positions for the groups attached. In the present clusters, the NHC and phosphine ligands attached to the metal centers adopt axial positions, located above and below the cluster plane. In the structures of **3**, **4** and **7**, two S^{t}Bu groups are also axial while the other two S^{t}Bu groups have equatorial positions (the molecular structure of **7** is illustrated as an example in Figure 2-1), which is the common orientation in previously reported clusters in this class of compounds.[14] In contrast, for complexes **1**, **2** and **5** all four S^{t}Bu groups occupy equatorial positions; the molecular structure of **2** is shown in Figure 2-2.

Table 2-3 $\%V_{bur}$ for selected NHCs and phosphines[41]

	$\%V_{bur}$ for M–P length at		
Ligand	2.00 Å	2.28 Å	Reference
^{i}Pr$_2$-bimy	27.9	23.9	48
^{i}Pr$_2$-mimy	38.4	33.9	49
P^{n}Pr$_3$	30.6	26.0	50
P^{i}Pr$_3$	37.6	32.3	50

For all of the clusters, all metal atoms are positioned in a single plane. The coordination around the sulfur atoms is pyramidal and each S atom is bridging between two metal centers. The M2–S (Figure 2-1) bond lengths in **1**–**4** range from 2.2951(10)–2.3093(4) Å and 2.4463(7)–2.5361(16) Å for the larger metals in **5** and **7**; there is no clear trend as a function of the nature of L. Selected bond lengths and angles for compounds **2** and **7** are listed in Table 2-4. Independent of the size and geometry of the supporting ligand used, all of the synthesized copper thiolate clusters exhibit the Cu_4S_4 framework in their solid-state structure. An eight membered ring with this chair conformation has shown to be one of the favorable structures for supported complexes with formula of $M_4(SR)_4L_2$ although a related, twisted boat conformation has been described using computational calculations.[52]

Krautscheid and co-workers have reported that structures of copper-phenylthiolato clusters can be influenced when extremely large or small phosphine ligands are employed, or when excess ligand is added.[53]

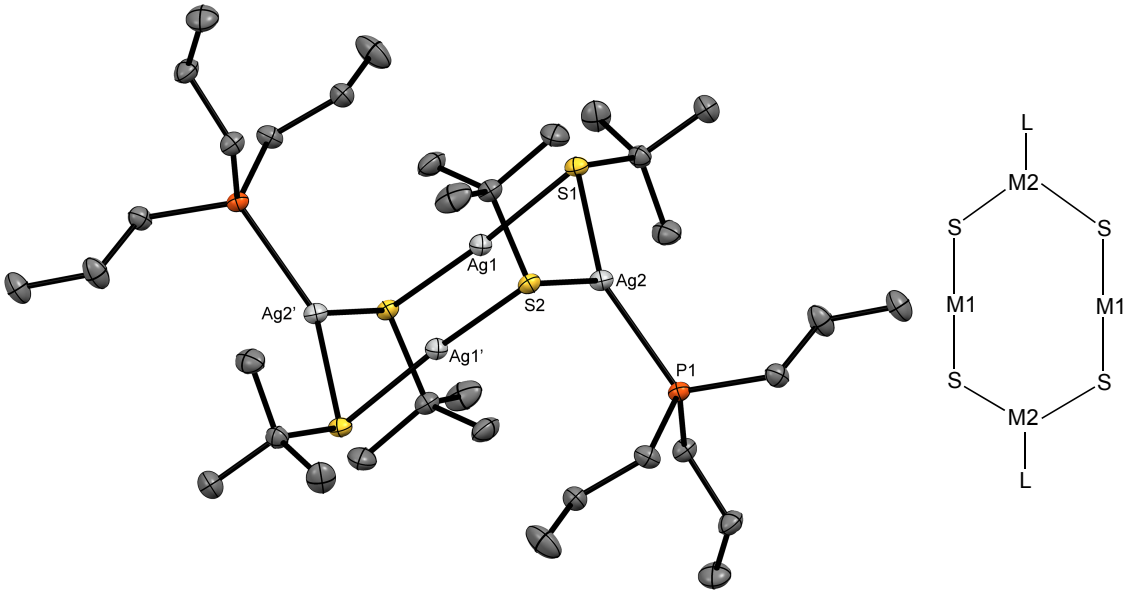

Figure 2-1 Left: The molecular structure of **7** in the solid state. Hydrogen atoms are omitted for clarity. Thermal ellipsoids are drawn at the 50% probability level. Right: M_4S_4 ring.

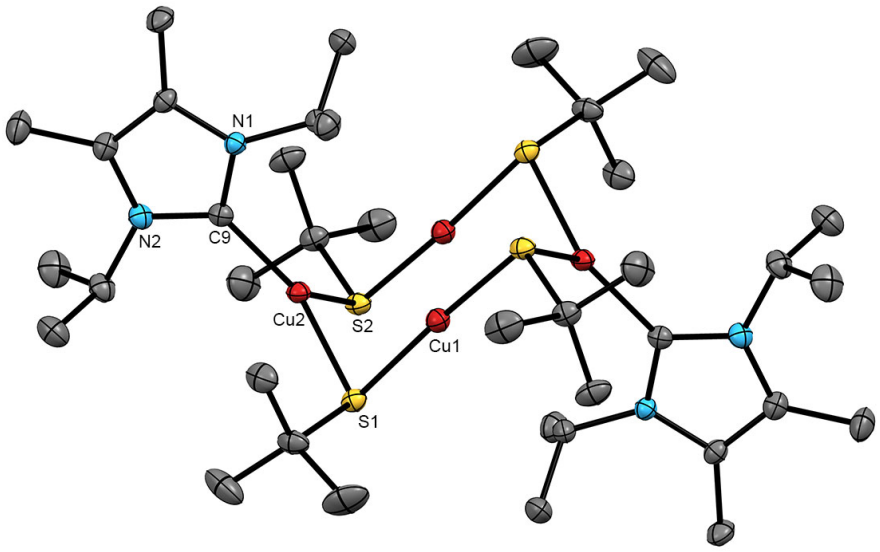

Figure 2-2 The molecular structure of **2** in the solid state. Hydrogen atoms are omitted for clarity. Thermal ellipsoids are drawn at the 50% probability level.

Table 2-4 Selected bond lengths (Å) and angles (°) for **2** and **7**

Compound **2**		Compound **7**	
Cu1–S1	2.1539(5)	Ag1–S2[2]	2.3512(8)
Cu1–S2[1]	2.1587(5)	Ag1–S1	2.3710(8)
Cu1–Cu2[1]	2.8131(7)	Ag1–Ag2	3.1235(10)
Cu1–Cu2	3.0447(5)	Ag1–Ag2[2]	3.3204(10)
Cu2–C9	1.9410(13)	Ag2–P1	2.4172(7)
Cu2–S1	2.2655(6)	Ag2–S1	2.4463(7)
Cu2–S2	2.2973(6)	Ag2–S2	2.5383(8)
N1–C9	1.3577(16)	Ag2–Ag1[2]	3.3204(10)
N2–C9	1.3581(17)	S1–C1	1.8563(14)
S1–Cu1–S2[1]	174.313(14)	S2–C5	1.8540(14)
S1–Cu1–Cu2[1]	130.136(16)	S2–Ag1[2]	2.3512(8)
S2[1]–Cu1–Cu2[1]	53.078(15)	S2[2]–Ag1–S1	169.999(12)
S1–Cu1–Cu2	47.996(16)	S2[2]–Ag1–Ag2	137.924(15)
S2[1]–Cu1–Cu2	136.928(16)	S1–Ag1–Ag2	50.639(15)
Cu2[1]–Cu1–Cu2	113.164(13)	S2[2]–Ag1–Ag2[2]	49.645(17)
C9–Cu2–S1	133.05(4)	S1–Ag1–Ag2[2]	137.845(14)
C9–Cu2–S2	129.03(4)	Ag2–Ag1–Ag2[2]	108.93(2)
S1–Cu2–S2	97.853(13)	P1–Ag2–S1	142.611(18)
C9–Cu2–Cu1[1]	116.62(4)	P1–Ag2–S2	104.08(2)
S1–Cu2–Cu1[1]	94.828(12)	S1–Ag2–S2	113.07(2)
S2–Cu2–Cu1[1]	48.696(13)	P1–Ag2–Ag1	125.34(2)
C9–Cu2–Cu1	115.42(4)	S1–Ag2–Ag1	48.54(2)
S2–Cu2–Cu1	101.81(2)	S2–Ag2–Ag1	105.26(2)
Cu1[1]–Cu2–Cu1	66.834(13)	P1–Ag2–Ag1[2]	101.29(3)
C1–S1–Cu1	106.35(5)	S1–Ag2–Ag1[2]	107.72(2)
C1–S1–Cu2	113.48(5)	S2–Ag2–Ag1[2]	44.900(18)
Cu1–S1–Cu2	87.054(15)	Ag1–Ag2–Ag1[2]	71.07(2)

1. 2–x, –y, –z 2. 1–x, 1–y, 2–z

Unlike the copper thiolate clusters, the structures of the silver thiolate complexes reported herein are influenced by the sizes of the supporting ligand used, even with a fixed metal:ligand reaction ratio. Cluster **6** consists of a $[Ag_5(S^tBu)_6]^-$ anion and a $[Ag(^iPr_2\text{-mimy})_2]^+$ cation and shows no Ag–S contact distances between the ion pairs that are shorter than the sum of the respective van der Waals radii. In the asymmetric unit of this cluster, one $[Ag_5(S^tBu)_6]^-$ is sitting on a general position while two independent $[Ag(^iPr_2\text{-mimy})_2]^+$ cations sit on special positions (2-fold rotation axes). In the cation, the geometry around the silver atom is slightly bent with a mean C–Ag–C angle of 178.3(7)°. Such a $[M_5(S^tBu)_6]^-$ fragment has been observed previously using PMe_3 as a stabilizing ligand for the complex cation $[Cu(PMe_3)_4][Cu_5(S^tBu)_6]$[9] as well as for $[NEt_3R]^+[M_5(S^tBu)_6]^-$, R = Et when M = Ag and R = H, Et when M = Cu.[54, 55] In this work, the anionic motif has been formed for silver with $^iPr_2$-mimy carbene as the stabilizing ligand for the cation complex. The structure of the core can be described as an expansion of the Ag_4S_4 rings in

5 and **7**. The 8-membered ring is folded about an Ag–Ag diagonal and another S–Ag–S group is added, which formed another Ag_4S_4 cycle.[14] The silver atoms in the core create an Ag_5 trigonal bipyramid in which each apical-equatorial edge is bridged by a S^{t}Bu with no bridging ligand along the equatorial-equatorial edges. Hence the equatorial Ag atoms are two-coordinate (mean S–Ag–S angle: 173.59(11)°) and the two apical Ag atoms are symmetrically bonded to three S^{t}Bu, with near planar coordination geometry (mean sum of the angles: 359.25(10)°). The sulfur centers define a trigonal prismatic S_6 cage that shows almost perfectly eclipsed triangular bases. Of the previously reported anions from this class only $[Cu(PMe_3)_4][Cu_5(S^tBu)_6]$ shows an almost perfect prismatic S_6 cage[9] whereas the others exhibit large antiprismatic twists.[54-56] The orientation of the silver and sulfur atoms in the core and the *tert*-butyl on the S centers gives an overall D_3 symmetry to the anion in **6**.

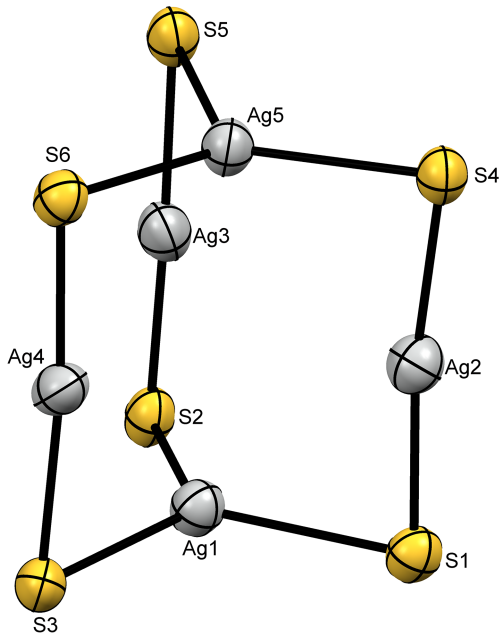

Figure 2-3 The molecular structure of the anion $[Ag_5(S^tBu)_6]^-$ in the solid state structure of **6**. Hydrogen and carbon atoms are omitted for clarity. Thermal ellipsoids are drawn at the 50% probability level.

The structure of the higher nuclearity cluster **8** is a new motif in this system. Although different from the others reported here, it expands upon some of the features present in the smaller ring systems (Figure 2-4). In the core of this cluster, an 8-membered ring of

silver and sulfur atoms (Ag_4S_4) is capped with a 4-membered ring (Ag_2S_2). Unlike the Ag_4S_4 rings in **5** and **7**, the 8-membered ring does not show a chair conformation in **8**; Instead a butterfly conformation is observed where the Ag_2S_2 fragment acts as two ligands for Ag1 and Ag1', and force the lower ring to bend to a butterfly conformation. The Ag_2S_2 also demonstrates a butterfly conformation. Two of the silver atoms in the 8-member ring (Ag2 and Ag2') are two-coordinated with sulfur atoms while the other two silver centers (Ag1 and Ag1') are three-coordinated (longer distances with S3 and S3'). Both of the silver atoms in the Ag_2S_2 ring are three-coordinated with two S^{t}Bu and one P^{i}Pr$_3$ groups. The mean Ag–S bond length for the Ag_4S_4 ring is 2.4047(18) Å while it is 2.5534(16) Å for the Ag_2S_2 ring. The shortest Ag–S distance between the atoms of these two rings is 2.8183(17) Å, which is the distance between Ag1 and S3 and its symmetry equivalent. In a different way, the core of this cluster is made of two 8-membered rings that share four of their atoms. The first ring consists of S3, Ag1, S1, Ag2', S2A', Ag1', S3' and Ag3' while the second one is formed by S3, Ag1, S2A, Ag2, S1', Ag1', S3' and Ag3. Both of these rings show a distorted boat conformation and each has a P^{i}Pr$_3$ group coordinating one of the silver centers.

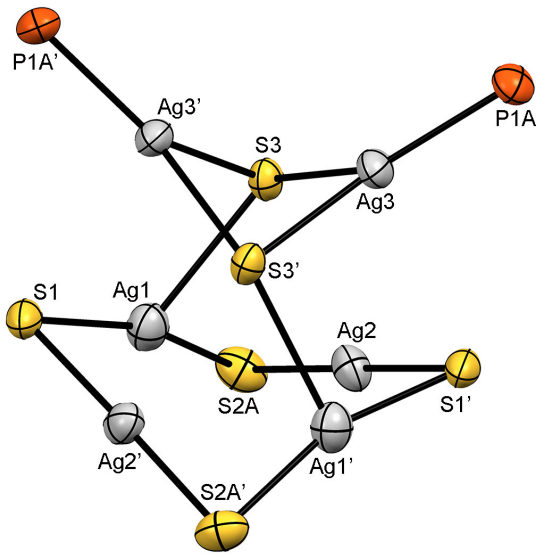

Figure 2-4 The molecular structure of **8** in the solid state. Hydrogen and carbon atoms are omitted for clarity. The center of the molecule is sitting on a 2-fold rotation axis. Thermal ellipsoids are drawn at the 50% probability level.

2.4 Conclusions

It was shown in this work that N-heterocylic carbenes can act as solubilising and stabilising reagents for [AgS^{t}Bu] and [CuS^{t}Bu] to form polynuclear copper and silver t-butylthiolate clusters, and can be considered as excellent alternatives for PR_3 in this area of chemistry. The clusters that are formed using NHCs are more stable under ambient lighting conditions compared to those that have PR_3 as a stabilizing ligand. The cluster frameworks are structurally related to those observed for copper and silver t-butylthiolate clusters stabilized with PR_3[8, 9, 14] and are affected by the nature of the ligand that is used. These clusters may be suitable molecular precursors in the synthesis of larger nanoclusters, nanoparticles and thin films. We are pursuing these possibilities actively.

2.5 References

1. V. W.-W. Yam, C. Lam, W. Fung and K. Cheung, *Inorg. Chem.,* 2001, **40**, 3435-3442.
2. R. Langer, M. Yadav, B. Weinert, D. Fenske and O. Fuhr, *Eur. J. Inorg. Chem.,* 2013, **2013**, 3623-3631.
3. E. Solomon, D. Randall and T. Glaser, *Coord. Chem. Rev.,* 2000, **200**, 595-632.
4. G. Henkel and B. Krebs, *Chem. Rev.,* 2004, **104**, 801-824.
5. J. T. Rubino and K. J. Franz, *J. Inorg. Biochem.,* 2012, **107**, 129-143.
6. S. A. Delp, C. Munro-Leighton, L. A. Goj, M. A. Ramirez, T. B. Gunnoe, J. L. Petersen and P. D. Boyle, *Inorg. Chem.,* 2007, **46**, 2365-2367.
7. M. D. Janssen, D. M. Grove and G. VanKoten, *Prog. Inorg. Chem.,* 1997, **46**, 97-149.
8. S. Schneider, Y. Yang and T. Marks, *Chem. Mater.,* 2005, **17**, 4286-4288.
9. S. Schneider, A. Dzudza, G. Raudaschl-Sieber and T. J. Marks, *Chem. Mater.,* 2007, **19**, 2768-2779.
10. C. Che, C. Li, S. S. Chui, V. A. L. Roy and K. Low, *Chem. Eur. J.,* 2008, **14**, 2965-2975.
11. D. Fenske, C. E. Anson, A. Eichhöfer, O. Fuhr, A. Ingendoh, C. Persau and C. Richert, *Angew. Chem. Int. Ed.,* 2005, **44**, 5242-5246.
12. C. E. Anson, A. Eichhöfer, I. Issac, D. Fenske, O. Fuhr, P. Sevillano, C. Persau,

D. Stalke and J. Zhang, *Angew. Chem. Int. Ed.,* 2008, **47**, 1326-1331.

13. (a) Z. Li, X. Li, P. Lin and S. Du, *J. Cluster Sci.,* 2008, **19**, 357-366; (b) K. Kim, Y. M. Lee, H. B. Lee and K. S. Shin, *Biosens. Bioelectron.,* 2009, **24**, 3615–3621.
14. I. Dance, L. Fitzpatrick, D. Craig and M. Scudder, *Inorg. Chem.,* 1989, **28**, 1853-1861.
15. I. Dance, *Polyhedron,* 1988, **7**, 2205-2207.
16. M. Baumgartner, H. Schmalle and C. Baerlocher, *J. Solid State Chem.,* 1993, **107**, 63-75.
17. G. Schrauzer and H. Prakash, *Inorg. Chem.,* 1975, **14**, 1200-1204.
18. P. Espinet, M. Lequerica and J. Martin-Alvarez, *Chem. Eur. J.,* 1999, **5**, 1982-1986.
19. N. Sandhyarani and T. Pradeep, *J. Mater. Chem.,* 2001, **11**, 1294-1299.
20. W. A. Herrmann, J. Schutz, G. D. Frey and E. Herdtweck, *Organometallics,* 2006, **25**, 2437-2448.
21. F. E. Hahn and M. C. Jahnke, *Angew. Chem. Int. Ed.,* 2008, **47**, 3122-3172.
22. H. Jacobsen, A. Correa, A. Poater, C. Costabile and L. Cavallo, *Coord. Chem. Rev.,* 2009, **253**, 687-703.
23. L. Benhamou, E. Chardon, G. Lavigne, S. Bellemin-Laponnaz and V. Cesar, *Chem. Rev.,* 2011, **111**, 2705-2733.
24. C. Crudden and D. Allen, *Coord. Chem. Rev.,* 2004, **248**, 2247-2273.
25. M. Poyatos, J. A. Mata and E. Peris, *Chem. Rev.,* 2009, **109**, 3677-3707.
26. G. Frenking, M. Sola and S. Vyboishchikov, *J. Organomet. Chem.,* 2005, **690**, 6178-6204.
27. J. C. Y. Lin, R. T. W. Huang, C. S. Lee, A. Bhattacharyya, W. S. Hwang and I. J. B. Lin, *Chem. Rev.,* 2009, **109**, 3561-3598.
28. F. Cisnetti, P. Lemoine, M. El-Ghozzi, D. Avignant and A. Gautier, *Tetrahedron Lett.,* 2010, **51**, 5226-5229.
29. D. V. Partyka and N. Deligonul, *Inorg. Chem.,* 2009, **48**, 9463-9475.
30. J. D. Egbert, C. S. J. Cazin and S. P. Nolan, *Catal. Sci. Tech.,* 2013, **3**, 912-926.
31. I. J. B. Lin and C. S. Vasam, *Coord. Chem. Rev.,* 2007, **251**, 642-670.
32. A. Kascatan-Nebioglu, M. J. Panzner, C. A. Tessier, C. L. Cannon and W. J.

Youngs, *Coord. Chem. Rev.,* 2007, **251**, 884-895.

33. I. Lin and C. Vasam, *Comments Inorg. Chem.,* 2004, **25**, 75-129.
34. S. Diez-Gonzalez and S. P. Nolan, *Aldrichimica Acta,* 2008, **41**, 43-51.
35. S. Diez-Gonzalez and S. P. Nolan, *Synlett,* 2007, 2158-2167.
36. J. Garrison and W. Youngs, *Chem. Rev.,* 2005, **105**, 3978-4008.
37. O. Kühl, *Functionalised N-Heterocyclic Carbene Complexes*, Wiley, Chichester, U.K., 2010.
38. W. J. Humenny, S. Mitzinger, C. B. Khadka, B. Khalili Najafabadi, I. Vieira and J. F. Corrigan, *Dalton Trans.,* 2012, **41**, 4413-4422.
39. A. Hillier, W. Sommer, B. Yong, J. Petersen, L. Cavallo and S. Nolan, *Organometallics,* 2003, **22**, 4322-4326.
40. A. Poater, B. Cosenza, A. Correa, S. Giudice, F. Ragone, V. Scarano and L. Cavallo, *Eur. J. Inorg. Chem.,* 2009, 1759-1766.
41. H. Clavier and S. P. Nolan, *Chem. Commun.,* 2010, **46**, 841-861.
42. B. Teo, Y. Xu, B. Zhong, Y. He, H. Chen, W. Qian, Y. Deng and Y. Zou, *Inorg. Chem.,* 2001, **40**, 6794-6801.
43. N. Kuhn and T. Kratz, *Synthesis-Stuttgart,* 1993, 561-562.
44. O. Starikova, G. Dolgushin, L. Larina, T. Komarova and V. Lopyrev, *Arkivoc,* 2003, 119-124.
45. Y. Han, H. V. Huynh and L. L. Koh, *J. Organomet. Chem.,* 2007, **692**, 3606-3613.
46. G. M. Sheldrick, *Acta Crystallogr. Sect. A,* 2008, **64**, 112-122.
47. T. Droege and F. Glorius, *Angew. Chem. Int. Ed.,* 2010, **49**, 6940-6952.
48. R. Jothibasu, H. V. Huynh and L. L. Koh, *J. Organomet. Chem.,* 2008, **693**, 374-380.
49. P. De Fremont, N. Scott, E. Stevens and S. Nolan, *Organometallics,* 2005, **24**, 2411-2418.
50. J. Bruckmann and C. Kruger, *Acta Crystallogr. Sect. C-Cryst. Struct. Commun.,* 1996, **52**, 1733-1736.
51. S. Groysman and R. H. Holm, *Inorg. Chem.,* 2009, **48**, 621-627.
52. J. A. S. Howell, *Polyhedron* 2006, **25**, 2993-3005.

53. O. Kluge, K. Grummt, R. Biedermann, H. Krautscheid, *Inorg. Chem.* 2011, **50**, 4742–4752.
54. I. Dance, *Chem. Commun.,* 1976, , 68-69.
55. G. Bowmaker, G. Clark, J. Seadon and I. Dance, *Polyhedron,* 1984, **3**, 535-544.
56. K. Fujisawa, S. Imai, N. Kitajima and Y. Moro-oka, *Inorg. Chem.,* 1998, **37**, 168-169.

Chapter 3

Enhanced Thermal Stability of Cu-Silylphosphido Complexes via NHC Ligation[‡]

3.1 Introduction

d-Block metal complexes containing $-P(SiMe_3)_2$ moieties have been shown to be useful precursors in solution-based routes to metal phosphide solid materials.[1] For example, Buhro and coworkers have reported the synthesis of Cd_3P_2 by alcoholysis and polycondensation of the molecular precursor $[Cd\{P(SiMe_3)_2\}_2]_2$,[2,3] such reactions proceeding by cleavage of the Si–P bonds and elimination of $SiMe_3$ groups.[4] Furthermore, such metal-phosphido complexes ($M-P(SiMe_3)_2$) have been used successfully for the synthesis of ternary metal-phosphide semiconductors in both crystalline and glassy form, taking advantage of the preformed metal-phosphorous bond, and the reactivity of the two remaining $P-SiMe_3$ towards a second metal salt.[5] Such metal-phosphido molecular precursors result in the formation of pure semiconductor solids; these materials attract interest due to the magnetic and electronic properties shown in the bulk, and the potential of unique, size-tunable properties in related nanoscale materials.[6] Transition-metal phosphides show high catalytic reactivity for hydroprocessing[7] and their magnetic properties can vary from

[‡] **B. Khalili Najafabadi**, J. F. Corrigan, *Dalton Trans*., **2015**, 44, 14235-14241. Reproduced by permission of The Royal Society of Chemistry.

antiferromagnetic to paramagnetic, leading to great interest in materials science and chemistry.[6] The electronic conductivity of metal phosphides vary from displaying metallic properties to semiconductor behavior with a corresponding band gap energy.[8]

It has been shown that metal chalcogenolates (M–E$SiMe_3$ E = S, Se, Te) can be used as precursors to prepare ternary metal-chalcogenide clusters.[9] In this vein, metal-P$(SiMe_3)_2$ complexes are promising candidates as precursors for the preparation of ternary metal-phosphide clusters using solution-phase methods and access to different "bottleable" reagents is desirable. In this report, the synthesis and characterization of homoleptic copper- and silver-bis(trimethylsilyl)phosphido compounds are described together with the more thermally stable mononuclear copper-phosphido complexes with differing N-heterocyclic carbene (NHC) ligands. It was found that the use of NHC ligands helps to stabilize copper-phosphido complexes when compared to their homoleptic counterparts.

3.2 Experimental

All syntheses were performed under an argon or N_2 atmosphere using standard Schlenk line and glovebox techniques unless otherwise stated. Chemicals were used as received from Strem Chemicals and/or Aldrich. Tetrahydrofuran, diethyl ether, hexanes, and pentane were purchased from Caledon and dried by passing through packed columns of activated alumina using a commercially available MBraun MB-SP Series solvent purification system. Dichloromethane (DCM) was purchased from Caledon and/or Aldrich and distilled over P_2O_5. Benzene-d_6 was dried and distilled over Na/K alloy. P$(SiMe_3)_3$,[10] [Ag-S^{t}Bu]$_n$[11] and [CuS^{t}Bu]$_n$[12] were prepared following literature procedures. 1,3-Di-isopropylbenzimidazole-2-ylidene (^{i}Pr$_2$-bimy)[13] was prepared from 1,3-di-isopropylbenzimidazoliumiodide.[14] [(IPr)CuOAc] (IPr = 1,3-bis(2,6-diisopropylphenyl)imidazol-2-ylidene) was prepared according to published methods.[15]

^{1}H and ^{13}C{^{1}H} NMR spectra were obtained on a Varian Inova 400 MHz spectrometer and are reported in ppm. These spectra were referenced internally to solvent peaks relative to $SiMe_4$ (δ = 0 ppm). ^{31}P{^{1}H} NMR spectra were recorded on the same spectrometer and are referenced to 85% H_3PO_4 (δ = 0 ppm). Although the complexes are temperature sensitive in solution, all of the NMR spectra were collected at room temperature due to the limited solubility of the complexes in common deuterated solvents.

Single crystal X-ray diffraction measurements were performed on Bruker APEXII and Nonius KappaCCD diffractometers, with the molecular structures determined via direct methods using the SHELX suite of crystallographic programs.[16] X-ray diffraction data resulting from a twinned crystal of **11** were analyzed with CELL_NOW to assign the reflections to different domains. The data were integrated using two major domains with a twin law of (0.999 -0.003 0.001, -0.511 -1.000 -0.001, -0.001 0.001 -1.000); the rest were discarded since they did not fit well into any specific cell. This resulted in an incomplete data set and larger thermal parameters for lighter atoms. Data were scaled and corrected for absorption using TWINABS. This structure was solved using the hklf4 file (reflections from the major domain) and refined with hklf5 file (reflections from both domains) with a BASF of 0.45932. Complex **12** crystallized in the form of very thin plates that diffracted poorly and were not suitable for X-ray diffraction analysis. After several attempts we were able to crystallize thicker plates of **12** but the poor quality of the crystals (reflections) suggested multiple contact twins and resulted in large thermal parameters for some atoms as well as a high weighted R factor of 0.263. Powder X-ray diffraction measurements were made on a Nonius KappaCCD diffractometer updated with a Bruker Apex2 detector at a temperature of 110 K and CuKα radiation. Crystals were crushed in a minimum amount of Paratone oil and mounted on a Mitegen polyimide micromount. The data collection strategy was a number of 360° φ scans which collected data over $-10° < 2\theta < 90°$ resulting images with the detector at the maximum distance of 165 mm. The frame integration was performed using XRD^2 Eval from the APEXII package.

3.2.1 $[Cu_6\{P(SiMe_3)_2\}_6]$ (9)[17]

In subdued light, $[CuS^tBu]_n$ (0.10 g, 0.65 mmol) was suspended in ~12 ml of DCM. $P(SiMe_3)_3$ (0.19 ml, 0.65 mmol) was added to this colourless suspension. The suspension turned to a golden orange, clear solution after a few minutes. 10 ml of pentane was added to the solution, mixed and kept at –25 °C. Colourless crystals formed after 1 week. Yield (isolated crystals): 0.10 g (48%). Crystals of isolated samples discolour significantly, even under inert atmosphere, at low temperatures in the absence of light. Sample homogeneity was confirmed via PXRD (See Results and Discussion).

^1H NMR (400 MHz, C_6D_6, 23 °C) δ = 0.50 (br). $^{31}P\{^1H\}$ NMR (C_6D_6, 23 °C) δ = –149.

3.2.2 $[Ag_6\{P(SiMe_3)_2\}_6]$ (10)

$[AgS^tBu]_n$ (0.10 g, 0.51 mmol) was suspended in 20 ml of THF. To this suspension, $P(SiMe_3)_3$ (0.15 ml, 0.51 mmol) was added at r.t. After ~10 min of stirring the solution started to change colour, yellow first and then orange. After the solid dissolved to yield a clear orange solution, it was cooled to –25 °C for crystallization. Colourless, cubic crystals formed after 1 day. Similar results were obtained using DCM as a solvent. Yield (isolated crystals): 0.12 g (66%). Crystals of isolated samples discolour significantly, even under inert atmosphere, at low temperatures in the absence of light. Sample homogeneity was confirmed via PXRD (See Results and Discussion).

^{1}H NMR (400 MHz, C_6D_6, 23 °C) δ = 0.48 (br). $^{31}P\{^1H\}$ NMR (C_6D_6, 23 °C) δ = –236.

3.2.3 $[(^iPr_2\text{-bimy})_2CuP(SiMe_3)_2]$ (11)

Copper(I) acetate (0.50 g, 4.02 mmol) was suspended in 10 ml of THF and cooled to 0 °C. Freshly prepared $^iPr_2$-bimy (1.36 g, 8.05 mmol) in THF was added to the solution at 0 °C. The reaction was stirred until it reached room temperature and was filtered to remove turbidity and obtain a clear light orange solution. This solution was cooled to –40 °C and $P(SiMe_3)_3$ (1.17 ml, 4.02 mmol) was added: after a few minutes, a pale yellow solid formed. The reaction mixture was stirred in the bath until the temperature gradually reached 0 °C. It was stirred at 0 °C for 30 min and the solid was isolated via filtration and washed with pentane. The yellow, hair-like crystalline solid was dried *in vacuo* yielding 0.62 g (25%) of **11**. Crystals suitable for X-ray analysis of **11** were obtained by layering a dilute solution in THF with pentane at –25 °C.

^{1}H NMR (400 MHz, C_6D_6, 23 °C) δ = 7.16 (br m, 4 H) (overlapping with the solvent peak), 6.96 (m, 4 H), 5.50 (br, 4 H), 1.48 (d, *J*=7 Hz, 24 H), 0.52 (d, *J*=3 Hz, 18 H). $^{13}C\{^1H\}$ NMR (100.5 MHz, C_6D_6) δ = 215.4, 112.4, 52.9, 42.1, 7.4. $^{31}P\{^1H\}$ NMR (C_6D_6, 23 °C) δ = –261. m.p.: 72°C (dec.).

3.2.4 $[(IPr)CuP(SiMe_3)_2]$ (12)

[(IPr)CuOAc] (0.10 g, 0.20 mmol) was dissolved in 10 ml of toluene and cooled to –60 °C. $P(SiMe_3)_3$ (0.06 ml, 0.20 mmol) was added to this solution and stirred with gradual warming to –25 °C. The solvent was reduced to about half in volume at this temperature and ~15 ml pentane was added to precipitate the product as a white solid. The solvent was

decanted and the solid was dried *in vacuo* yielding 0.06 g of **12** (47%). Colourless plate crystals were formed from cooling a concentrated toluene solution of **12** at –25 °C over ~2 weeks.

^{1}H NMR (400 MHz, C_6D_6, 23 °C): δ = 7.25 (t, *J*=8 Hz, 2 H), 7.10 (d, *J*=8 Hz, 4 H), 6.28 (s, 2 H), 2.61 (m, 4 H), 1.45 (d, *J*=7 Hz, 12 H), 1.07 (d, *J*=7 Hz, 12 H), 0.28 (d, *J*=3 Hz, 18 H). ^{13}C{^{1}H} NMR (100.5 MHz, C_6D_6) δ = 186.6, 145.7, 135.2, 130.5, 124.3, 122.2, 29.0, 25.1, 24.0, 7.5 (d, *J*=11 Hz). ^{31}P{^{1}H} NMR (C_6D_6, 23 °C) δ = –268. m.p.: 85.5 °C (dec.).

3.3 Results and Discussion

Due to the potential reactivity and application of copper-phosphido complexes in organic and organometallic synthesis, a few homoleptic copper–PR_2 compounds have been prepared and structurally characterized.[18-20] In most of these complexes, the PR_2 groups act as a bridge between the copper centers and form cyclic structures such as $[CuP^tBu_2]_4$.[19] On the other hand, different homoleptic metal–$P(SiMe_3)_2$ complexes have been reported with both terminal and bridging $P(SiMe_3)_2$ (metal = Zn, Cd, Hg, Sn, Pb, Mn)[1, 2], among them $[Cu_6\{P(SiMe_3)_2\}_6]$ **9** by Buhro and co-workers.[17] Unfortunately we were unable to locate detailed preparation or characterization data for this complex. We were able to successfully synthesize and characterize $[Cu_6\{P(SiMe_3)_2\}_6]$ **9** and the isostructural $[Ag_6\{P(SiMe_3)_2\}_6]$ **10** from the straightforward reaction of polymeric $[CuS^tBu]_n$ and $[AgS^tBu]_n$ with $P(SiMe_3)_3$, respectively (Scheme 3-1). These metal thiolate complexes show an ideal, slow reactivity towards the addition of $P(SiMe_3)_3$ at ambient conditions with little competition for the formation of higher nuclearity complexes via activation of additional P–Si bonds. Reactions progress by the cleavage of S^tBu groups and formation of $^tBuSSiMe_3$ as a byproduct, while solubilizing the coordination polymers.

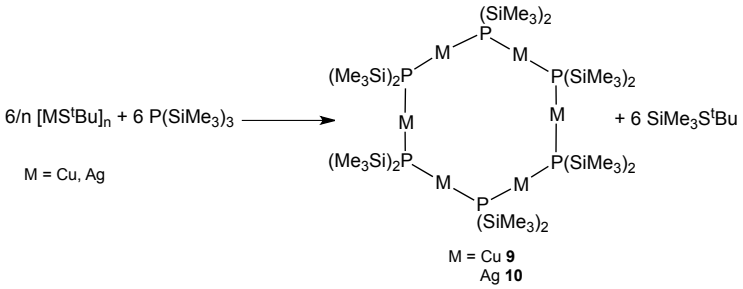

Scheme 3-1 Preparation of **9** and **10**

We have recently shown that $[CuS^tBu]_n$ and $[AgS^tBu]_n$ can be used to synthesize corresponding metal-thiolate ring complexes when ligated with carbene ligands.[21] It has also been reported that $[AgS^tBu]_n$ can be used as a source of Ag(I) in the reaction with $S(SiMe_3)_2$ and $Se(SiMe_3)_2$ to prepare large polynuclear silver-sulfide and selenide clusters under mild conditions.[22] The addition of $P(SiMe_3)_3$ to a suspension of $[CuS^tBu]_n$ or $[AgS^tBu]_n$ in THF (or DCM) at room temperature resulted in the formation of **9** and **10** as white solids. Single crystals of **9** and **10** were obtained from cooling the reaction mixtures to –25 °C. X-ray diffraction analysis of colourless crystals of **9** and **10** (space group $P\bar{1}$) indicated hexagonal molecules residing about an inversion center in the unit cell. The crystal structure of **10** is shown in Figure 3-1 and bond lengths and angles ranges are mentioned in the caption. In these isostructural molecules, the phosphorus atoms are positioned on the corners of the hexagon and the two-coordinate, near linear metal atoms reside on the edges. Each of the $P(SiMe_3)_2$ groups bridges two metal atoms symmetrically (P–Cu bond lengths of 2.2043(16)–2.2094(15) Å). The metal atoms exhibit a slightly bent geometry (P–Ag–P ~177° and P–Cu–P ~178°) in these structures and, together with the phosphorus atoms, form a planar M_6P_6 array. P–Cu–P angles are less distorted from linear (177.97(4)–178.29(4)°) in **9** compared to the smaller cyclic copper-phosphido complexes (*e.g.* 169° in $[Cu_4(P^tBu_2)_4]$[19]) due to the formation of the larger polygon (hexagon compared to square). As a consequence of the overall geometry the Cu–P–Cu angles are also larger in **9** (~118°) compared to those in $[Cu_4(P^tBu_2)_4]$ (~100.5°).[19] The atoms bonded to each phosphorus center form a distorted tetrahedral geometry in such a way that $SiMe_3$ groups are arranged above and below the plane defined by M_6P_6 of the molecule (Figure 3-1). Metal-metal distances are in the range of 3.779–3.810 Å and 4.084–4.134 Å in **9** and **10** respectively, which preclude metallophilic interactions in these structures.[23]

Table 3-1 Ranges of bond lengths (Å) and angles (°) for **9** and **10**

Compound	$[Cu_6\{P(SiMe_3)_2\}_6]$ (**9**)	$[Ag_6\{P(SiMe_3)_2\}_6]$ (**10**)
M–P	2.2043(16)–2.2094(15)	2.3930(14)–2.4107(15)
P–Si	2.2326(16)–2.2431(19)	2.2457(17)–2.253(2)
Si–C	1.814(8)–1.862(6)	1.843(6)–1.894(6)
P–M–P	177.97(4)–178.29(4)	177.28(4)–177.64(4)
M–P–M	117.79(4)–119.40(6)	117.04(6)–118.75(5)
Si–P–Si	106.60(7)–107.20(7)	108.73(7)–109.78(7)

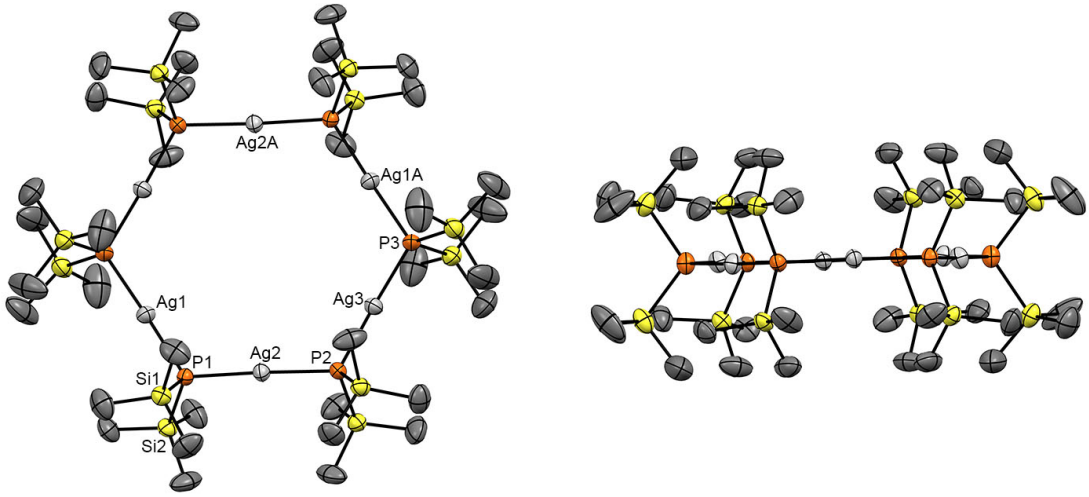

Figure 3-1 Molecular structure of $[Ag_6\{P(SiMe_3)_2\}_6]$ (**10**) (two different views). Ellipsoids are at the 50% probability level and hydrogen atoms were omitted for clarity. The molecule resides about a crystallographic inversion centre. Ag: silver, P: orange, Si: yellow, C: grey. Bond lengths (Å) and angles (°) ranges: 2.393(1)<Ag–P<2.411(2), 2.246(2)<P–Si<2.253(2), 177.28(4)<P–Ag–P<177.64(4), 117.04(6)<Ag–P–Ag<118.75(5), 108.73(7)<Si–P–Si<109.78(7).

In both of these structures the voids directly above and below the center of the hexagon (side length = 4.4 Å (for **9**) and 4.8 Å (for **10**)) are filled with (disordered) THF solvent molecules of crystallization. We believe that the presence of solvent is crucial for the formation of these structures and may explain their sensitivity to the loss of solvent, evidenced by discolouring and decomposition of **9** and **10** in the solid state even at low temperatures when removed from their mother liquor. In comparison, crystals of **9** and **10** are stable while they are kept under reaction solvent at low temperature, with no sign of decomposition or desolvation. Crystals of the Cu_6 and Ag_6 complexes both contain THF solvent molecules of crystallization that were satisfactorily modeled in the refinement of structures **9** and **10**.

Despite their marked sensitivity to air and lattice solvent loss resulting in decomposition of the molecular species (as evidenced by a rapid darkening of the solids from colourless to black) sample homogeneity of **9** and **10** can be confirmed via powder X-ray diffraction data. Data collection at low temperature of crystals that were partially crushed and ground into a minimum amount of Paratone oil to minimize decomposition yielded powder patterns that were compared with those simulated from the single crystal diffraction data.

The higher sensitivity of **9** is reflected in poorer quality of powder diffraction data. (Figure 3-2 and Figure 3-3).

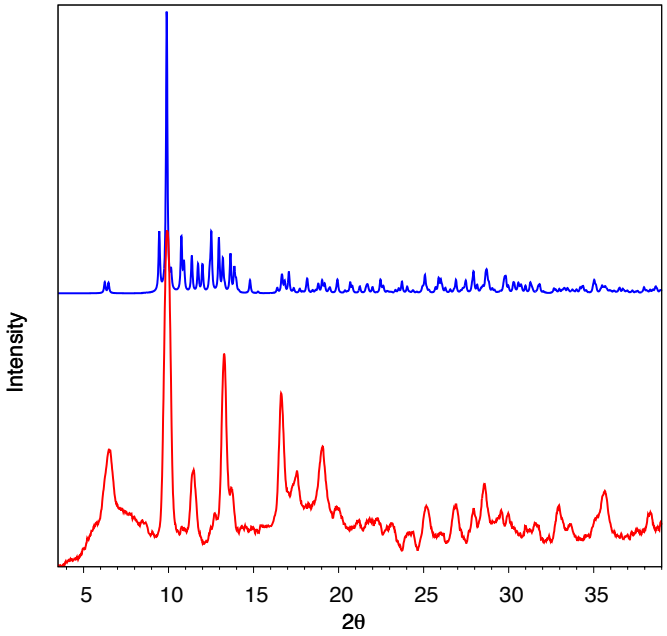

Figure 3-2 Powder X-ray diffraction pattern of $[Cu_6\{P(SiMe_3)_2\}_6]$ (**9**), blue: simulated, red: observed.

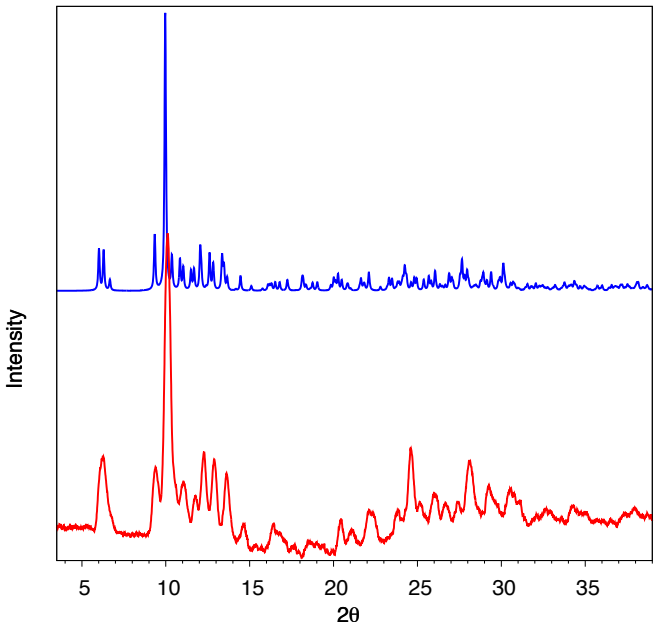

Figure 3-3 Powder X-ray diffraction pattern of $[Ag_6\{P(SiMe_3)_2\}_6]$ (**10**), blue: simulated, red: observed.

As in the solid state, **9** and **10** are thermally sensitive when redissolved in solvent. Compounding this situation is their limited solubility in common solvents at low temperatures. However, NMR data could be obtained prior to visible signs of decomposition (darkening) from freshly prepared solutions at room temperature. The presence of only one peak in the solution ^{1}H NMR spectrum of **9** (0.50 ppm) and **10** (0.48 ppm) shows that a symmetrical structure is retained in solution. Similarly, ^{31}P{^{1}H} NMR spectra display only one peak for each of these complexes (δ = –149 ppm for **9** and –236 ppm for **10**), with no Ag–P J-coupling resolved for **10**. The observed chemical shifts are in agreement with those reported for other metal bis(trimethylsilyl)phosphido compounds, where chemical shifts are in the range of –60 to –290 ppm for 3d and 4d metal-P(SiMe$_3$)$_2$ complexes.[1, 24, 25]

Table 3-2 Crystallographic information for compounds **9**-**12**

Compound	**9**·THF	**10**·THF	**11**	**12**
Formula	$C_{40}H_{116}Si_{12}P_6OCu_6$	$C_{40}H_{116}Si_{12}P_6OAg_6$	$C_{32}H_{54}N_4Si_2PCu$	$C_{40}H_{62}CuN_2PSi_2$
Formula weight	1517.46	1783.44	645.48	721.60
Temperature/K	150	150	150	110
Crystal system	Triclinic	Triclinic	Triclinic	Monoclinic
Space group	$P\bar{1}$	$P\bar{1}$	$P\bar{1}$	$P2_1/c$
a/Å	9.813(7)	9.836(2)	9.611(4)	22.988(7)
b/Å	15.477(10)	15.683(3)	20.206(8)	10.325(3)
c/Å	16.325(9)	16.709(3)	20.631(6)	18.132(4)
α/°	62.453(15)	63.81(3)	102.042(13)	90
β/°	73.25(2)	74.78(3)	89.995(9)	94.917(8)
γ/°	77.325(18)	79.34(3)	96.848(8)	90
Volume/Å^3	2094(2)	2224.6(10)	3889(2)	4288(2)
Z	1	1	4	4
ρ (g/cm^3)	1.203	1.331	1.102	1.118
μ (mm^{-1})	1.806	1.587	0.688	0.629
F(000)	796.0	904	1384.0	1552.0
Reflections collected	46231	18731	9151	57174
GooF on F^2	1.033	1.048	1.323	1.110
Final R indexes [I>=2σ (I)]	R_1 = 0.0585 wR_2 = 0.1510	R_1 = 0.0490 wR_2 = 0.1319	R_1 = 0.1280 wR_2 = 0.3310	R_1 = 0.0925 wR_2 = 0.2521

The use of NHCs as stabilizing ligands for the synthesis of the mononuclear copper phosphido complexes [(^{i}Pr$_2$-bimy)$_2$CuP(SiMe$_3$)$_2$] **11** and [(IPr)CuP(SiMe$_3$)$_2$] **12** leads to a marked, enhanced stability of the Cu–P(SiMe$_3$)$_2$ moiety. 1,3-Di-isopropylbenzimidazole-2-ylidene (^{i}Pr$_2$-bimy) and 1,3-bis(2,6-diisopropylphenyl)imidazol-2-ylidene (IPr) were chosen as stabilizing ligands for the formation of mononuclear copper phosphido complexes. Terminal copper-phosphido complexes are rare, with only one structurally charac-

terized complex reported.[19] We have recently shown that NHCs, and specifically $^{i}Pr_2$-bimy, can be used to prepare cyclic clusters of copper and silver with chalcogenolate ligands.[21, 26] $^{i}Pr_2$-bimy has an ideal size that is not too large to limit the coordination number around the metal to which it ligates and has shown to be appropriate for stabilizing large metal-phosphide clusters.[27]

[($^{i}Pr_2$-bimy)$_2$CuP(SiMe$_3$)$_2$] (**11**) was synthesized by the reaction of CuOAc, solubilized by two equivalents of $^{i}Pr_2$-bimy, with P(SiMe$_3$)$_3$ (Scheme 3-2). The formation of **11** results in its precipitation in the form of a pale yellow solid. Attempts to synthesize the analogous Cu–P(SiMe$_3$)$_2$ complex with only one $^{i}Pr_2$-bimy ligand on the copper center also result in the formation of **11**, although a darkening of reaction solutions suggests competition for the formation of larger Cu–P cluster complexes.[20, 28] Crystals of **11** for X-ray diffraction were obtained by layering a dilute solution in THF with pentane. The formation of twinned, needle shaped crystals resulted in highly twinned X-ray diffraction data sets. After several attempts, a usable, un-twinned data set was obtained. However, the lower quality of the diffraction data is such that we limit the discussion of the structural parameters to the overall molecular features (Figure 3-4). The structure was refined as a two-component twin and SQUEEZE/PLATON[29] was used to treat the electron density resulting from disordered solvent molecules present in the unit cell. PLATON calculates a solvent accessible volume of 399 Å^3, which contains 82 electrons.

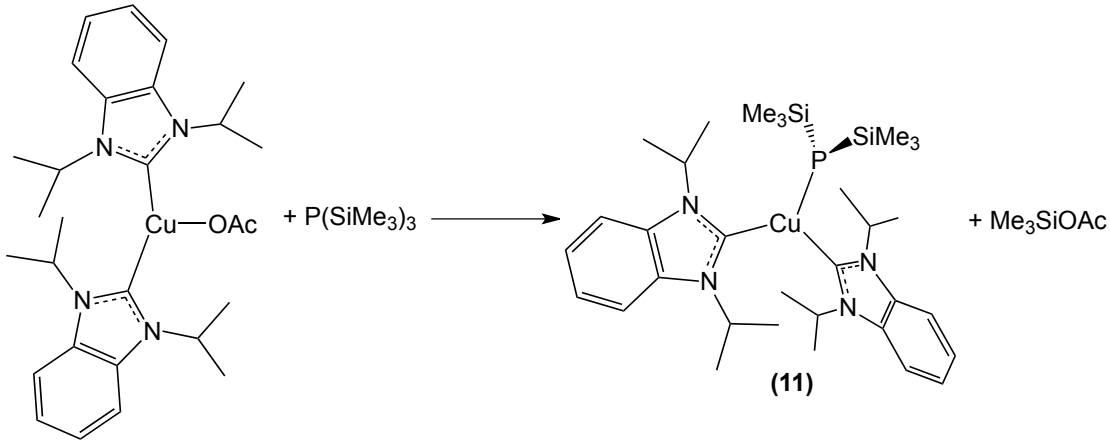

Scheme 3-2 Preparation of **11**

This air sensitive but thermally stable molecule **11** crystallizes in the triclinic space group $P\bar{1}$ with a $Z = 4$. In both crystallographically independent but otherwise identical molecules, the copper centre displays a distorted, trigonal planar geometry and the coordination about phosphorus is distorted trigonal pyramidal. The terminal coordination of $P(SiMe_3)_2$ is the first example reported for copper. Crystallographically characterized examples of $M–P(SiMe_3)_2$ have been described for other d-block metals, where the additional electron pair on phosphorus can also contribute to metal-P bonding.[24, 30] Similar to the formation of the silyl-chalcogenolato complexes $(R_3P)_3Cu–ESiMe_3$[31, 32] as intermediates in the formation of copper-chalcogenides, complex **11** is representative of the first step en route to the formation of polynuclear copper-phosphide clusters using $P(SiMe_3)_3$.[28, 33] The isolation of similar, terminally bonded phosphido complexes when CuOAc was ligated with PR_3 has, to date, not proven to be possible in our hands, demonstrating a significant benefit of using a NHC in this area.

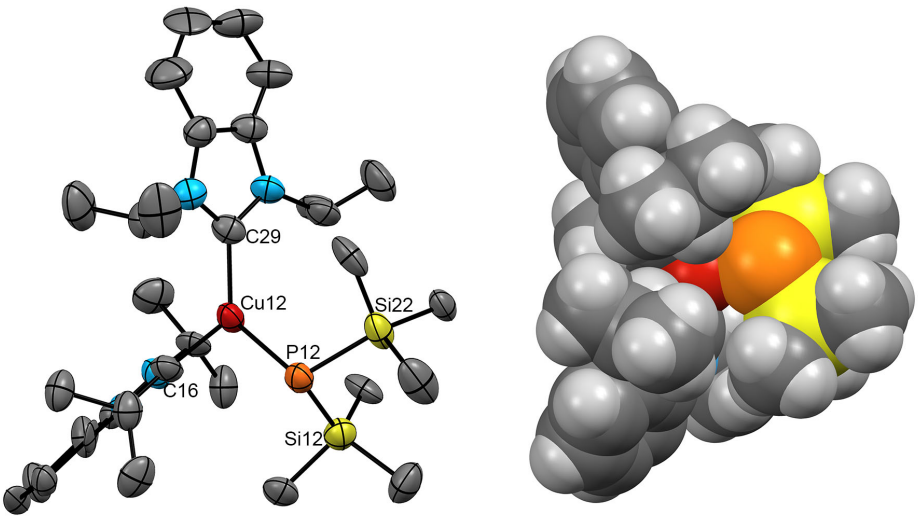

Figure 3-4 Left: molecular structure of one of two independent molecules of [(^{i}Pr$_2$-bimy)$_2$CuP(SiMe$_3$)$_2$] (**11**). Ellipsoids are at the 50% probability level and hydrogen atoms omitted for clarity. Right: space filling model of **11**. Cu: red, P: orange, Si: yellow, N: blue, C: dark grey, H: light grey. Selected bond lengths (Å) and angles (°): Cu12–P12 2.284(5), Cu12–C16 1.994(13), Cu12–C29 1.923(15), P12–Si12 2.195(6), C29–Cu12–C16 123.4(6), C29–Cu12–P12 125.8(4), Si12–P12–Cu12 103.9(2), Si12–P12–Si22 102.3(2).

NMR spectra of **11** in solution correlate with the molecular structure observed in the solid state. Integration values of the peaks related to the protons of $^{i}Pr_2$-bimy ligands with the peak related to the $SiMe_3$ groups shows a 2:1 ratio of $^{i}Pr_2$-bimy:$P(SiMe_3)_2$. Only one peak was observed in ^{31}P NMR spectrum of **11** (δ = –261 ppm), shifted upfield compared to the signal for the μ-$P(SiMe_3)_2$ in **9** (δ = –149 ppm). This chemical shift is close to those observed for the other terminally bonded metal–$P(SiMe_3)_2$ groups in related complexes.[1] Compound **11** is thermally sensitive in solution, however, it is far more stable than **9** in the solid state and decomposes only above 72 °C.

Using a much larger NHC, [(IPr)CuP$(SiMe_3)_2$] (**12**) was synthesized by reacting [(IPr)CuOAc][15] with $P(SiMe_3)_3$ in toluene (Scheme 3-3). Cooling a concentrated toluene solution of **12** resulted in the formation of thin, plate-like, colourless crystals, which were used for single crystal X-ray diffraction.

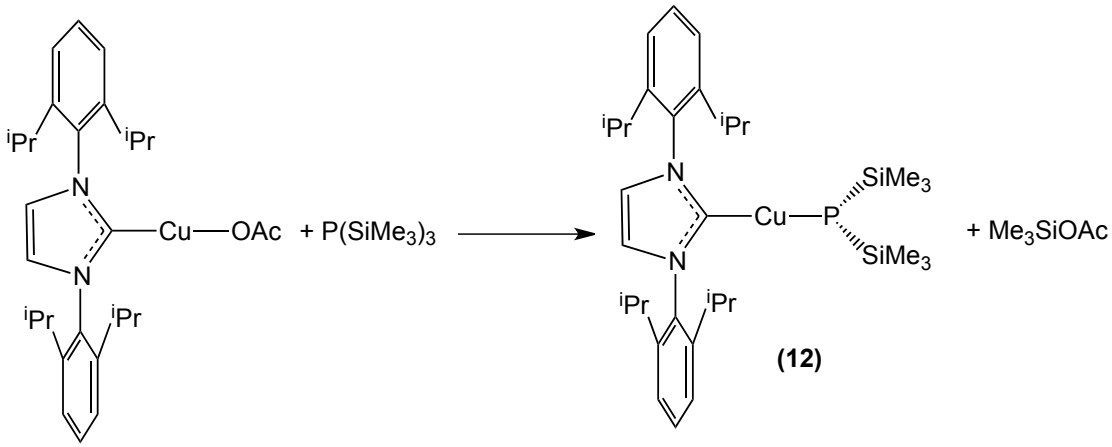

Scheme 3-3 Preparation of **12**

This molecule crystalizes in space group $P2_1/c$ with a $Z = 4$. Due to the presence of larger groups attached to nitrogen atoms ($\%V_{bur}$ for M–NHC length at 2.00 Å: $^{i}Pr_2$-bimy = 27.9 and IPr = 44.5)[34] the copper center in **12** has a coordination number of two and exhibits slightly distorted, linear coordination geometry (P–Cu–C = 173.39(17)°). This value is similar to reported mononuclear complex [Cu(IPr)($P^{t}Bu_3$)][BF_4], the copper coordinated to one IPr and one phosphine ligand (P–Cu–C = 178.38(17)°). Interestingly the Cu–C and Cu–P bond lengths in **12** (1.898(5) and 2.1913(15) Å respectively) are also very similar to those reported in [Cu(IPr)($P^{t}Bu_3$)][BF_4] (1.918(5) and 2.2147(15) Å respectively)[35]. The Cu–P bond length in **12** is somewhat shorter than those observed in the linear

bis(dialkylphosphido) complex $[Cu(P^tBu_2)_2]^-$ (2.266(4) and 2.246(5) Å) and longer than those observed in **9** (2.2043(16)–2.2094(15)).[19] Together with phosphorus centre in **12** displaying a distorted trigonal pyramidal geometry similar to that observed in **11**, the metrical parameters illustrate that the additional electron pair on phosphorus in **12** does not contribute to copper-phosphorus bonding. The possibility of protonation of the P centre in **12** is ruled out by examining the IR and ^{1}H NMR spectra of this complex, which confirm the lack of an identifiable P–H stretch and P–H related chemical shift, respectively (see Supporting Information in section 7.2).

^{1}H NMR spectroscopy of **12** shows that the solid-state connectivity is maintained in solution. The integration of the peaks confirms a 1:1 ratio of IPr:$P(SiMe_3)_2$. Only one peak was observed in ^{31}P NMR spectrum of **12** (δ = –268 ppm), which is related to the one phosphorus centre present in its structure and is in good agreement with the value reported for **11**. Although **12** is relatively reactive and sensitive in the solution state, it too is thermally stable to 85 °C as a crystalline solid, decomposing above this temperature.

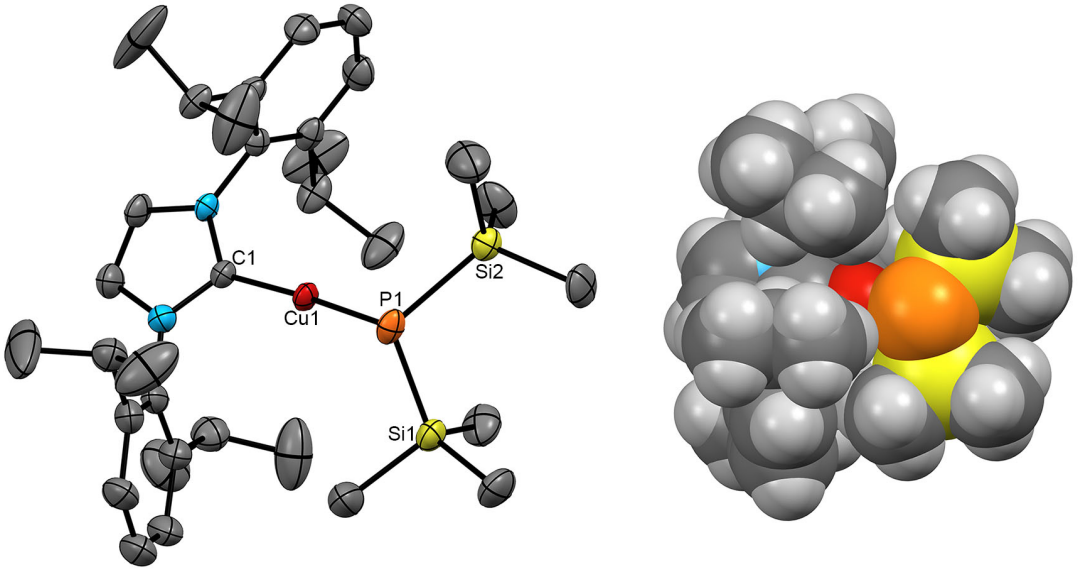

Figure 3-5 Left: Molecular structure of [(IPr)CuP$(SiMe_3)_2$] (**12**) with ellipsoids at the 50% probability level and hydrogen atoms omitted for clarity. Right: Space filling model of **12.** Cu: red, P: orange, Si: yellow, N: blue, C: dark grey, H: light grey. Selected bond lengths (Å) and angles (°): Cu1–C1 1.898(5), Cu1–P1 2.1913(15), P1–Si1 2.219(2), C1–Cu1–P1 173.39(17), Cu1–P1–Si1 97.90(7), Si1–P1–Si2 104.95(9).

We have recently communicated that the NHC $^{i}Pr_2$-bimy can be employed as a ligand with the reaction of AgOAc with $P(SiMe_3)_3$, ultimately yielding the polynuclear complexes $[Ag_{12}(PSiMe_3)_6(^{i}Pr_2\text{-bimy})_6]$ and $[Ag_{26}P_2(PSiMe_3)_{10}(^{i}Pr_2\text{-bimy})_8]$.[27] To date, our attempts at isolating the (expected) first formed, mononuclear complexes of NHC ligated Ag-$P(SiMe_3)_2$ with either $^{i}Pr_2$-bimy or IPr have not proven to be possible. Whilst the clusters above are isolated with $^{i}Pr_2$-bimy, reaction of (IPr)AgOAc[36] or $[AgS^{t}Bu]_n$ solubilized by free IPr[37] with $P(SiMe_3)_3$ ultimately yield $[(IPr)_2Ag]^+$ as the identifiable silver complex, confirmed by NMR spectroscopy and mass spectrometry.[38] Although the initial formation of $[(IPr)AgP(SiMe_3)_2]$ is suggested by the appearance of a new doublet at 0.27 ppm (for $-P(SiMe_3)_2$ which compares well with the corresponding peak in the ^{1}H NMR of **12**, a shift of the peaks assigned to the IPr ligand as well as the disappearance of the Ag–OAc and formation of Me_3SiOAc in *in situ* ^{1}H NMR studies, rapid decomposition was invariably observed through darkening of the reaction solution and isolation of $[(IPr)_2Ag]^+$ species. This decomposition likely proceeds by the formation of $[Ag_6\{P(SiMe_3)_2\}_6]$ as observed transiently in the $^{31}P\{^1H\}$ NMR spectrum of these solutions. Similarly, the attempted reaction of IPr with $[Ag_6\{P(SiMe_3)_2\}_6]$ in order to prepare IPr ligated Ag-$P(SiMe_3)_2$ only lead to decomposition.

3.4 Conclusions

The NHC ligated coordination complexes **11** and **12** are easily synthesized and thermally stable in the solid state under inert atmosphere. Although they are temperature sensitive in solution, their enhanced stability may make them better candidates for binary and ternary copper-phosphide cluster assembly compared to **9**, which is markedly more sensitive to temperature and solvent loss, decomposing at very low temperatures (~ –40 °C). By employing NHC ligands that have dramatically different sizes ($\%V_{bur}$ for M–NHC length at 2.00 Å: $^{i}Pr_2$-bimy = 27.9 and IPr = 44.5)[34] together with different NHC ligand to metal ratios, **11** and **12** may be useful precursors for ternary phosphide nanocluster assembly. We are actively exploring the chemistry of these complexes in our laboratories.

3.5 References

1. S. C. Goel, M. Y. Chiang, D. J. Rauscher and W. E. Buhro, *J. Am. Chem. Soc.*,

1993, **115**, 160-169.

2. S. C. Goel, M. Y. Chiang and W. E. Buhro, *J. Am. Chem. Soc.*, 1990, **112**, 5636-5637.
3. M. A. Matchett, A. M. Viano, N. L. Adolphi, R. D. Stoddard, W. E. Buhro, M. S. Conradi and P. C. Gibbons, *Chem. Mater.*, 1992, **4**, 508-511.
4. G. Fritz and P. Scheer, *Chem. Rev.*, 2000, **100**, 3341-3402.
5. S. C. Goel, W. E. Buhro, N. L. Adolphi and M. S. Conradi, *J. Organomet. Chem.*, 1993, **449**, 9-18.
6. S. L. Brock, S. C. Perera and K. L. Stamm, *Chem. Eur. J.*, 2004, **10**, 3364-3371.
7. S. T. Oyama, *J. Catal.*, 2003, **216**, 343-352.
8. M. Sharon and G. Tamizhmani, *J. Mater. Sci.*, 1986, **21**, 2193-2201.
9. C. B. Khadka, A. Eichhöfer, F. Weigend and J. F. Corrigan, *Inorg. Chem.*, 2012, **51**, 2747-2756.
10. H. Karsch, F. Bienlein, T. Rupprich, F. Uhlig, E. Herrmann and M. Scheer, in *Synthetic methods of organometallic and inorganic chemistry :(HerrmannBrauer)*, ed. W. A. Herrmann, Georg Thieme Verlag ; Stuttgart ; New York, 1996, pp. 58-65.
11. B. K. Teo, Y. H. Xu, B. Y. Zhong, Y. K. He, H. Y. Chen, W. Qian, Y. J. Deng and Y. H. Zou, *Inorg. Chem.*, 2001, **40**, 6794-6801.
12. S. Schneider, Y. Yang and T. J. Marks, *Chem. Mater.*, 2005, **17**, 4286-4288.
13. O. V. Starikova, G. V. Dolgushin, L. I. Larina, T. N. Komarova and V. A. Lopyrev, *Arkivoc*, 2003, 119-124.
14. Y. Han, H. V. Huynh and L. L. Koh, *J. Organomet. Chem.*, 2007, **692**, 3606-3613.
15. N. P. Mankad, T. G. Gray, D. S. Laitar and J. P. Sadighi, *Organometallics*, 2004, **23**, 1191-1193.
16. G. M. Sheldrick, *Acta Crystallogr. Sect. A: Found. Crystallogr.*, 2008, **64**, 112-122.
17. S. C. Goel, M. A. Matchett, D. K. Cha, M. Y. Chiang and W. E. Buhro, *Phosphorus, Sulfur Silicon Relat. Elem.*, 1993, **76**, 289-292.
18. P. J. Harford, J. Haywood, M. R. Smith, B. N. Bhawal, P. R. Raithby, M. Uchiyama and A. E. H. Wheatley, *Dalton Trans.*, 2012, **41**, 6148-6154.

19. A. H. Cowley, D. M. Giolando, R. A. Jones, C. M. Nunn and J. M. Power, *J. Chem. Soc., Chem. Commun.*, 1988, 208-209.
20. A. Eichhöfer, D. Fenske and W. Holstein, *Angew. Chem. Int. Ed.*, 1993, **32**, 242-245.
21. B. Khalili Najafabadi and J. F. Corrigan, *Dalton Trans.*, 2014, **43**, 2104-2111.
22. C. E. Anson, A. Eichhöfer, I. Issac, D. Fenske, O. Fuhr, P. Sevillano, C. Persau, D. Stalke and J. Zhang, *Angew. Chem. Int. Ed.*, 2008, **47**, 1326-1331.
23. H. Schmidbaur and A. Schier, *Angew. Chem. Int. Ed.*, 2015, **54**, 746 - 784.
24. L. Weber, G. Meine, R. Boese and N. Augart, *Organometallics*, 1987, **6**, 2484-2488.
25. H. Schafer, *Z. Anorg. Allg. Chem.*, 1979, **459**, 157-169.
26. W. J. Humenny, S. Mitzinger, C. B. Khadka, B. Khalii Najafabadi, I. Vieira and J. F. Corrigan, *Dalton Trans.*, 2012, **41**, 4413-4422.
27. B. Khalili Najafabadi and J. F. Corrigan, *Chem. Commun.*, 2015, **51**, 665-667.
28. D. Fenske and W. Holstein, *Angew. Chem. Int. Ed.*, 1994, **33**, 1290-1292.
29. A. L. Spek, *J. Appl. Crystallogr.*, 2003, **36**, 7-13.
30. D. Fenske, A. Grissinger, E. M. Hey-Hawkins and J. Magull, *Z. Anorg. Allg. Chem.*, 1991, **595**, 57-66.
31. D. T. T. Tran and J. F. Corrigan, *Organometallics*, 2000, **19**, 5202-5208.
32. D. T. T. Tran, N. J. Taylor and J. F. Corrigan, *Angewandte Chemie-International Edition*, 2000, **39**, 935-937.
33. P. M. Allen, B. J. Walker and M. G. Bawendi, *Angew. Chem. Int. Ed.*, 2010, **49**, 760-762.
34. H. Clavier and S. P. Nolan, *Chem. Commun.*, 2010, **46**, 841-861.
35. F. Lazreg, A. M. Z. Slawin and C. S. J. Cazin, *Organometallics*, 2012, **31**, 7969-7975.
36. D. V. Partyka and N. Deligonul, *Inorg. Chem.*, 2009, **48**, 9463-9475.
37. L. Jafarpour, E. D. Stevens and S. P. Nolan, *J. Organomet. Chem.*, 2000, **606**, 49-54.
38. S. F. Zhu, R. X. Liang and H. F. Jiang, *Tetrahedron*, 2012, **68**, 7949-7955.

Chapter 4

N-Heterocyclic Carbene Stabilized Ag-P Nanoclusters[§]

4.1 Introduction

Compared with tertiary phosphines, NHCs have been shown to form stronger bonds with coinage metals due to their excellent σ-donating property[1] and may thus be developed for the stabilization of new coinage metal containing cluster frameworks.[2] Indeed, their excellent ligating properties have been exploited recently for the preparation and stabilization of novel polymetallic main group cluster complexes[3] and have emerged as viable ligands for the tailored surface functionalization of precious metal nanoparticles.[4]

Stabilizing ligands are also often required on the surface of semiconductor nanoclusters in order to prevent their aggregation and formation of bulk material. It has been shown that tertiary phosphines[5] and amines[6] are good ancillary ligands for the preparation of metal-chalcogenide clusters. The incorporation of ancillary ligands on the surface of a cluster restricts the number of vacant coordination sites about the metals and stabilizes the cluster core. Despite these successes, these two classes of ligands have demonstrated only limited utility at passivating high nuclearity group 11-phosphide architectures.[7]

[§] **B. Khalili Najafabadi**, J. F. Corrigan, *Chem. Commun.,* **2015**, 51, 665-667. Reproduced by permission of The Royal Society of Chemistry.

Due in part to the coordination flexibility of the metal, the preparation of a series of nanoscale Ag phosphide clusters represents an excellent opportunity to explore the molecule to nanocluster evolution but such a series has yet to be developed.[8] The NHC 1,3-di-isopropylbenzimidazole-2-ylidene ($^{i}Pr_2$-bimy) can be used as a ligand to coordinate Ag(I) centres but where its steric requirements are not so large as to limit the coordination number around the metal to a point where cluster formation would not be possible.[9a] Herein we describe initial results on the formation of AgP architectures stabilized by this NHC, with the facile preparation and structural analysis of $[Ag_{12}(PSiMe_3)_6(^{i}Pr_2\text{-bimy})_6]$ (**13**) and $[Ag_{26}P_2(PSiMe_3)_{10}(^{i}Pr_2\text{-bimy})_8]$ (**14**).

4.2 Experimental

All syntheses were performed under an inert atmosphere using standard Schlenk line and glovebox techniques. Chemicals were used as received from Strem Chemicals and/or Aldrich. Tetrahydrofuran, diethyl ether, and pentane were purchased from Caledon and dried by passing through packed columns of activated alumina using a commercially available MBraun MB-SP Series solvent purification system. $(^{i}Pr_2\text{-bimy})_2AgOAc$[9a] and $P(SiMe_3)_3$,[9b] were prepared according to published methods.

$^{31}P\{^{1}H\}$ NMR spectrum was recorded on Inova 400 MHz spectrometer and is referenced to 85% H_3PO_4 ($\delta = 0$ ppm).

Data collection for X-ray structure determination was performed on a Bruker APEX-II CCD diffractometer at 110(2) K (for **13**) and 150(2) K (for **14**) using graphite-monochromated MoKα radiation ($\lambda = 0.71073$ Å). Frame integration was performed with SAINT software (Bruker AXS Inc., Madison, Wisconsin, USA, 2007). The structures were solved by direct methods and refined by full-matrix least-squares cycles.[10] The resulting raw data were scaled and corrected for absorption using a multi-scan averaging of symmetry equivalent data using SADABS (Bruker-AXS, SADABS version 2012.1, **2012**, Bruker-AXS, Madison, WI 53711, USA).

4.2.1 $[Ag_{12}(PSiMe_3)_6(^{i}Pr_2\text{-bimy})_6]$ (13)

$(^{i}Pr_2\text{-bimy})_2AgOAc$[9a] (0.35 g, 0.60 mmol) was dissolved in 25 ml of diethyl ether and cooled to –67 °C. $P(SiMe_3)_3$[9b] (0.09 ml, 0.30 mmol) was added at –67 °C. The solution

was stirred as the acetone-dry ice bath warmed gradually to –25 °C. The clear red solution was stirred for ~30 min at this temperature and then kept at –25 °C over night. This solution was layered with cold pentane for crystallization at –25 °C. Orange crystals of **13** formed after a few days beside some black powder. Yield: ~10 %. $^{31}P\{^{1}H\}$ (C_7D_8, 200 K) +31.8 ppm. EDX analysis of the black material was consistent with formulation Ag_3P.

4.2.2 $[Ag_{26}P_2(PSiMe_3)_{10}(^{i}Pr_2\text{-bimy})_8]$ (14)

($^{i}Pr_2$-bimy)$_2$AgOAc[9a] (0.37 g, 0.65 mmol) was dissolved in 25 ml of THF and cooled to –67 °C. P(SiMe$_3$)$_3$[9b] (0.09 ml, 0.30 mmol) was added at –67 °C. The solution was stirred as the acetone-dry ice bath warmed gradually to –25 °C. The clear dark-red solution was stirred for ~30 min at this temperature and then kept at –25 °C over night. The solvent was removed cold *in vacuo* and 25 ml of diethyl ether was added to dissolve the solid. This solution was layered with cold pentane for crystallization at –25 °C. Dark-red crystals of **14** formed after two weeks beside some black powder. Yield: ~5 %.

4.3 Results and Discussion

The reaction of ($^{i}Pr_2$-bimy)$_2$AgOAc[9a] and P(SiMe$_3$)$_3$[9b] in a 2:1 ratio yields $[Ag_{12}(PSiMe_3)_6(^{i}Pr_2\text{-bimy})_6]$ (**13**) (diethyl ether as solvent). $[Ag_{26}P_2(PSiMe_3)_{10}(^{i}Pr_2\text{-bimy})_8]$ (**14**) (with THF as solvent) is isolated from these reagents when a higher ($^{i}Pr_2$-bimy)$_2$AgOAc to P(SiMe$_3$)$_3$ ratio (2:0.9) is used. Both products arise via activation of P–Si bonds and illustrate the use of $^{i}Pr_2$-bimy as a stabilizing ligand on the surface of metal-phosphide clusters. The presence of both SiMe$_3$ and $^{i}Pr_2$-bimy groups on the surface of the formed clusters prevents their aggregation to extended solids.

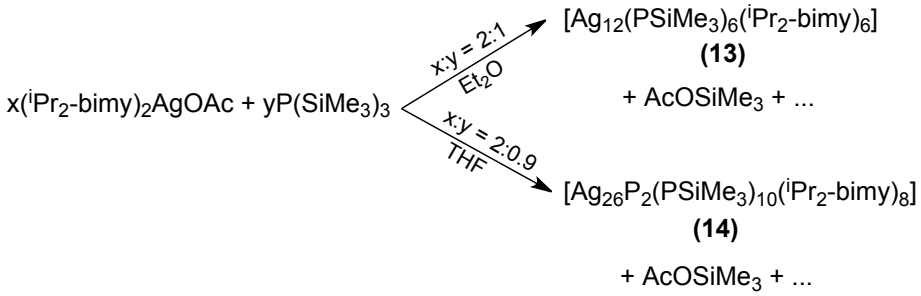

Scheme 4-1 Preparation of **13** and **14**

Single crystals of **13** and **14** were formed by layering their solutions in diethyl ether with pentane. Molecules of **13** crystallize in the monoclinic space group $P2_1$ with a Z of 2 (Table 4-1). This structure was refined as an inversion twin (R = (-1 0 0, 0 -1 0, 0 0 -1)) with a Flack parameter of 0.29(5). The molecular structure of **13** in the solid state is shown in Figure 4-1 with selected ranges of bond lengths listed in the caption. The $PSiMe_3$ centres, formed via the cleavage of two $–SiMe_3$ moieties per phosphorus, arrange themselves at the vertices of a (non-bonded) distorted P_6 trigonal prism where the two normally congruent P_3 triangles are offset by ~18° from one another; the silver atoms are positioned above the edges of this arrangement. The three *inter*-triangle edges are each linked by two Ag(I). These are each coordinated by two $PSiMe_3$, as well as one $^iPr_2$-bimy ligand and display distorted trigonal planar geometries (average sum of the angles = 359.0(4)°) with the average C–Ag–P and P–Ag–P angles of 133.9(5) and 91.28(17)°, respectively. Coordination by $^iPr_2$-bimy forces these silver atoms to move out from the trigonal prism arrangement of the phosphorus centres. The additional six Ag(I) are located along the *intra*-triangular edges of the trigonal prism, coordinated by two $PSiMe_3$. These latter silver centres adopt bent geometries with an average P–Ag–P angle of 165.2(2)°. The twelve silvers form a distorted anti-cuboctahedron (Figure 4-1, bottom) and each of the $PSiMe_3$ is bonded to four Ag(I).

Molecules of **14** represent the first example of a condensed silver-phosphide nanocluster with NHC ligands on the surface. Indeed, such condensed, molecular AgP frameworks are exceptionally rare with only one other structure reported.[7c] Nanocluster **14** crystallizes in the triclinic space group $P\bar{1}$ with a *Z* of 2 (Table 4-1). Although the preparative procedure for **14** is similar, to that for **13**, the higher Ag:P reaction stoichiometry results in the formation and incorporation of two P^{3-} and the assembly of a larger framework. The molecular structure of **14** is illustrated in Figure 4-2 (top) as is the construction of the AgP core (bottom); a selection of bond length parameters is listed in the caption. This binary silver phosphide cluster consists of an $Ag_{26}P_{12}$ core, which has 8 $^iPr_2$-bimy ligands on its surface. 10 of the P centres retain one (surface) $SiMe_3$ moiety. As observed for **13**, the presence of $SiMe_3$ on the surface of **14** makes this cluster extremely sensitive to air and moisture. On the other hand, these groups may lend themselves to further functionalization of the cluster surface.

Table 4-1 Crystallographic information for compounds **13**-**14**

Compound	**13**·$(C_4H_{10}O)_{0.5}$	**14**·$(C_5H_{12})_{1.4}$
Formula	$C_{98}H_{167}Ag_{12}N_{12}O_{0.50}P_6Si_6$	$C_{141}H_{250.80}Ag_{26}N_{16}P_{12}Si_{10}$
Formula Weight (*g/mol*)	3170.23	5627.52
Crystal Color and Habit	orange plate	red plate
Crystal System	monoclinic	triclinic
Space Group	$P2_1$	$P\bar{1}$
Temperature, K	110(2)	150(2)
a, Å	15.889(8)	17.285(4)
b, Å	18.207(12)	20.433(5)
c, Å	23.994(15)	29.512(8)
α,°	90	95.465(12)
β,°	95.206(15)	91.603(9)
γ,°	90	90.317(19)
V, Å^3	6913(7)	10371(4)
Z	2	2
F(000)	3162	5502
ρ (g/cm^3)	1.523	1.802
μ (mm^{-1})	1.821	2.582
Max 2θ for data collection, °	51.414	49.556
R_{merge}	0.0616	0.0846
R_1	0.0572	0.0555
wR_2	0.1149	0.1142
GOF	1.024	1.016
Maximum shift/error	0.041	0.001

In the structure of this cluster, there are two phosphorus centres that are present as phosphide ligands and each bridges six silver atoms. Both display one longer contact to a silver atom, which is in the middle of the core. The other 10 phosphorus atoms are present as phosphinidines that retain one $SiMe_3$ group connected to them. Each of these 10 phosphorus atoms bridge 4 silver atoms. There are two types of silver atoms in this structure: 18 Ag are coordinated with only two phosphorus and show a bent geometry (153.58(10) < P–Ag–P < 177.50(10)°). The other 8 Ag atoms have one $^iPr_2$-bimy coordinated to them as well as two phosphorus, similar to the Ag(I) present in **13**. These silver atoms exhibit distorted trigonal planar geometry albeit with markedly differing P–Ag–P angles of ~93 to 130°. All of the Ag…Ag contacts are greater than 2.8 Å, which is consistent with +1 oxidation state for the silver centres.[5a] To confirm the homogeneity of the compounds **13** and **14** (for which combustion analyses was not possible due to their sensitivity), EDX analysis was performed on single crystals and the atomic ratio of Ag:P and P:Si were calculated. The determined ratios are in agreement with the information obtained from single crystal X-ray diffraction analysis (Figure 4-3 and Figure 4-4).

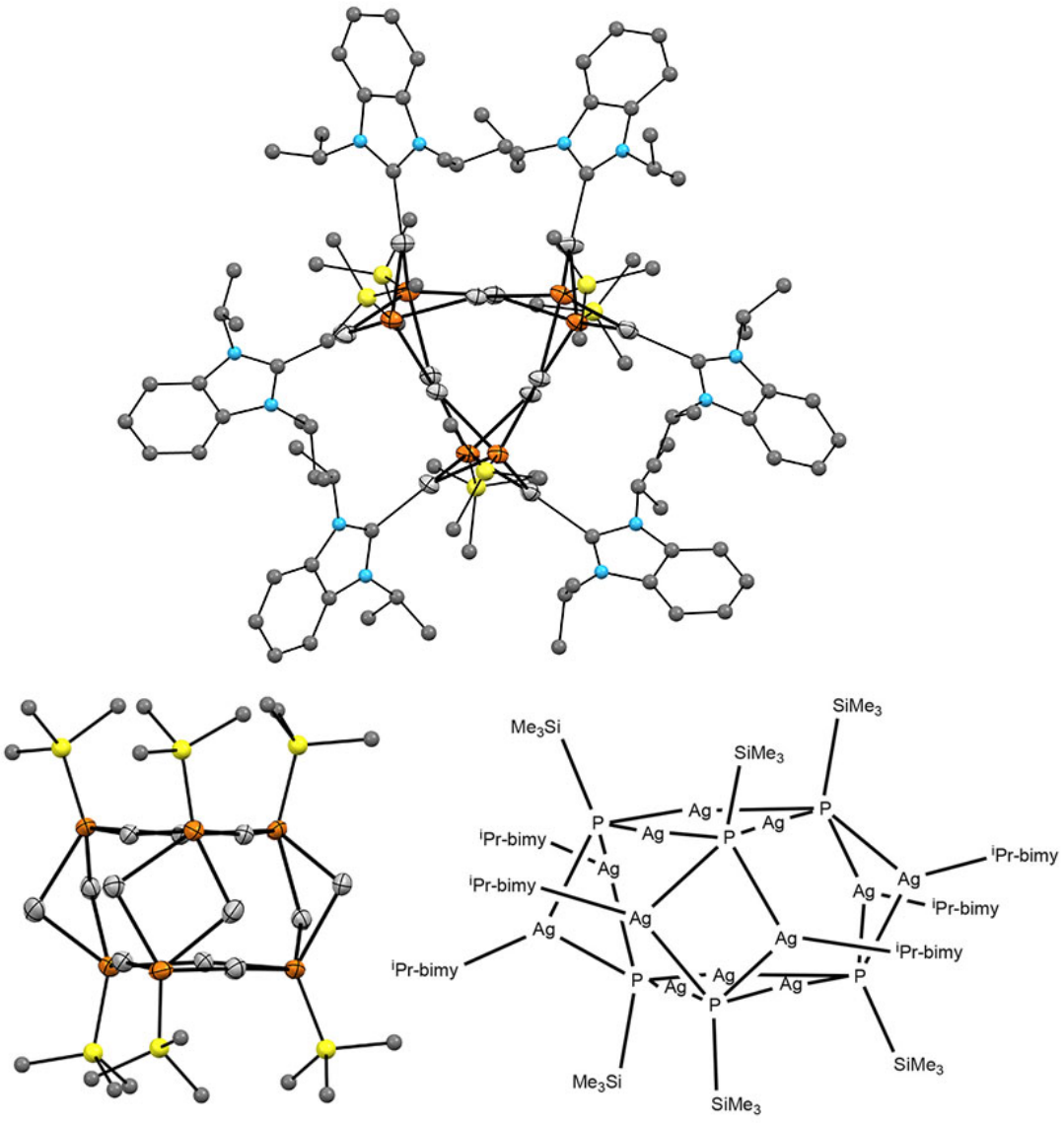

Figure 4-1 Top: Molecular structure of **13** in the solid state. Bottom right: Line diagram of the molecular structure of **13**. Bottom left: Side view of the molecular structure of **13** where ^{i}Pr-bimy groups are omitted for clarity. Ag: silver, P: orange, Si: yellow, N: blue, C: grey. The hydrogen atoms are omitted for clarity. Selected bond length ranges: 2.406(6) < Ag–P < 2.480(6) (two co-ordinate Ag), 2.509(5) < Ag–P < 2.605(5) (3 coordinate Ag), 2.145(18) < Ag–C < 2.194(19), 2.198(7) < P–Si < 2.223(8) Å.

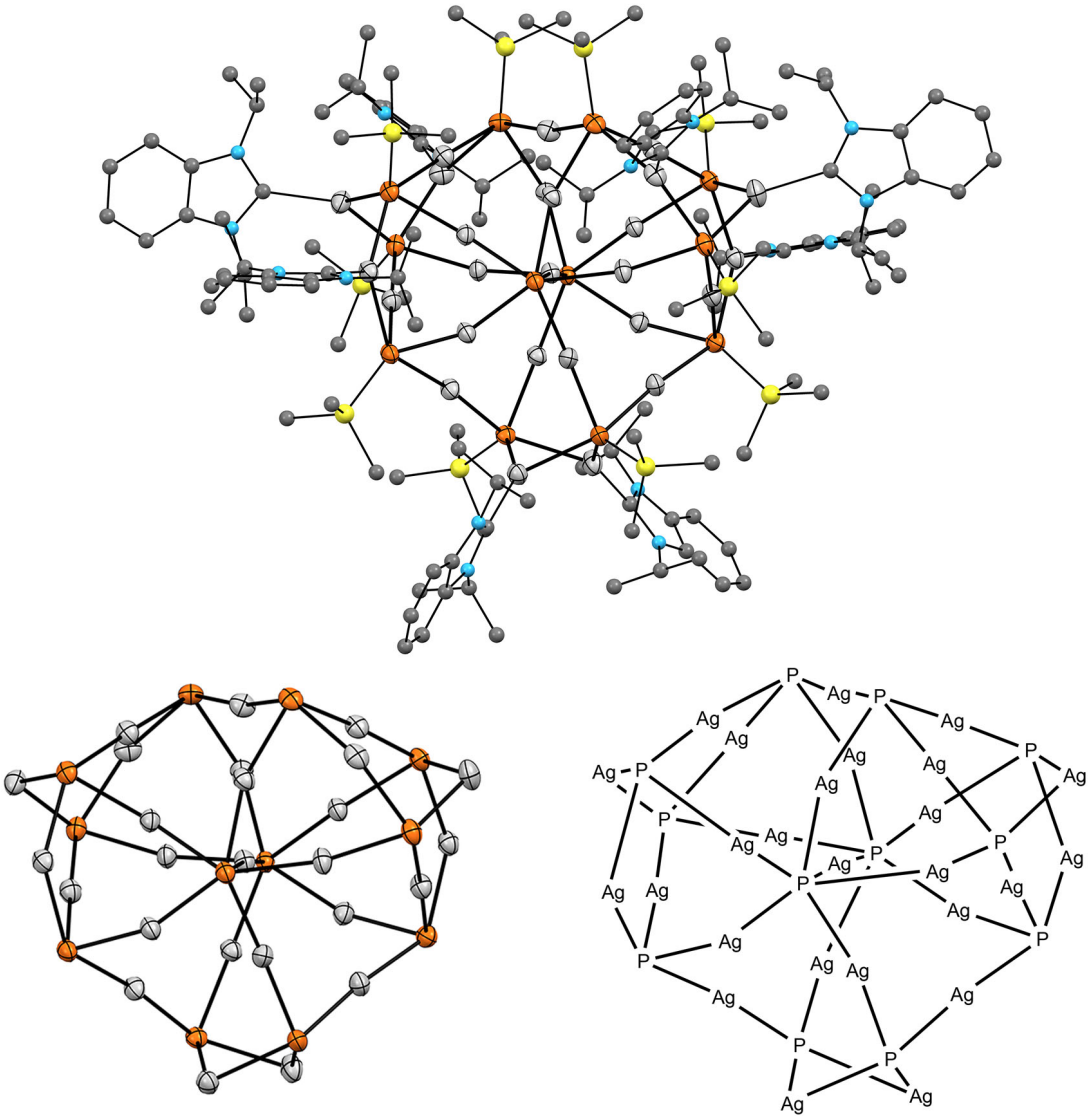

Figure 4-2 Top: Molecular structure of **14** in the solid state. Bottom right: Line diagram of the molecular structure of the AgP core of **14**. Bottom left: structure of the AgP core of **14**. Ag: silver, P: orange, Si: yellow, N: blue, C: grey. The hydrogen atoms are omitted for clarity. Selected bond length ranges: 2.375(3) < Ag–P < 2.579(3), 2.169(12) < Ag–C < 2.215(11), 2.203(4) < P–Si < 2.230(4) Å.

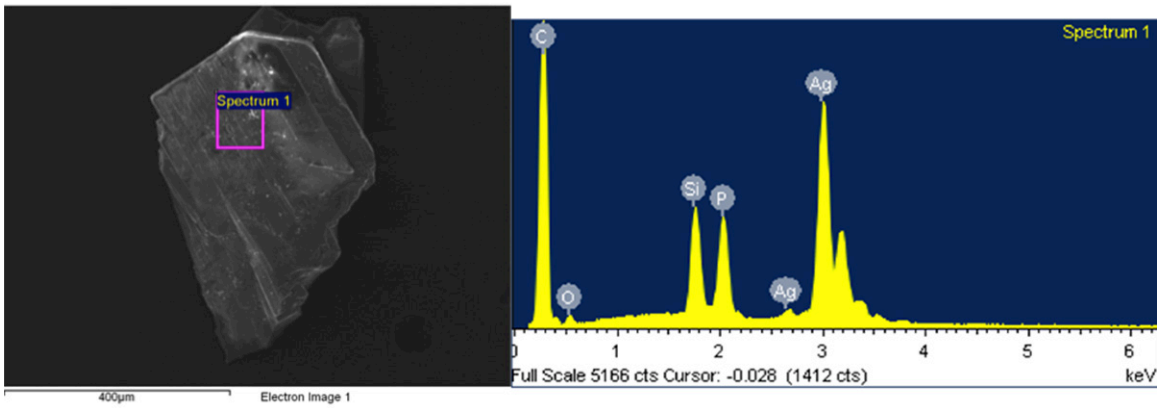

Figure 4-3 SEM image (left) and EDX spectrum (right) for the crystals of $[Ag_{12}(PSiMe_3)_6(^iPr_2\text{-bimy})_6]$ (**13**). Similar spectra were collected over three areas and the average Ag/P/Si ratios obtained are tabulated below.

Table 4-2 Average Ag/P and P/Si ratios for crystals of **13**

	Ag/P	P/Si
Calculated	2.00	1.00
Observed	1.80	0.99

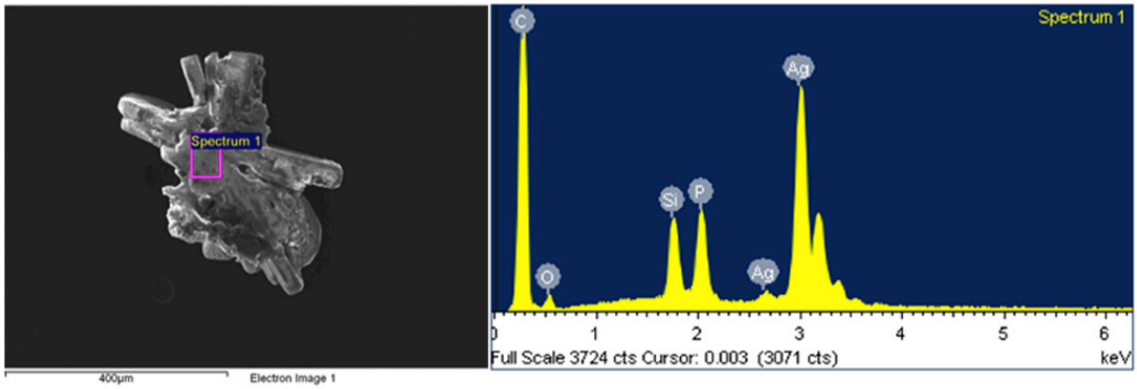

Figure 4-4 SEM image (left) and EDX spectrum (right) for the crystals of $[Ag_{26}P_2(PSiMe_3)_{10}(^iPr_2\text{-bimy})_8]$ (**14**). Similar spectra were collected over three areas and the average Ag/P/Si ratios obtained are tabulated below.

Table 4-3 Average Ag/P and P/Si ratios for crystals of **14**

	Ag/P	P/Si
Calculated	2.16	1.20
Observed	2.04	1.18

4.4 Conclusions

The synthesis of nanoscale metal-phosphide architectures remains an active area of research, with a focus on developing new methods of preparation.[11] This research area is less developed when compared to the materials chemistry of other nanocluster semiconductors such as the metal-chalcogenides.[8, 12] Approaches that can be used to prepare polymetallic phosphide complexes with sources of phosphorus include P_4, PH_3, Na_3P and $P(SiMe_3)_3$.[11, 13] In a complementary vein, Scheer and coworkers have elegantly developed fullerene-like metal-phosphorous materials using the *cyclo*-P_5 ligand complex ((η^5-C_5Me_5)Fe(η^5-P_5)) as linking units between copper(I) halides.[14] The formation and structural characterization of **13** and **14**, which are the first examples of using NHCs to stabilize such nanoscopic AgP clusters, shows that NHCs are excellent ancillary ligands to be exploited in the synthesis of high nuclearity metal-main group clusters and expands the accessibility of well-defined metal-phosphide architectures. We are actively developing this area of nanocluster chemistry in order to develop and cement structure/property relationships for this system.

4.5 References

1. J. C. Y. Lin, R. T. W. Huang, C. S. Lee, A. Bhattacharyya, W. S. Hwang and I. J. B. Lin, *Chem. Rev*. 2009, **109**, 3561-3598.
2. a) A. Rit, T. Pape and F. E. Hahn, *J. Am. Chem. Soc*. 2010, **132**, 4572-4573. b) A. Rit, T. Pape, A. Hepp and F. E. Hahn, *Organometallics*, 2011, **30**, 334-347.
3. B. Quillian, P. Wei, C. S. Wannere, P. V. R. Schleyer and G. H. Robinson, *J. Am. Chem. Soc*. 2009, **131**, 3168-3169.
4. See, for example, a) C. Richter, K. Schaepe, F. Glorius and B. J. Ravoo, *Chem. Commun*. 2014, **50**, 3204-3207. b) P. Lara, O. Rivada-Wheelaghan, S. Conejero, R. Poteau, K. Philippot and B. Chaudret, *Angew. Chem., Int. Ed*. 2011, **50**, 12080-12084. c) J. Vignolle and T. D. Tilley, *Chem. Commun*. 2009, 7230-7232; and references therein.
5. a) C. E. Anson, A. Eichhöfer, I. Issac, D. Fenske, O. Fuhr, P. Sevillano, C. Persau,

D. Stalke and J. Zhang, *Angew. Chem. Int. Ed* 2008, **47**, 1326-1331. b) M. Fu, I. Issac, D. Fenske and O. Fuhr, *Angew. Chem. Int. Ed.* 2010, **49**, 6899-6903. c) R. Langer, B. Breitung, L. Wuensche, D. Fenske and O. Fuhr, *Z. Anorg. Allg. Chem.* 2011, **637**, 995-1006. d) S. Dehnen, A. Schäfer, D. Fenske and R. Ahlrichs, *Angew. Chem. Int. Ed. Engl.* 1994, **33**, 746-749.

6. C. B. Khadka, A. Eichhöfer, F. Weigend and J. F. Corrigan, *Inorg. Chem.* 2012, **51**, 2747-2756.
7. a) D. Fenske and W. Holstein, *Angew. Chem. Int. Ed.* 1994, **33**, 1290-1292. b) P. Sevillano, O. Fuhr, O. Hampe, S. Lebedkin, E. Matern, D. Fenske and M. M. Kappes, *Inorg. Chem.* 2007, **46**, 7294-7298. c) D. Fenske and F. Simon, *Angew. Chem. Int. Ed. Engl.* 1997, **36**, 230-233.
8. O. Fuhr, S. Dehnen and D. Fenske, *Chem. Soc. Rev.* 2013, **42**, 1871-1906.
9. a) W. J. Humenny, S. Mitzinger, C. B. Khadka, B. Khalili Najafabadi, I. Vieira and J. F. Corrigan, *Dalton Trans.* 2012, **41**, 4413-4422. b) H. H. Karsch, F. Bienlein, T. Rupprich, F. Uhlig, E. Herrmann, M. Scheer, in *Synthetic Methods of Organometallic and Inorganic Chemistry*, Herrmann, W. A., Ed.; Stuttgart; New York, 1996, pp. 58-65.
10. G. M. Sheldrick, *Acta. Crystallogr. Sect. A* 2008, **64**, 112-122.
11. S. Carenco, D. Portehault, C. Boissiere, N. Mezailles and C. Sanchez, *Chem. Rev.* 2013, **113**, 7981-8065.
12. a) M. W. Degroot and J. F. Corrigan, in *Comprehensive Coordination Chemistry II*, Vol.7 (Eds: J. A. McCleverty, T. J. Meyer) Elsevier Ltd., UK, 2004, pp. 57-123. b) P. Y. Feng, X. H. Bu and N. F. Zheng, *Acc. Chem. Res.* 2005, **38**, 293-303. c) S. Dehnen, A. Eichhöfer, J. F. Corrigan, O. Fuhr and D. Fenske, in Nanoparticles: From Theory to Application (G. Schmid, Ed.) 2nd Ed. Synthesis and Characterization of Ib-VI Nanoclusters, Wiley-VCH, 2010, pp. 127-239.
13. a) S. L. Brock, S. C. Perera and K. L. Stamm, *Chem. Eur. J.* 2004, **10**, 3364-3371. b) W. Buhro, *Polyhedron* 1994, **13**, 1131-1148. c) E. Arushanov, *Prog. Cryst. Growth Charact. Mater.* 1980, **3**, 211-255.
14. S. Welsch, C. Groeger, M. Sierka and M. Scheer, *Angew. Chem. Int. Ed.* 2011, **50**, 1435-1438.

Chapter 5

Silylphosphido Gold Complexes Coordinated by NHC Ligands

5.1 Introduction

It has been shown that metal complexes that contain main group elements retaining $-SiMe_3$ groups are suitable molecular precursors for the preparation of metal-chalcogenide[1,2] and metal-phosphide[3,4] polynuclear materials. As described in Chapter 4, NHC–Cu–$P(SiMe_3)_2$ complexes are much more stable than homoleptic copper phosphido complex with $-P(SiMe_3)_2$. NHC-gold complexes[5] are widely synthesized and their application as catalysts[6,7] and anticancer agents[8] has been studied. Despite the several reports of bridging gold phosphidos in the literature,[9-11] only few structurally characterized terminal L–Au–PR_2 complexes (L = IPr[12], PPh_3[13], $PCyp_3$[14]) are reported, with gold being coordinated by NHC only in one report.[12]

Gold polynuclear clusters have attracted a lot of research interest due to their fascinating supramolecular architectures and optical properties arising from noncovalent metal-metal interactions.[15-18] Despite these interesting characteristics, the chemistry of gold phosphide clusters is not well established.[19-28] Phosphine ligands are the dominant stabilizing ligands for the formation of group 11 nanoclusters while N-heterocyclic carbenes (NHC) have emerged as strong substituents for phosphines recently.[29]

Herein we report the synthesis and characterization of a series of mononuclear gold complexes that are coordinated with NHC ligands as well as $-P(SiMe_3)_2$ or $-P(Ph)SiMe_3$. These complexes are potential molecular precursors for the preparation of larger gold-phosphide clusters since they carry $-SiMe_3$ groups attached to the phosphorus center that can be eliminated upon the reaction with suitable polar compounds.[30] We have tested the reactivity of the P–Si bond in two of the synthesized complexes by the addition of an acyl chloride and elimination of $ClSiMe_3$ via the cleavage of P–Si bonds and the formation of new P–C interactions.

5.2 Experimental

All syntheses were performed under an inert atmosphere using standard Schlenk line and glovebox techniques unless otherwise stated. Chemicals were used as received from Strem Chemicals and/or Aldrich. Tetrahydrofuran and pentane were purchased from Caledon and dried by passing through packed columns of activated alumina using a commercially available MBraun MB-SP Series solvent purification system. Chloroform-d was purchased from Aldrich and distilled over P_2O_5. Benzene-d_6 was dried and distilled over Na/K. $PPh(SiMe_3)_2$,[31] $P(SiMe_3)_3$,[32] IPrAuCl[33] (IPr = 1,3-bis(2,6-diisopropylphenyl)imidazol-2-ylidene) and $^{i}Pr_2$-bimyAuCl[34] ($^{i}Pr_2$-bimy = 1,3-di-isopropylbenzimidazole-2-ylidene) were prepared following literature procedures.

^{1}H and $^{13}C\{^{1}H\}$ NMR spectra were obtained on a Varian Inova 400 MHz spectrometer and are reported in ppm. These spectra were referenced internally to solvent peaks relative to $SiMe_4$ ($\delta = 0$ ppm). $^{31}P\{^{1}H\}$ NMR spectra were recorded on the same spectrometer and are referenced to 85% H_3PO_4 ($\delta = 0$ ppm).

Single crystal X-ray diffraction measurements were performed on a Bruker APEXII or a Nonius KappaCCD diffractometer, with the molecular structures determined via direct methods using the SHELX suite of crystallographic programs.[35, 36]

5.2.1 [(IPr)AuP(Ph)SiMe$_3$] (15)

IPrAuCl (0.10 g, 0.16 mmol) was dissolved in 10 ml of THF. This cloudy solution was cooled to 0 °C and $PPh(SiMe_3)_2$ (0.05 ml, 0.16 mmol) was added. The solution turned to a yellow suspension by this addition. It was stirred at 0 °C for 15 min until the solid materi-

al dissolved and yielded a clear solution. The volume was reduced to about half and 20 ml of pentane was added, which precipitated out the product as an orange solid. The solvent was removed with a pipette and the solid was washed with pentane (2×10 ml) and dried *in vacuo*. Yield = 0.08 g (62%)

^{1}H NMR (400 MHz, C_6D_6, 23 °C) δ = 7.48 (m, 2 H), 7.27 (t, *J*=8 Hz 2 H), 7.09 (d, *J*=8 Hz, 4 H), 7.03 (overlapping peaks, 3 H), 6.30 (s, 2 H), 2.62 (sep, *J*=7 Hz, 4 H), 1.43 (d, *J*=7 Hz, 12 H), 1.06 (d, *J*=7 Hz, 12 H), 0.24 (d, *J*=4 Hz, 9 H). ^{13}C{^{1}H} NMR (100.5 MHz, C_6D_6) δ = 179.5, 145.9, 137.1 (d, *J*=13 Hz), 134.8, 130.6, 126.9, 124.3, 122.4, 29.1, 24.7, 24.1, 3.4 (d, *J*=11 Hz). ^{31}P{^{1}H} NMR (C_6D_6, 23 °C) δ = –95.5. m.p.: 140 °C (dec.)

5.2.2 [(IPr)AuP(SiMe$_3$)$_2$] (16)

Complex **16** was prepared analogously to **15** except that P(SiMe$_3$)$_3$ was used instead of PPh(SiMe$_3$)$_2$. Yield = 0.13 g (70%).

^{1}H NMR (400 MHz, C_6D_6, 23 °C) δ = 7.26 (t, *J*=7 Hz, 2 H), 7.09 (d, *J*=7 Hz, 4 H), 6.27 (s, 2 H), 2.61 (sep, *J*=7 Hz, 4 H), 1.49 (d, *J*=7 Hz, 12 H), 1.06 (d, *J*=7 Hz, 12 H), 0.30 (d, *J*=4 Hz, 18 H). ^{13}C{^{1}H} NMR (100.5 MHz, C_6D_6) δ = 186.6, 145.8, 135.0, 130.5, 124.2, 122.2, 29.0, 24.7, 24.1, 6.9 (d, *J*=11 Hz). ^{31}P{^{1}H} NMR (C_6D_6, 23 °C) δ = –235.7. m.p.: 136 °C (dec.)

5.2.3 [(^{i}Pr$_2$-bimy)AuP(Ph)SiMe$_3$] (17)

^{i}Pr$_2$-bimyAuCl (0.10 g, 0.23 mmol) was dissolved in 10 ml of THF and cooled to 0 °C. PhP(SiMe$_3$)$_2$ was added to this solution, which resulted in a suspension. It was stirred in the ice bath for ~15 min until the solution turned clear. The volume of the solution was reduced to half under vacuum and then 20 ml pentane was added to precipitate complex **17** as a yellow solid. Yield = 0.09 g (67%)

^{1}H NMR (400 MHz, C_6D_6, 23 °C) δ = 8.29 (t, *J*=7 Hz, 2 H), 7.26 (t, *J*=7 Hz, 2 H), 7.15 (overlapping with solvent peak, 1 H), 6.94 (overlapping peaks, 4 H), 5.17 (br, 2 H), 1.31 (d, *J*=5 Hz, 12 H), 0.67 (d, *J*=4 Hz, 9 H). ^{13}C{^{1}H} NMR (100.5 MHz, C_6D_6) δ = 179.5, 137.9, 137.2 (d, *J*=13 Hz), 133.0, 127.4, 123.5, 112.8, 52.9, 21.8, 3.0 (d, *J*=11 Hz). ^{31}P{^{1}H} NMR (C_6D_6, 23 °C) δ = –94.9. m.p.: 128 °C (dec.)

5.2.4 [($^{i}Pr_2$-bimy)AuP($SiMe_3$)$_2$] (18)

18 was synthesized via the same method as for **17** where P($SiMe_3$)$_3$ was used instead of PPh($SiMe_3$)$_2$. Yield = 0.08 g (56%)

^{1}H NMR (400 MHz, C_6D_6, 23 °C) δ = 6.91 (overlapping peaks, 4 H), 5.23 (sep, *J*=7 Hz, 2 H), 1.31 (d, *J*=7 Hz, 12 H), 0.73 (d, *J*=4 Hz, 18 H). ^{13}C{^{1}H} NMR (100.5 MHz, C_6D_6) δ = 185.5, 122.9, 112.3, 52.3, 21.2, 6.9 (d, *J*=11 Hz). ^{31}P{^{1}H} NMR (C_6D_6, 23 °C) δ = –235.0. m.p.: 122 °C (dec.)

5.2.5 [(IPrAu)$_2$PPhC(O)Ph][$AuCl_2$] (19)

0.14 g (0.18 mmol) of **15** was dissolved in 10 ml of THF and cooled to 0 °C. PhC(O)Cl (0.02 ml, 0.18 mmol) was added to this solution which was stirred at 0 °C for 30 min. Some black solid formed which was filtered and the filtrate collected. The solvent was removed *in vacuo* and then the white solid was washed with pentane (3×10 ml). Layering of a THF solution of this solid with pentane resulted colourless crystals of **19**. Yield = 0.06 g (60%, based on Au).

^{1}H NMR (400 MHz, $CDCl_3$, 23 °C) δ = 7.55–7.48 (overlapping peaks, 6 H), 7.40–7.27 (overlapping peaks, 16 H), 7.17 (s, 4 H), 2.56 (sep, *J*=7 Hz, 8 H), 1.34 (d, *J*=7 Hz, 24 H), 1.22 (d, *J*=7 Hz, 24 H). ^{13}C{^{1}H} NMR (100.5 MHz, $CDCl_3$) δ = 220.1, 186.3, 145.6, 134.0, 130.7, 124.2, 124.0, 123.3, 123.06, 28.8, 24.5, 24.0. ^{31}P{^{1}H} NMR ($CDCl_3$, 23 °C) δ = 27.4. Anal. Calcd **19**.(C_4H_8O)$_2$: C, 50.78; H, 5.72; N, 3.00. Found: C, 50.36; H, 5.88; N, 3.18. HRMS: Calc. for [$C_{67}H_{82}Au_2N_4OP$]$^{-}$ *m/z* = 1383.55576. Found. *m/z* = 1383.55571.

5.2.6 PPh(C(O)Ph)$_2$[37] (20)

Freshly made **17** (0.10 g, 0.17 mmol) was dissolved in 10 ml of THF. PhCOCl (0.04 ml, 0.34 mmol) was added to this solution. A white solid was formed right after this addition. The solution was stirred at r.t. for 1 hr and then the solid was separated via filtration. NMR spectroscopy and mass spectrometry confirmed the solid to be $^{i}Pr_2$-bimyAuCl.[34] 20 ml of pentane was added to the filtrate and filtered again in order to remove all $^{i}Pr_2$-bimyAuCl from the solution. The solvent was removed *in vacuo* to yield **20** as a yellow solid. Crystals suitable for X-ray crystallography were formed from cooling the THF/pentane solution to –25 °C. Yield = 0.04 g (75%)

^{1}H NMR (400 MHz, C_6D_6, 23 °C) δ = 8.06 (d, *J*=7 Hz, 4 H), 7.61 (t, *J*=8 Hz, 2 H), 7.00–6.91 (overlapping peaks, 9 H). ^{13}C{^{1}H} NMR (100.5 MHz, C_6D_6) δ = 208.51 (d, *J*=34 Hz), 140.23 (d, *J*=36 Hz), 137.57 (d, *J*=19 Hz), 133.47, 130.74, 129.11–128.95 (overlapping peaks). ^{31}P{^{1}H} NMR (C_6D_6, 23 °C) δ = 29.42. HRMS: Calc. for $C_{20}H_{15}PO_2$ *m/z* = 318.0809. Found. *m/z* = 318.0806.

5.3 Results and Discussion

Recently a NHC ligated digold(I)-di(bis(trimethylsilyl)phosphido complex of [Au_2(^{n}Bu_4-benzo(imy)$_2$){P($SiMe_3$)$_2$}$_2$] (^{n}Bu_4-benzo(imy)$_2$ = tetrakis(nbutyl)benzobis(imidazolium)) has been prepared in our group from the reaction of [Au_2Cl_2(^{n}Bu_4-benzo(imy)$_2$)][38] with Li[P($SiMe_3$)$_2$].[39] We have also shown that NHC ligated copper-trimethylsilyl phosphido complexes can be synthesized via the reaction of NHCCuOAc with P($SiMe_3$)$_3$. In this Chapter we report a convenient route to synthesize **15**–**18**, which involved the simple addition of phosphine (P($SiMe_3$)$_3$ or PhP($SiMe_3$)$_2$) to a solution of NHC–Au–Cl (NHC = ^{i}Pr_2-bimy or IPr) at 0 °C and elimination of $ClSiMe_3$ via the cleavage of a P–Si bond (Scheme 5-1 to Scheme 5-4). Formation of these complexes was confirmed by ^{1}H, ^{13}C{^{1}H} and ^{31}P{^{1}H} NMR spectroscopy. It was found that the byproduct ($ClSiMe_3$) should be removed as soon as the reaction is done due to the competitive reactions that result in other NHC containing compounds (*e.g.* NHC.HCl, [(NHC)$_2$Au]$^{+}$).

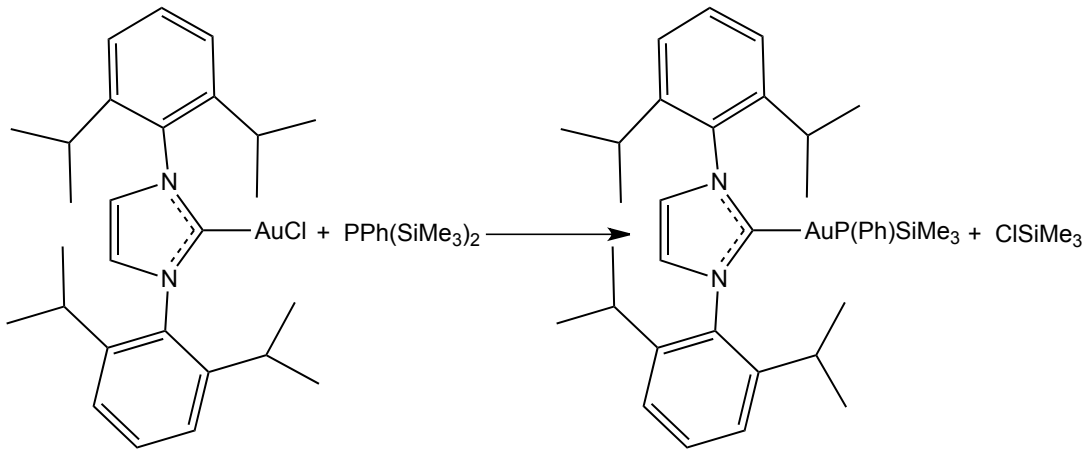

15

Scheme 5-1 Preparation of **15**

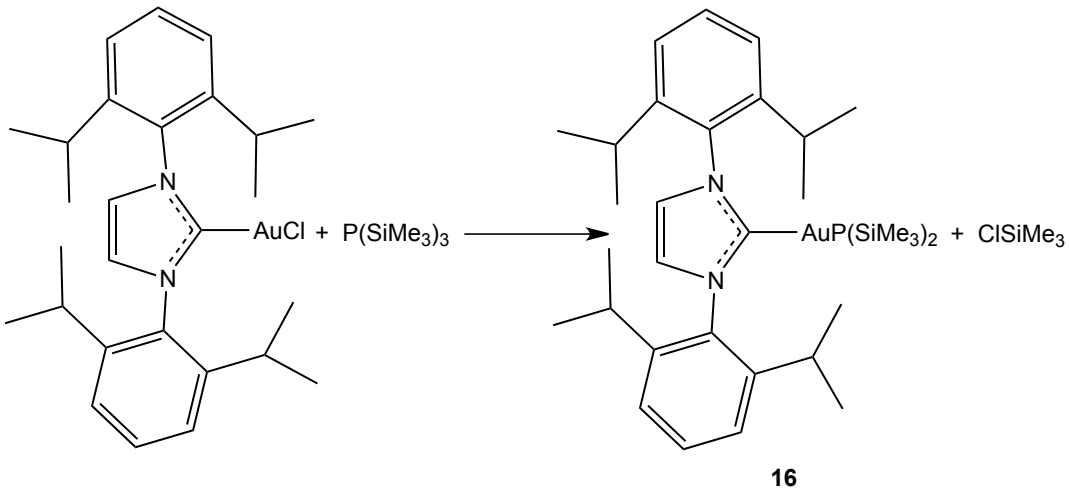

Scheme 5-2 Preparation of **16**

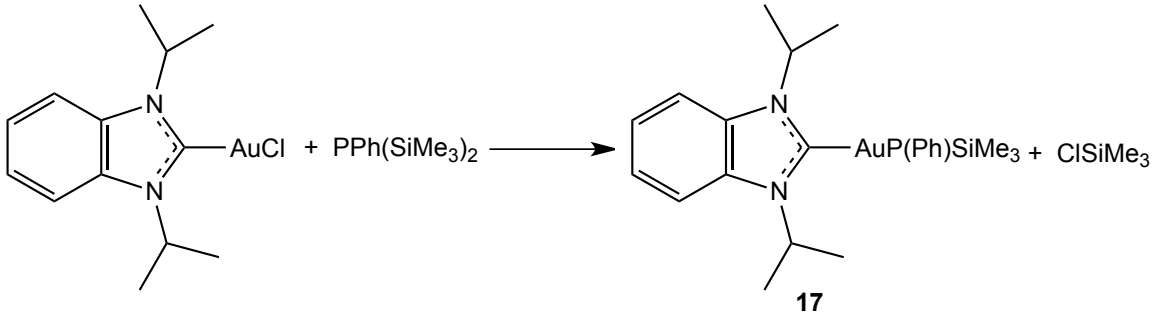

Scheme 5-3 Preparation of **17**

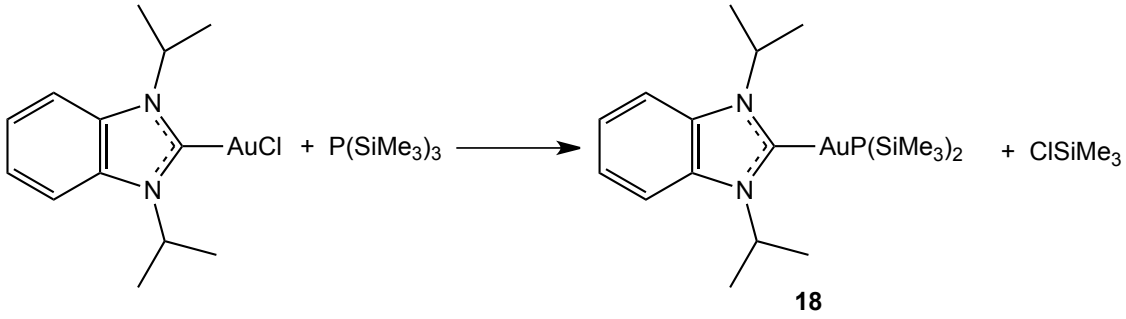

Scheme 5-4 Preparation of **18**

Complexes **15**–**18** could also be synthesized from the reaction of [$^{i}Pr_2$-bimyAuOAc] or [IPrAuOAc] with the corresponding silylphosphines, starting at –25 °C and gradually warming the reaction solution to r.t. This method adds another step to the preparation of the starting materials since [NHCAuOAc] (NHC = $^{i}Pr_2$-bimy or IPr) compounds are synthesized from [NHCAuCl] complexes.[40, 41]

The reaction of silylphosphines with acid chlorides in order to prepare related acylphosphides has been well established.[30, 42] Becker has also demonstrated the formation of P=C bonds from the reaction of $RP(SiMe_3)_2$ with pivalic chloride and elimination of one of the $-SiMe_3$ moieties followed by rearrangement of the second silyl group.[43] Our group has successfully applied this method for the preparation of $[MI(^iPr_2\text{-bimy})_2P\{C(O)Ph\}_2]$ complexes (M = Pd, Ni) from $[MI(^iPr_2\text{-bimy})_2\{P(SiMe_3)_2\}]$ (M = Pd, Ni) and two equivalents of benzoyl chloride.[39]

Complexes **15** and **17** were reacted with PhC(O)Cl to investigate the accessibility of the $-SiMe_3$ groups via the elimination of $ClSiMe_3$. $[(IPrAu)_2PPhC(O)Ph][AuCl_2]$ (**19**) was formed from the reaction of **15** with benzoyl chloride. Although isolation of this product confirms the reactivity of the $-SiMe_3$ group in **15**, it also illustrates the elimination of some of the IPr ligands and breakage of some of the Au–P bonds.

When **17** was reacted with PhC(O)Cl, $PPh(C(O)Ph)_2$[37] (**20**) was isolated as product, which exhibits the reactivity and accessibility of the $-SiMe_3$ group in **17**. However, this experiment also demonstrates the cleavage of all of the Au–P bonds. This could be the result of a consequent nucleophilic attack to the gold centre in a pre-formed NHC–Au–P(Ph)C(O)Ph and breakage of the Au–P bond. In order to explore this hypothesis, the reaction of *in situ* prepared $[(^iPr_2\text{-bimy})AuP(Ph)SiMe_3]$ (**17**) (using $[^iPr_2\text{-bimyAuOAc}]$) with PhC(O)Cl (Scheme 5-5) was monitored by NMR spectroscopy. After the addition of one equivalent of PhC(O)Cl, the peak related to $-SiMe_3$ group in **17** disappeared and an intermediate was detected along with the $PPh(C(O)Ph)_2$ (Figure 5-1) and precipitation of a small amount of solid ($[^iPr_2\text{-bimyAuCl}]$). This intermediate, that is believed to be $[(^iPr_2\text{-bimy})AuP(Ph)C(O)Ph]$ ($^{31}P\{^1H\}$ NMR (C_6D_6, 23 °C) δ = 146.7), could not be isolated and fully characterized. After the addition of the second equivalent of benzoylchloride, all of that intermediate was converted to $[^iPr_2\text{-bimyAuCl}]$ and $PPh(C(O)Ph)_2$.

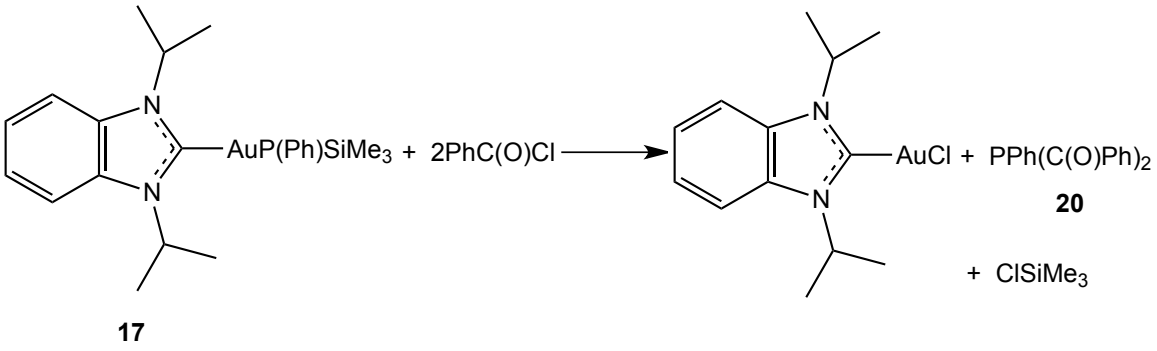

Scheme 5-5 Activation of **17** with PhC(O)Cl

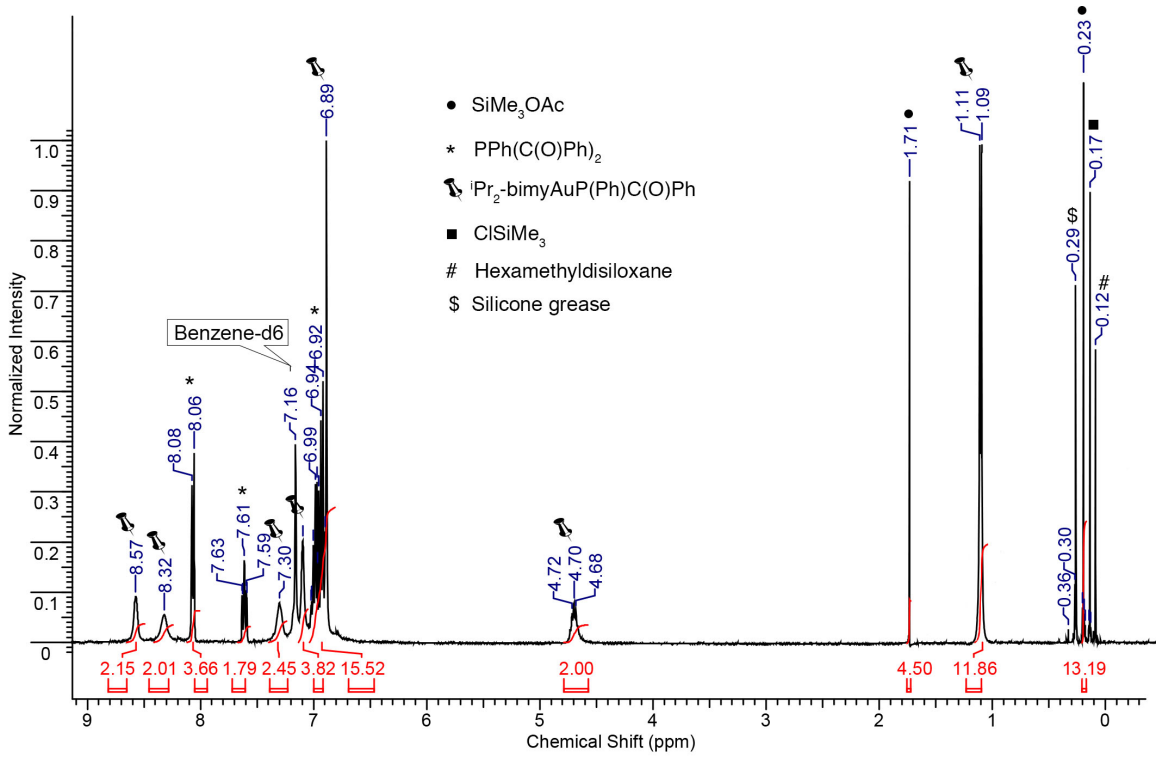

Figure 5-1 ^{1}H NMR spectrum of the reaction of **17** with PhC(O)Cl.

The ^{1}H chemical shifts of the P–SiMe$_3$ moieties of **15** and **16** (0.24 ppm and 0.30 ppm respectively) don't exhibit a significant difference compared to those for PhP(SiMe$_3$)$_2$ and P(SiMe$_3$)$_3$ (0.25 ppm and 0.30 ppm, respectively). ^{13}C{^{1}H} and ^{31}P{^{1}H} chemical shifts of the aforementioned groups however, show significant changes versus the corresponding chemical shifts in their starting materials. Both ^{13}C{^{1}H} and ^{31}P{^{1}H} chemical shifts of the P–SiMe$_3$ groups in **15** (3.4 ppm and –95.5 ppm, respectively) appear to lower field when compared to the corresponding peaks in the NMR spectra of PhP(SiMe$_3$)$_2$ (1.34 ppm and –137.6 ppm, respectively). The same trend is observed in the NMR spectra of **16** where

$^{13}C\{^{1}H\}$ (6.9 ppm) and $^{31}P\{^{1}H\}$ (–235.7 ppm) NMR spectra show higher chemical shift values versus $P(SiMe_3)_3$ (4.25 ppm and –252.4 ppm, respectively). ^{1}H NMR chemical shifts related to the IPr carbene have shifted to lower field for both **15** and **16** compared to the corresponding peaks in the spectrum of [IPrAuCl].

On the other hand, differences in the chemical shifts of the P–$SiMe_3$ moieties of **17** and **18** versus their starting materials are pronounced in all NMR spectra. ^{1}H, $^{13}C\{^{1}H\}$ and $^{31}P\{^{1}H\}$ NMR spectra of **17** exhibit chemical shifts at 0.67, 3.0 and –94.9 ppm respectively that are moved to the lower field when compared to the corresponding peaks in the NMR spectra of $PhP(SiMe_3)_2$. Complex **18** also shows peaks with more positive chemical shift values in its ^{1}H, $^{13}C\{^{1}H\}$ and $^{31}P\{^{1}H\}$ NMR spectra (0.73, 6.9 and –235.0 ppm) compared to $P(SiMe_3)_3$. These comparisons show that $^{i}Pr_2$-bimy has more effect on the ^{1}H NMR chemical shifts of the groups that are attached to the P center compared to IPr at the same position. This has been also observed previously in the ^{1}H NMR spectra of [($^{i}Pr_2$-bimy)$_2$CuP($SiMe_3$)$_2$] (**11**) and [(IPr)CuP($SiMe_3$)$_2$] (**12**). The peaks corresponding to the $^{i}Pr_2$-bimy ligand in **17** and **18** have also shifted to higher chemical shift values when compared to the NMR spectrum of [$^{i}Pr_2$-bimyAuCl]. All of the observed chemical shifts in the NMR spectra of **15**–**18** are in close agreement with those reported for metal-(trimethylsilyl)phosphido complexes with a terminal –$P(SiMe_3)$[3, 44-48] especially with our recently reported NHC–M–$P(SiMe_3)_2$ complexes (M = Cu (Chapter 4), Au[39]).

Complex **19** also exhibits characteristic chemical shifts in ^{1}H, $^{13}C\{^{1}H\}$ and $^{31}P\{^{1}H\}$ NMR spectra. Peaks corresponding to the silyl group in the starting material (complex **15**) have disappeared from ^{1}H and $^{13}C\{^{1}H\}$ NMR spectra and the only $^{31}P\{^{1}H\}$ resonance has shifted from –95.5 ppm in **15** to 27.4 ppm in **19**. This significant downfield shift of 123 ppm confirms the replacement of the electron-donating trimethylsilyl moiety with the electron-withdrawing benzoyl group. The phosphine **20** has been synthesized previously[37] but no NMR chemical shifts were reported. ^{1}H and $^{13}C\{^{1}H\}$ NMR spectra for this compound exhibit characteristic peaks in the aromatic region and one peak at 29.42 ppm is observed in the $^{31}P\{^{1}H\}$ NMR spectrum.

Molecular structures of **15**, **16**, **19**, and **20** in the solid state have been determined by single crystal X-ray diffraction technique. Suitable single crystals of **15** and **16** were formed from layering of their solutions in THF with pentane at –25 °C while crystals of **19** were

prepared via the same method at room temperature. Single crystals of **20** were formed from cooling its solution in THF/pentane to –25 °C. Molecules of **15** were crystallized in the space group $P\bar{1}$ with $Z = 4$. In this structure two independent molecules are present in an asymmetric unit that are otherwise the same. Molecule 1 is considered here for the structural discussion. The gold center in this molecule exhibits a slightly bent geometry with an angle of 177.19(4)° and the coordination around the phosphorus atom is distorted trigonal pyramidal with a slightly larger Au–P–C(Ph) angle. The angles around this phosphorus centre range from 95.09(3)° to 105.95(6)° which are in average smaller than those reported for angles around the phosphorus in IPrAuP(Mes)$_2$ (101.22(11)° to 117.98(13)°) with bulkier mesityl groups.[12] However, the Au–C and Au–P bond lengths for **15** (2.0342(17) and 2.3225(8) Å respectively) are almost the same as those in IPrAuP(Mes)$_2$ (2.043(3) and 2.3195(9) Å respectively).[12] A comparison of these bond lengths with Au–C and Au–P bond lengths in [IPrAuPPh$_3$][BF$_4$] (2.039(5) and 2.2939(15) Å respectively)[49] in addition to the trigonal pyramidal geometry around the phosphorus center, confirms that the lone pair on the P center is not contributing to the Au–P bond. Having three different groups coordinated to the P atom in **15**, in addition to the lone pair, phosphorus is considered to be a chiral centre. Although the environment around the isopropyl groups on the IPr ligands are different in the solid state, but in the solution NMR there are only two chemical shifts observed for the protons of the isopropyl moieties, which is the same as more symmetrical IPr ligated complexes.[33, 49] Table 5-1 lists selected bond lengths and angles for **15**.

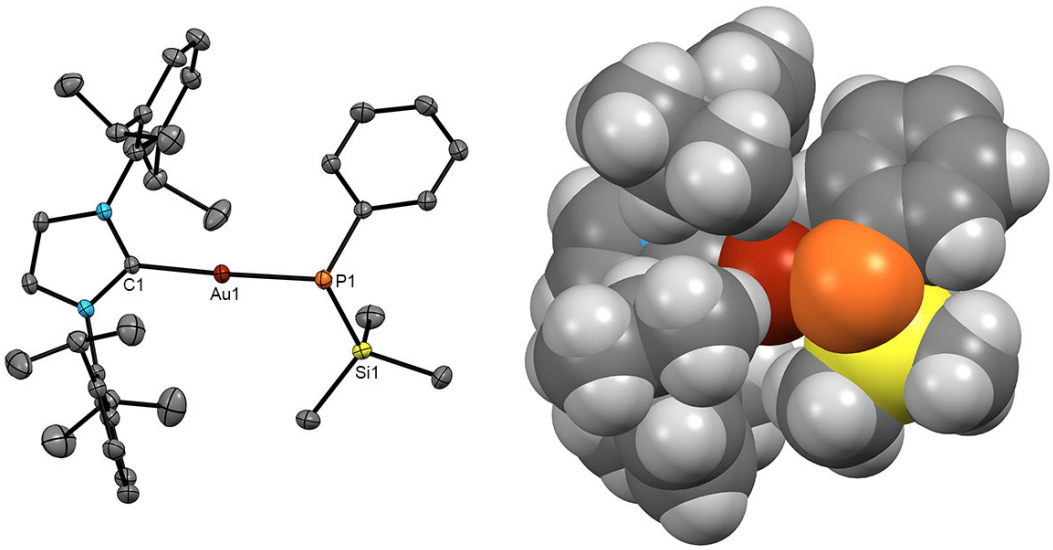

Figure 5-2 Left: Molecular structure of one of two independent molecules of [IPrAuP(Ph)$SiMe_3$] (**15**). Ellipsoids are at the 50% probability level and hydrogen atoms were omitted for clarity. Right: Space filling model. Au: dark red, P: orange, Si: yellow, N: blue, C: grey.

Table 5-1 Selected bond lengths (Å) and angles (°) for **15**

Au1–C1	2.0342(17)	C1–Au1–P1	177.19(4)
Au1–P1	2.3225(8)	C28–P1–Si1	99.02(6)
P1–C28	1.8514(19)	C28–P1–Au1	105.95(6)
P1–Si1	2.2337(9)	Si1–P1–Au1	95.09(3)

Complex **16** also crystallizes in the space group $P\bar{1}$ with $Z = 4$ and thus two independent molecules in the asymmetric unit as well as a disordered pentane molecule that sits on a centre of symmetry. In molecule 1, the coordination around the gold centre is bent with a C–Au–P angle of 175.74(4)°, which is slightly smaller than the corresponding angle in **15**. Phosphorus atom also displays distorted trigonal pyramidal geometry with angles around the phosphorus ranging from 100.54(3)° to 105.74(3)°. Au–C and Au–P bond lengths for **16** are 2.0326(14) Å and 2.3197(6) Å respectively that are very similar to the corresponding angles in **15** and IPrAuP$(Mes)_2$[12] as described above. Selected bond lengths and angles for complex **16** are listed in Table 5-2.

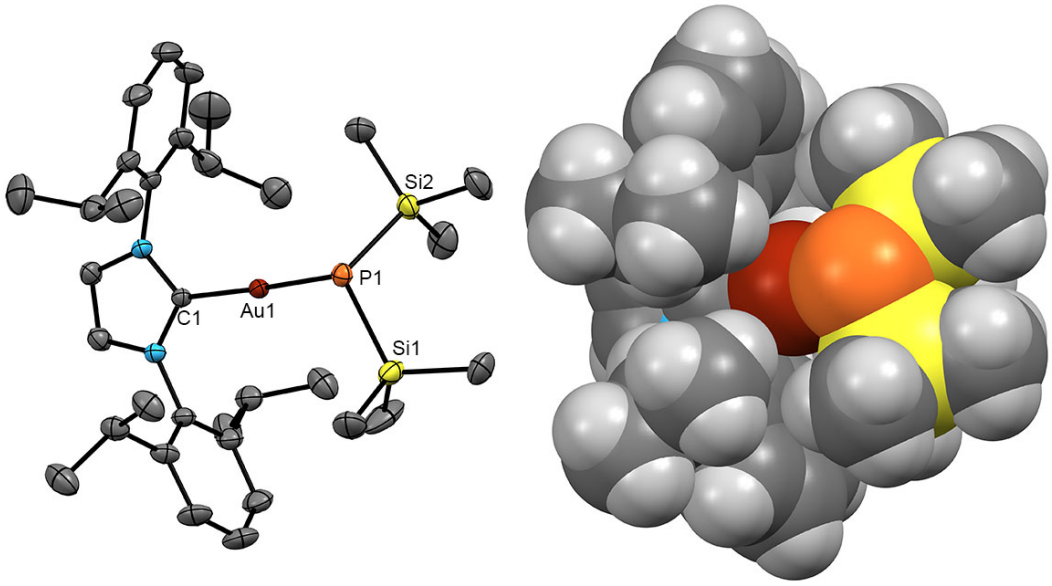

Figure 5-3 Left: Molecular structure of one of two independent molecules of [IPrAuP($SiMe_3$)$_2$] (**16**). Ellipsoids are at the 50% probability level and hydrogen atoms were omitted for clarity. Right: Space filling model. Au: dark red, P: orange, Si: yellow, N: blue, C: grey.

Table 5-2 Selected bond lengths (Å) and angles (°) for **16**

Au1–C1	2.0326(14)	C1–Au1–P1	175.74(4)
Au1–P1	2.3197(6)	Si1–P1–Si2	105.74(3)
P1–Si1	2.2228(8)	Si1–P1–Au1	101.50(2)
P1–Si2	2.2244(7)	Si2–P1–Au1	100.54(3)

Complex **19** was also structurally characterized by single crystal X-ray diffraction technique. This compound crystallizes in the space group *Pca*2$_1$ with Z = 4 with two THF molecules of crystallization. Two gold centers in the cation display bent geometry with an average angle of 173.3° while the phosphorus center has a distorted tetrahedral coordination around it with the angles ranging from 105.4(8)° to 121.46(15)°. In this cation, gold atoms show a distance of 3.996 Å, which is close to other non-cyclic phosphido bridging complexes,[11, 50] and illustrates that there is no significant aurophilic interaction between these gold centers.[51] Selected bond lengths and angles for **19** are listed in Table 5-4.

Table 5-3 Crystallographic information for **15**, **16**, **19**, **20**

Compound	**15**	**16**·$(C_5H_{12})_{0.25}$	**19**·$(C_4H_8O)_2$	**20**
Formula	$C_{36}H_{50}AuN_2PSi$	$C_{34.25}H_{56.75}AuN_2PSi_2$	$C_{75}H_{98}Au_3Cl_2N_4O_3P$	$C_{20}H_{15}O_2P$
Formula Weight (g/mol)	766.80	780.68	1796.34	318.29
Crystal Color and Habit	colourless block	yellow block	colourless plate	yellow needle
Crystal System	triclinic	triclinic	orthorhombic	triclinic
Space Group	$P\bar{1}$	$P\bar{1}$	$Pca2_1$	$P\bar{1}$
Temperature, K	110	110	110	110
a, Å	13.049(3)	12.547(3)	20.843(4)	5.9715(6)
b, Å	16.047(5)	16.043(4)	14.477(3)	8.3046(9)
c, Å	17.969(5)	20.509(5)	24.559(5)	16.379(2)
α,°	77.745(14)	89.721(9)	90	79.725(5)
β,°	89.241(10)	78.309(12)	90	87.641(4)
γ,°	86.737(10)	77.757(15)	90	78.852(5)
V, Å^3	3671.1(17)	3947.8(16)	7411(2)	784.11(15)
Z	4	4	4	2
F(000)	1552	1593	3544	332
ρ (g/cm^3)	1.387	1.313	1.610	1.348
μ (mm^{-1})	4.108	3.850	12.170	1.606
R_1	0.0367	0.0326	0.0540	0.0330
wR_2	0.0657	0.0613	0.1546	0.0868
GOF	0.985	0.995	1.047	1.072
Maximum shift/error	0.004	0.007	0.348	0.000

Although compound **20** was reported in a patent previously,[37] it has not been structurally characterized. This molecule crystallizes in the space group $P\bar{1}$ with $Z = 2$. The geometry around the P center is distorted trigonal pyramid with angles range from 96.74(7)° to 102.83(7)° where C7–P1–C14 is the smallest. The P1–C1, P1–C7, and P1–C17 bond lengths are 1.8195(15), 1.8822(16), and 1.8841(15) Å respectively (Figure 5-5).

Table 5-4 Selected bond lengths (Å) and angles (°) for **19**

Au1–C1	2.024(13)	C1–Au1–P1	175.5(4)
Au1–P1	2.288(3)	C28–Au2–P1	173.1(4)
Au2–C28	2.067(14)	C62–P1–C55	105.4(8)
Au2–P1	2.292(3)	C62–P1–Au1	111.2(6)
P1–C62	1.833(17)	C55–P1–Au1	104.6(6)
P1–C55	1.856(18)	C62–P1–Au2	107.5(5)
O1–C55	1.23(2)	C55–P1–Au2	105.5(6)

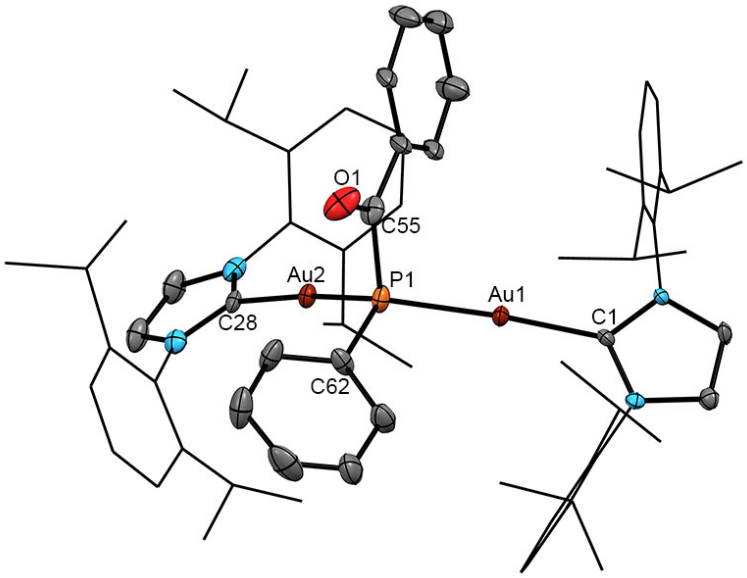

Figure 5-4 Molecular structure of $[(IPrAu)_2P(Ph)C(O)Ph]^+$ in the solid state. Ellipsoids are at the 50% probability level and hydrogen atoms were omitted for clarity. Au: dark red, P: orange, O: red, N: blue, C: grey.

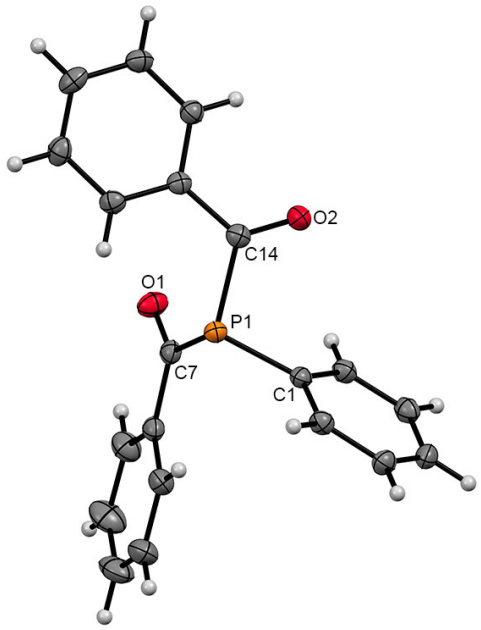

Figure 5-5 Molecular structure of **20** in the solid state. Ellipsoids are at the 50% probability. P: orange, O: red, C: grey, H: white.

5.4 Conclusions

Four new NHC coordinated gold silylphosphido complexes were successfully synthesized and characterized. Although the consequent reaction of **15** and **17** with benzoyl chloride confirmed the reactivity and accessibility of $–SiMe_3$ groups, the cleavage of Au–P bond occurred which resulted in the elimination of NHC–Au moieties. This may not be an issue when these complexes react with other metal sources (such as metal acetates) that do not contain strong nucleophiles (such as Cl^-) and hence those reactions should be investigated to take advantage of the accessible $–SiMe_3$ groups in **15**–**18**, in order to synthesize multinuclear complexes coordinated by NHC ligands. On the other hand, NMR studies showed that reaction of **17** with benzoyl chloride is a stepwise reaction. So it might be possible to synthesize asymmetric phosphines (PRR'R") by the addition of a different acylchloride in the second step of the reaction.

5.5 References

1. D. T. T. Tran, N. J. Taylor and J. F. Corrigan, *Angew. Chem. Int. Ed.*, 2000, **39**, 935-937.
2. C. B. Khadka, A. Eichhöfer, F. Weigend and J. F. Corrigan, *Inorg. Chem.*, 2012, **51**, 2747-2756.
3. S. C. Goel, M. Y. Chiang and W. E. Buhro, *J. Am. Chem. Soc.*, 1990, **112**, 5636-5637.
4. M. A. Matchett, A. M. Viano, N. L. Adolphi, R. D. Stoddard, W. E. Buhro, M. S. Conradi and P. C. Gibbons, *Chem. Mater.*, 1992, **4**, 508-511.
5. I. J. B. Lin and C. S. Vasam, *Can. J. Chem.*, 2005, **83**, 812-825.
6. S. Gaillard, C. S. J. Cazin and S. P. Nolan, *Acc. Chem. Res.*, 2012, **45**, 778-787.
7. S. P. Nolan, *Acc. Chem. Res.*, 2011, **44**, 91-100.
8. K. M. Hindi, M. J. Panzner, C. A. Tessier, C. L. Cannon and W. J. Youngs, *Chem. Rev.*, 2009, **109**, 3859-3884.
9. E. J. Fernández, A. Taguna and M. E. Olmos, *J. Chil. Chem. Soc.*, 2007, **52**, 1200-1205.
10. D. M. Stefanescu, H. F. Yuen, D. S. Glueck, J. A. Golen and A. L. Rheingold, *Angew. Chem. Int. Ed.*, 2003, **42**, 1046-1048.

11. D. M. Stefanescu, H. F. Yuen, D. S. Glueck, J. A. Golen, L. N. Zakharov, C. D. Incarvito and A. L. Rheingold, *Inorg. Chem.*, 2003, **42**, 8891-8901.
12. M. W. Johnson, S. L. Shevick, F. D. Toste and R. G. Bergman, *Chem. Sci.*, 2013, **4**, 1023-1027.
13. C. C. Cummins, C. Huang, T. J. Miller, M. W. Reintinger, J. M. Stauber, I. Tannou, D. Tofan, A. Toubaei, A. Velian and G. Wu, *Inorg. Chem.*, 2014, **53**, 3678-3687.
14. S. Gomez-Ruiz, R. Wolf, S. Bauer, H. Bittig, A. Schisler, P. Lonnecke and E. Hey-Hawkins, *Chem. Eur. J.*, 2008, **14**, 4511-4520.
15. H. Schmidbaur, *Chem. Soc. Rev.*, 1995, **24**, 391-400.
16. H. Schmidbaur, *Gold Bull.*, 2000, **33**, 3-10.
17. V. W. W. Yam and E. C. C. Cheng, *Chem. Soc. Rev.*, 2008, **37**, 1806-1813.
18. M. C. Gimeno and A. Laguna, *Chem. Soc. Rev.*, 2008, **37**, 1952-1966.
19. H. Schmidbaur, G. Weidenhiller, O. Steigelmann and G. Muller, *Z. Naturforsch. B: Chem. Sci.*, 1990, **45**, 747-752.
20. H. Schmidbaur, G. Weidenhiller, O. Steigelmann and G. Muller, *Chem. Ber.*, 1990, **123**, 285-287.
21. B. Assmann and H. Schmidbaur, *Chem. Ber. Recl.*, 1997, **130**, 217-219.
22. H. Schmidbaur, G. Weidenhiller and O. Steigelmann, *Angew. Chem. Int. Ed.*, 1991, **30**, 433-435.
23. H. Schmidbaur, E. Zeller and J. Ohshita, *Inorg. Chem.*, 1993, **32**, 4524-4526.
24. H. Schmidbaur, E. Zeller, G. Weidenhiller, O. Steigelmann and H. Beruda, *Inorg. Chem.*, 1992, **31**, 2370-2376.
25. E. Zeller, H. Beruda, J. Riede and H. Schmidbaur, *Inorg. Chem.*, 1993, **32**, 3068-3071.
26. T. K.-M. Lee, E. C.-C. Cheng, N. Zhu and V. W.-W. Yam, *Chem. Eur. J.*, 2014, **20**, 304-310.
27. M. C. Blanco, E. J. Fernandez, M. E. Olmos, J. Perez, O. Crespo, A. Laguna and P. G. Jones, *Organometallics*, 2004, **23**, 4373-4381.
28. P. Sevillano, O. Fuhr, E. Matern and D. Fenske, *Z. Anorg. Allg. Chem.*, 2006, **632**, 735-738.

29. B. Khalili Najafabadi and J. F. Corrigan, *Chem. Commun.*, 2015, **51**, 665-667.
30. G. Fritz and P. Scheer, *Chem. Rev.*, 2000, **100**, 3341-3402.
31. J. Hahn and T. Nataniel, *Z. Anorg. Allg. Chem.*, 1986, **543**, 7-21.
32. H. Karsch, F. Bienlein, T. Rupprich, F. Uhlig, E. Herrmann and M. Scheer, in *Synthetic methods of organometallic and inorganic chemistry :(HerrmannBrauer)*, ed. W. A. Herrmann, Georg Thieme Verlag , Stuttgart ; New York, 1996, pp. 58-65.
33. G. A. Fernandez, A. S. Picco, M. R. Ceolin, A. B. Chopa and G. F. Silbestri, *Organometallics*, 2013, **32**, 6315-6323.
34. R. Jothibasu, H. V. Huynh and L. L. Koh, *J. Organomet. Chem.*, 2008, **693**, 374-380.
35. G. M. Sheldrick, *Acta Crystallogr. Sect. C: Cryst. Struct. Commun.*, 2015, **71**, 3-8.
36. G. M. Sheldrick, *Acta Crystallogr. Sect. A: Found. Crystallogr.*, 2015, **71**, 3-8.
37. US3668093A, 1972.
38. C. Radloff, J. J. Weigand and F. E. Hahn, *Dalton Trans.*, 2009, 9392-9394.
39. M. Madadi, Dissertation/Thesis, School of Graduate and Postdoctoral Studies, University of Western Ontario, 2014.
40. S. Guo, H. Sivaram, D. Yuan and H. V. Huynh, *Organometallics*, 2013, **32**, 3685-3696.
41. A. Iglesias and K. Muniz, *Chem. Eur. J.*, 2009, **15**, 10563-10569.
42. H. J. Becher, D. Fenske and E. Langer, *Chem. Ber. Recl.*, 1973, **106**, 177-187.
43. G. Becker, *Z. Anorg. Allg. Chem.*, 1976, **423**, 242-254.
44. S. C. Goel, W. E. Buhro, N. L. Adolphi and M. S. Conradi, *J. Organomet. Chem.*, 1993, **449**, 9-18.
45. S. C. Goel, M. Y. Chiang, D. J. Rauscher and W. E. Buhro, *J. Am. Chem. Soc.*, 1993, **115**, 160-169.
46. F. Lindenberg and E. Heyhawkins, *J. Organomet. Chem.*, 1992, **435**, 291-297.
47. H. Schafer, *Z. Anorg. Allg. Chem.*, 1980, **467**, 105-122.
48. H. Schafer and D. Binder, *Z. Anorg. Allg. Chem.*, 1987, **546**, 55-78.
49. S. Gaillard, P. Nun, A. M. Z. Slawin and S. P. Nolan, *Organometallics*, 2010, **29**, 5402-5408.

50. R. G. Pritchard, D. B. Dyson, R. V. Parish, C. A. McAuliffe and B. Beagley, *J. Chem. Soc., Chem. Commun.*, 1987, 371-372.

51. H. Schmidbaur and A. Schier, *Chem. Soc. Rev.*, 2008, **37**, 1931-1951.

Chapter 6

Conclusions and Future Directions

N-Heterocyclic carbenes have been extensively studied during the past few decades, highlighting their unique characteristics in organometallic synthesis and their numerous applications as catalysts. However, their usage as ligands in stabilizing nanoclusters has been much less explored. On the other hand, metal silylphosphido complexes have been proven to be efficient molecular precursors for the formation of metal-phosphides. This thesis discussed the synthesis and characterization of coinage metal silylphosphido and t-butylthiolate complexes that are coordinated by NHC ligands and are promising molecular precursors for the synthesis of larger nanoclusters.

Chapter 2 illustrates a comparison between NHC and PR_3 ligands in solubilizing and stabilizing [CuS^tBu] and [AgS^tBu] coordination polymers to form polynuclear copper and silver t-butylthiolate clusters. It was found that NHCs are excellent alternatives for PR_3 ligands; furthermore, polynuclear clusters that had NHCs as stabilizing groups were more stable under ambient lighting conditions compared to those that were coordinated by PR_3 ligands. Molecular structures of the eight synthesized polynuclear clusters were characterized by X-ray diffraction technique, and were found to be related to the previously reported copper and silver t-butylthiolate clusters stabilized with PR_3 ligands. The cluster frameworks were found to be structurally affected by the steric demands of the ligands that were used to stabilize them.

It was shown in Chapter 3 that NHC coordinated copper silylphosphido complexes, [$^{i}Pr_2$-bimy)$_2$CuP(SiMe$_3$)$_2$] (**11**) and [(IPr)CuP(SiMe$_3$)$_2$] (**12**), exhibit enhanced thermal stability in the solid state, compared to the very sensitive homoleptic copper silylphosphido complex [Cu$_6${P(SiMe$_3$)$_2$}$_6$] (**9**). Their improved stability makes them better candidates for binary and ternary copper-phosphide cluster assembly, compared to the homoleptic copper silylphosphido complex (**9**). By means of employing two NHC ligands with very different steric characteristics, and different ligand-to-metal ratios, **11** and **12** become potential precursors for ternary phosphide nanocluster assembly.

Although similar mononuclear NHC ligated silver silylphosphido complexes were not isolated from analogous reactions with silver, two polynuclear AgP clusters [Ag$_{12}$(PSiMe$_3$)$_6$($^{i}Pr_2$-bimy)$_6$] (**13**) and [Ag$_{26}$P$_2$(PSiMe$_3$)$_{10}$($^{i}Pr_2$-bimy)$_8$] (**14**) were formed by applying the $^{i}Pr_2$-bimy ligand. These were the first examples of NHC-stabilized nanoscopic AgP clusters, whose synthesis and characterizations were discussed in Chapter 4. Formation and structural features of these isolated clusters indicate that NHCs are excellent ancillary ligands to be exploited in the synthesis of high-nuclearity frameworks.

Chapter 5 describes the synthesis of gold silylphosphido complexes coordinated with two NHC ligands: $^{i}Pr_2$-bimy and IPr. They both were successfully utilized in the facile preparation of gold complexes coordinated with either −P(SiMe$_3$)$_2$ or –P(Ph)SiMe$_3$ moieties. Furthermore, reactivity of the P−Si bond in [IPrAuP(Ph)SiMe$_3$] (**15**) and [($^{i}Pr_2$-bimy)AuP(Ph)SiMe$_3$] (**17**) was explored via the addition of PhC(O)Cl. The product of such reactions was the formation of [(IPrAu)$_2$PPhC(O)Ph][AuCl$_2$] (**19**) and PPh(C(O)Ph)$_2$ (**20**), respectively, as well as the elimination of ClSiMe$_3$. This confirms that the P−Si bond is indeed accessible, and thus, synthesized gold silylphosphido complexes are promising candidates for preparation of larger gold-phosphide clusters.

Further investigation in this area involves the application of the aforementioned synthesized molecular precursors in order to form large nanoclusters. This can be accomplished by reacting the copper and gold silylphosphido complexes with other metal salts in targeting ternary metal-phosphide clusters. It was shown in Chapter 5 that the chloride ion might result in the cleavage of Au–P bond as a result of its high nucleophilicity. Acetate ion, on the other hand, has lower nucleophilicity and thus, metal acetates could be more suitable reagents. Metal acetates have the potential to be coordinated by phosphine or

carbene ligands, which could further help stabilize the formed nanoclusters.

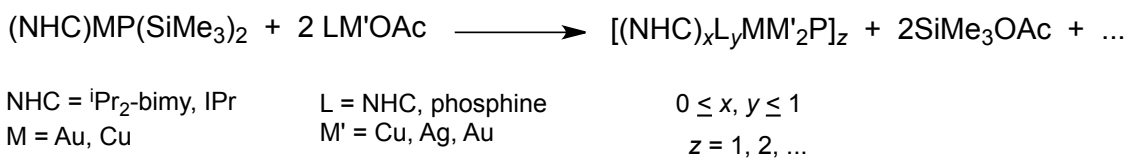

Scheme 6-1 General reaction of metal silylphosphido complexes with metal acetates to form metal phosphide clusters.

Molecular precursors containing –P(Ph)$SiMe_3$ are expected to form smaller multinuclear complexes via the reaction with other metal salts. This is due to the presence of only one $SiMe_3$ group attached to the phosphorus center in such precursors, to be eliminated via the activation reaction. Such smaller multinuclear complexes should be targeted as a starting point for this new area of cluster chemistry.

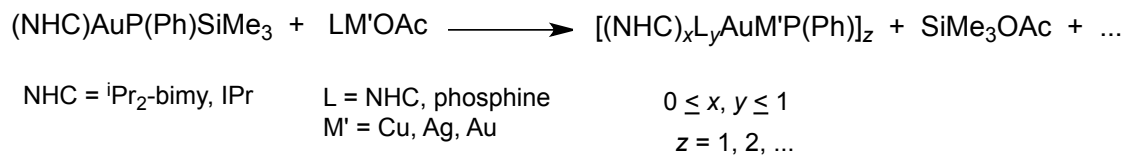

Scheme 6-2 General reaction of gold complexes containing –P(Ph)$SiMe_3$ with metal acetates to form multinuclear metal phosphide complexes.

During the course of this study, it was observed that IPr and especially $^{i}Pr_2$-bimy are not suitable ligands in terms of the formation of single crystals. Thus, exploration of other NHC ligands that improve crystallization of formed complexes is suggested. Employment of other NHC ligands with different steric demands should affect the size and stability of the formed clusters and even mononuclear complexes.

Appendices

A. Permission to Reuse Copyrighted Material

Copyright Clearance Center RightsLink®

Home | Create Account | Help | Live Chat

ACS Publications Most Trusted. Most Cited. Most Read.

Title: Synthesis of Cu-Doped InP Nanocrystals (d-dots) with ZnSe Diffusion Barrier as Efficient and Color-Tunable NIR Emitters

Author: Renguo Xie, Xiaogang Peng

Publication: Journal of the American Chemical Society

Publisher: American Chemical Society

Date: Aug 1, 2009

Copyright © 2009, American Chemical Society

LOGIN

If you're a copyright.com user, you can login to RightsLink using your copyright.com credentials. Already **a RightsLink user** or want to learn more?

PERMISSION/LICENSE IS GRANTED FOR YOUR ORDER AT NO CHARGE

This type of permission/license, instead of the standard Terms & Conditions, is sent to you because no fee is being charged for your order. Please note the following:

- Permission is granted for your request in both print and electronic formats, and translations.
- If figures and/or tables were requested, they may be adapted or used in part.
- Please print this page for your records and send a copy of it to your publisher/graduate school.
- Appropriate credit for the requested material should be given as follows: "Reprinted (adapted) with permission from (COMPLETE REFERENCE CITATION). Copyright (YEAR) American Chemical Society." Insert appropriate information in place of the capitalized words.
- One-time permission is granted only for the use specified in your request. No additional uses are granted (such as derivative works or other editions). For any other uses, please submit a new request.

If credit is given to another source for the material you requested, permission must be obtained from that source.

BACK | CLOSE WINDOW

RSC | Advancing the Chemical Sciences

Royal Society of Chemistry
Thomas Graham House
Science Park
Milton Road
Cambridge
CB4 0WF

Tel: +44 (0)1223 420 066
Fax: +44 (0)1223 423 623
Email: contracts-copyright@rsc.org

www.rsc.org

Acknowledgements to be used by RSC authors

Authors of RSC books and journal articles can reproduce material (for example a figure) from the RSC publication in a non-RSC publication, including theses, without formally requesting permission providing that the correct acknowledgement is given to the RSC publication. This permission extends to reproduction of large portions of text or the whole article or book chapter when being reproduced in a thesis.

The acknowledgement to be used depends on the RSC publication in which the material was published and the form of the acknowledgements is as follows:

- For material being reproduced from an article in *New Journal of Chemistry* the acknowledgement should be in the form:
  - [Original citation] - Reproduced by permission of The Royal Society of Chemistry (RSC) on behalf of the Centre National de la Recherche Scientifique (CNRS) and the RSC
- For material being reproduced from an article *Photochemical & Photobiological Sciences* the acknowledgement should be in the form:
  - [Original citation] - Reproduced by permission of The Royal Society of Chemistry (RSC) on behalf of the European Society for Photobiology, the European Photochemistry Association, and RSC
- For material being reproduced from an article in *Physical Chemistry Chemical Physics* the acknowledgement should be in the form:
  - [Original citation] - Reproduced by permission of the PCCP Owner Societies
- For material reproduced from books and any other journal the acknowledgement should be in the form:
  - [Original citation] - Reproduced by permission of The Royal Society of Chemistry

The acknowledgement should also include a hyperlink to the article on the RSC website.

The form of the acknowledgement is also specified in the RSC agreement/licence signed by the corresponding author.

Except in cases of republication in a thesis, this express permission does not cover the reproduction of large portions of text from the RSC publication or reproduction of the whole article or book chapter.

A publisher of a non-RSC publication can use this document as proof that permission is granted to use the material in the non-RSC publication.

VAT Registration Number: GB 342 1764 71 Registered Charity Number: 207890

B. Supporting Information for Chapter 2

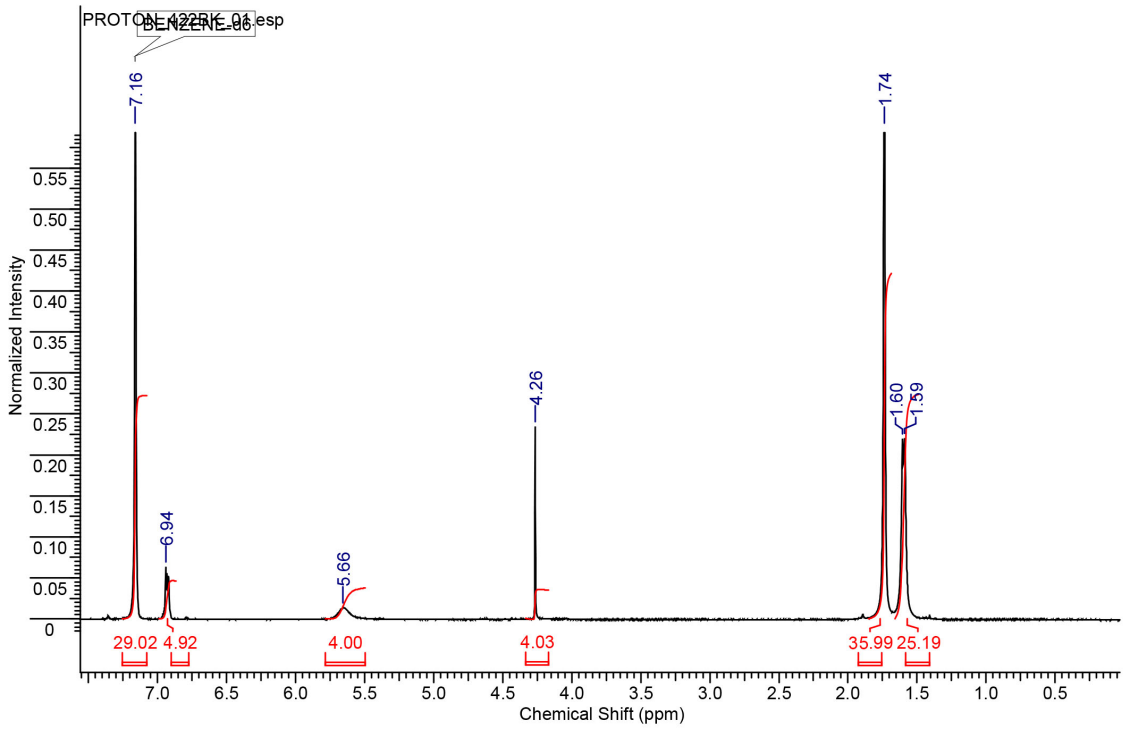

Figure B. 1 ^{1}H NMR spectrum of **1**

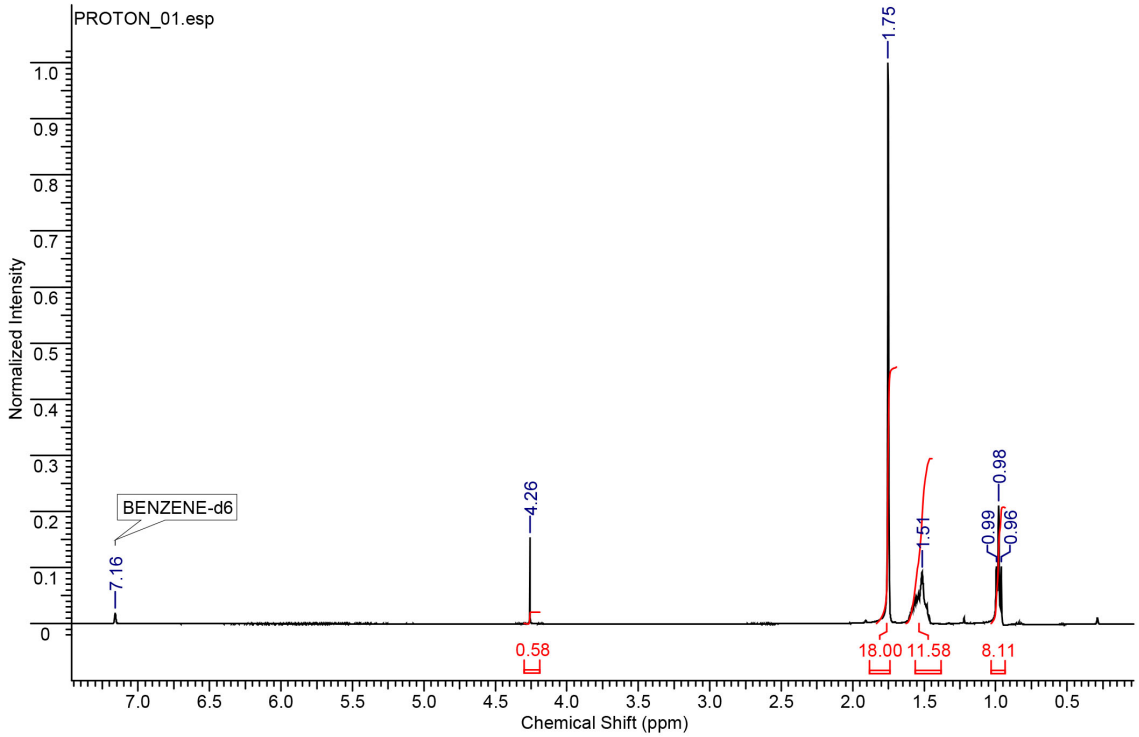

Figure B. 2 ^{1}H NMR spectrum of **3**

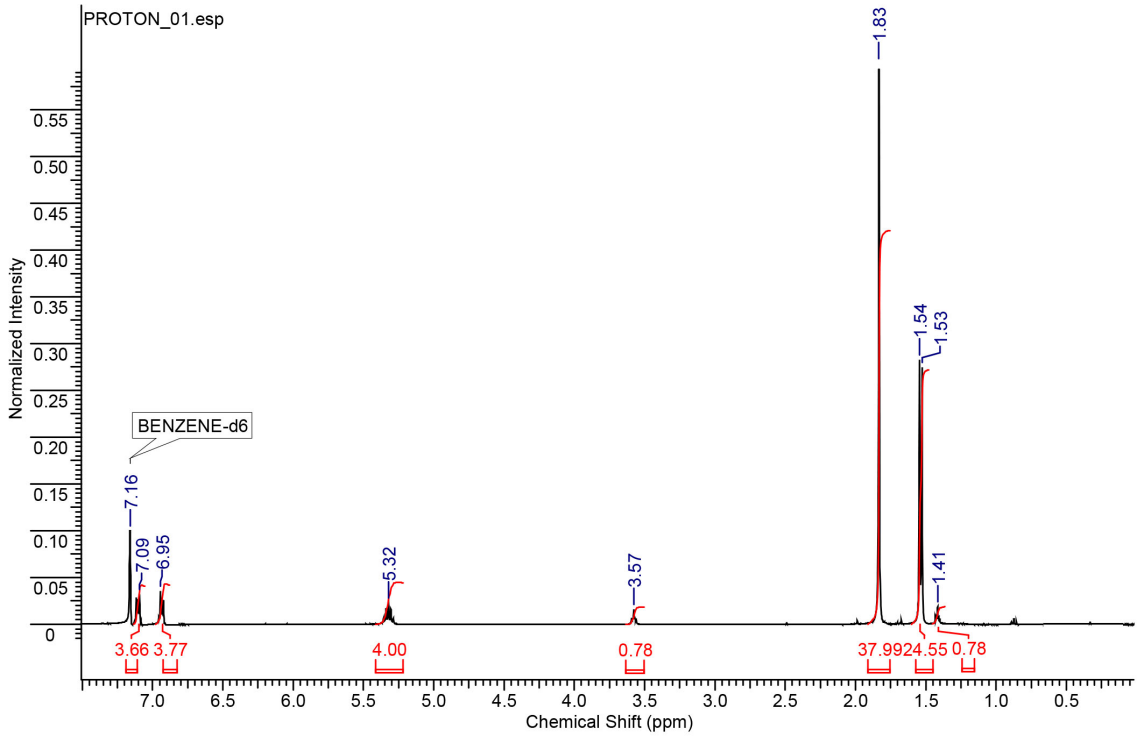

Figure B. 3 ^{1}H NMR spectrum of **5**

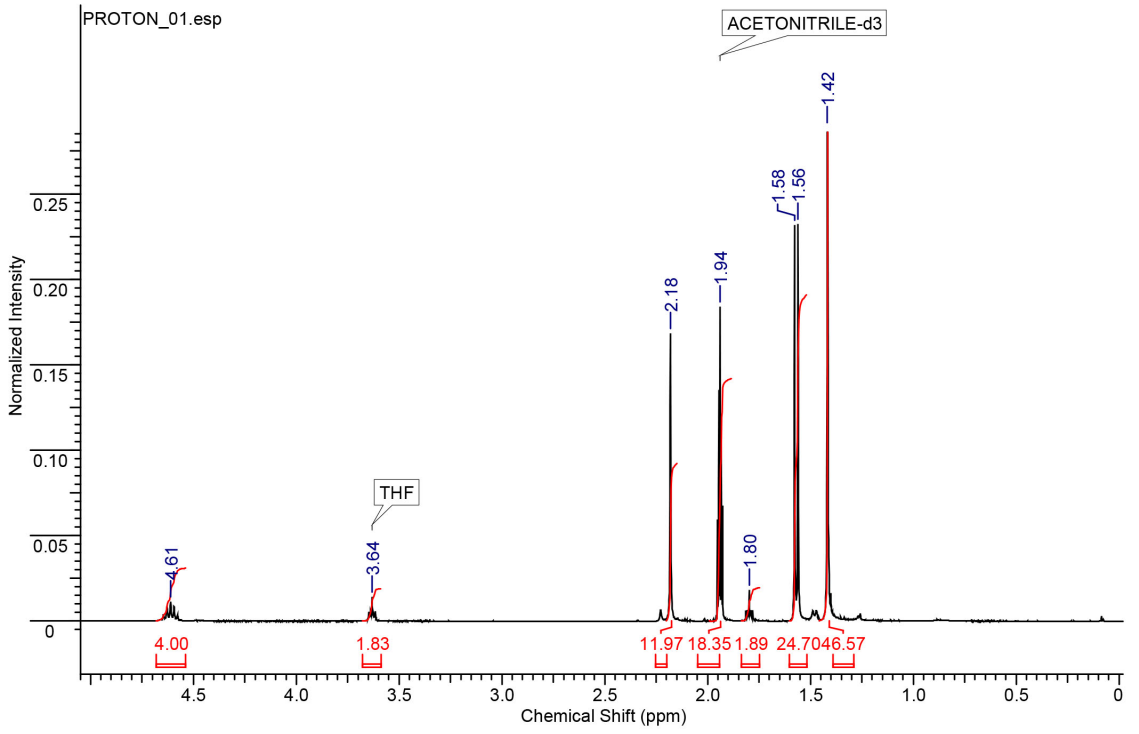

Figure B. 4 ^{1}H NMR spectrum of **6**

C. Supporting Information for Chapter 3

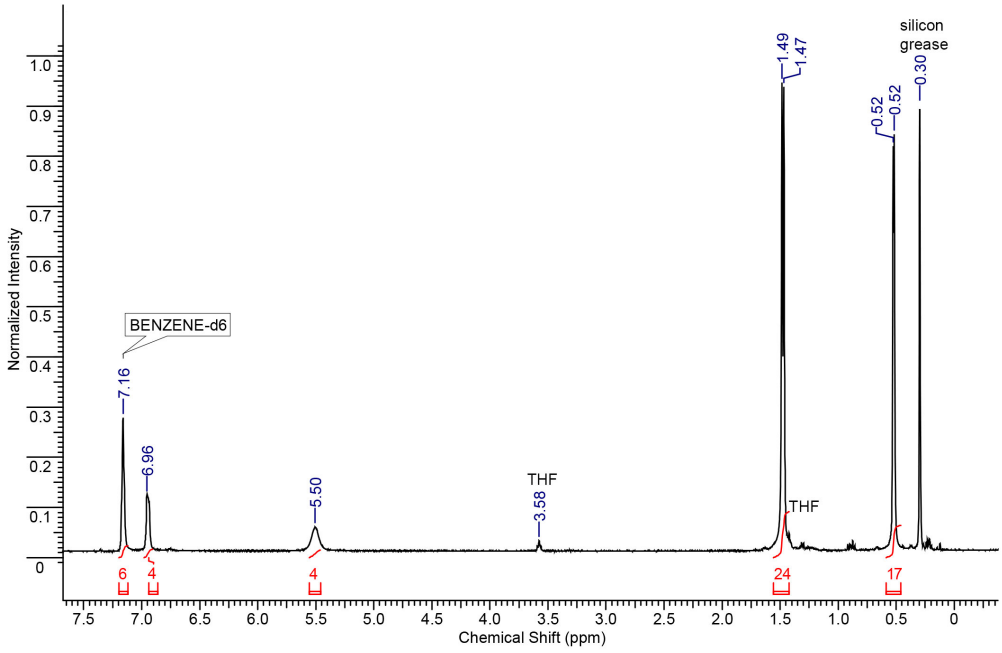

Figure C. 1 ^{1}H NMR spectrum of **11**

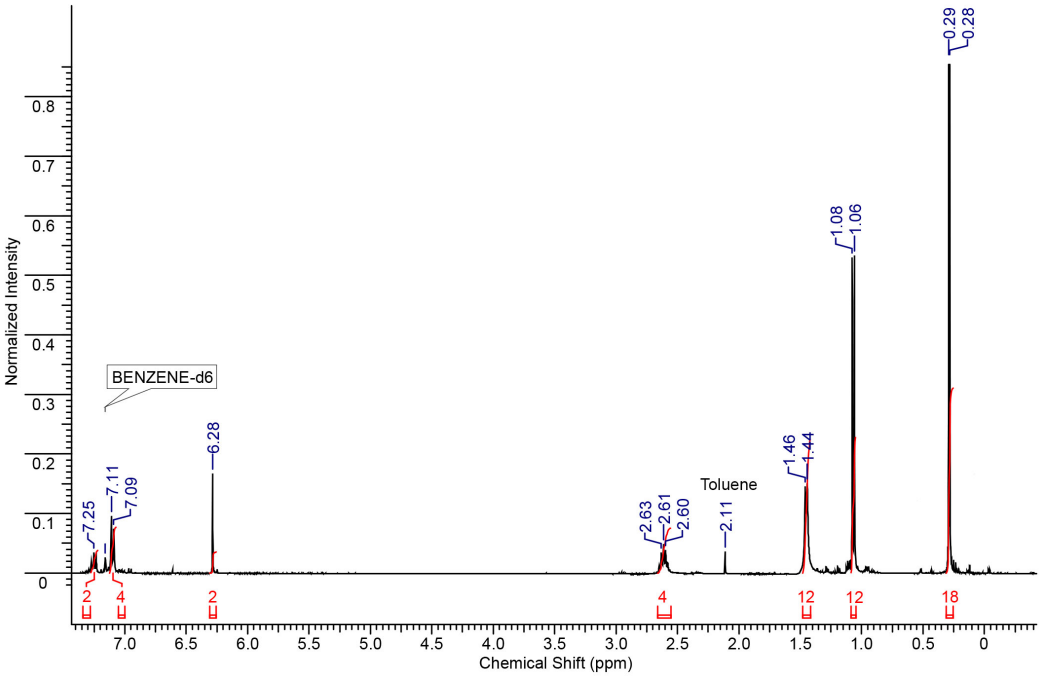

Figure C. 2 ^{1}H NMR spectrum of **12**

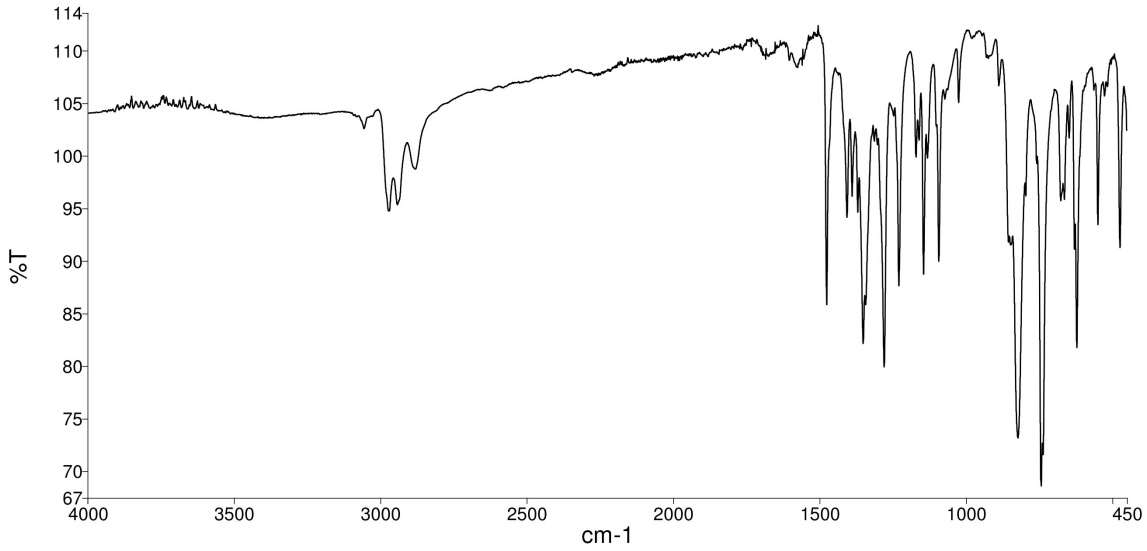

Figure C. 3 IR spectrum of **11**

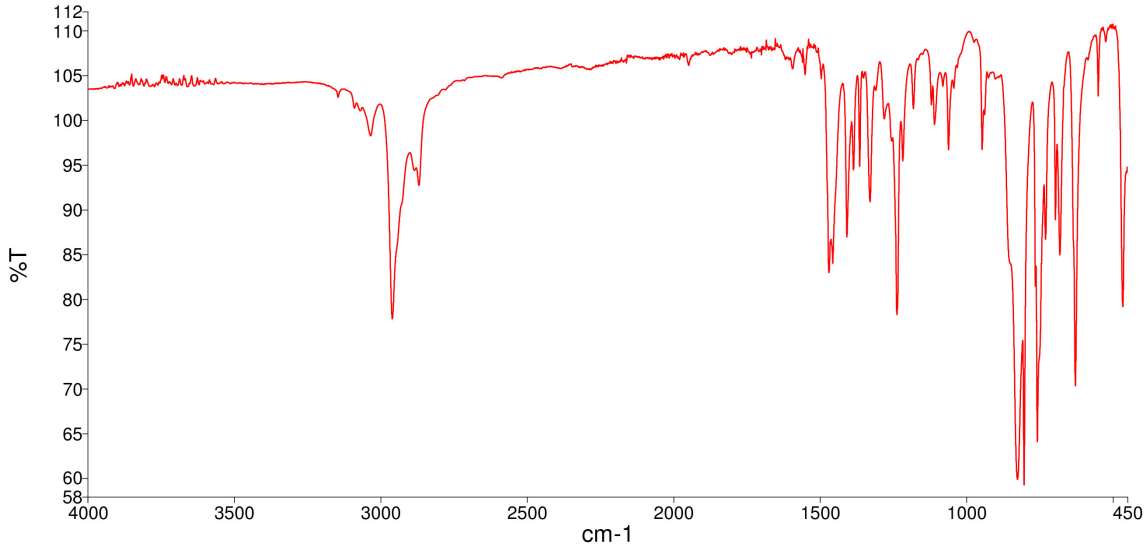

Figure C. 4 IR spectrum of **12**

D. X-ray Crystallographic Data Parameters for Compounds 1–16, 19, and 20

Table D. 1 Summary of Crystal Data for **1**

Formula	$C_{44}H_{76}Cl_4Cu_4N_4S_4$
Formula Weight (*g/mol*)	1185.28
Crystal Dimensions (*mm*)	0.352 × 0.333 × 0.198
Crystal Color and Habit	colourless block
Crystal System	monoclinic
Space Group	P $2_1/c$
Temperature, K	110(2)
a, Å	10.315(2)
b, Å	24.927(7)
c, Å	11.256(2)
α,°	90
β,°	104.654(10)
γ,°	90
V, $Å^3$	2800.0(12)
Number of reflections to determine final unit cell	5711
Min and Max 2θ for cell determination, °	19.1, 66.34
Z	2
F(000)	1232
ρ (g/cm^3)	1.406
λ, Å, (MoKα)	0.71073
μ (mm^{-1})	1.871
Diffractometer Type	Bruker APEX-II CCD
Scan Type(s)	φ and ω scans
Max 2θ for data collection, °	77.448
Measured fraction of data	0.998
Number of reflections measured	118869
Unique reflections measured	15872
R_{merge}	0.0408
Number of reflections included in refinement	15872
Cut off Threshold Expression	$I > 2\sigma(I)$
Structure refined using	full matrix least-squares using F^2
Number of parameters in least-squares	331
R_1	0.0315
wR_2	0.0680
R_1 (all data)	0.0518
wR_2 (all data)	0.0743
GOF	1.034
Maximum shift/error	0.002
Min & Max peak heights on final ΔF Map (e^-/Å)	-0.623, 0.851

Table D. 2 Summary of Crystal Data for **2**

Formula	$C_{40}H_{80}Cl_4Cu_4N_4S_4$
Formula Weight (*g/mol*)	1141.28
Crystal Dimensions (*mm*)	0.32 × 0.14 × 0.10
Crystal Color and Habit	colourless tetragonal prism
Crystal System	Monoclinic
Space Group	P2(1)/c
Temperature, K	110(2)
a, Å	10.363(2)
b, Å	23.568(6)
c, Å	11.579(3)
α,°	90.00
β,°	106.670(4)
γ,°	90.00
V, $Å^3$	2709.0(12)
Number of reflections to determine final unit cell	2759
Min and Max 2θ for cell determination, °	6.46, 64.9
Z	2
F(000)	1192
ρ (g/cm^3)	1.399
λ, Å, (MoKα)	0.71073
μ (mm^{-1})	1.930
Diffractometer Type	Bruker APEX-II CCD
Scan Type(s)	φ and ω scans
Max 2θ for data collection, °	66.4
Measured fraction of data	0.998
Number of reflections measured	126773
Unique reflections measured	10352
R_{merge}	0.0381
Number of reflections included in refinement	10352
Cut off Threshold Expression	>2σ(I)
Structure refined using	full matrix least-squares using F^2
Number of parameters in least-squares	284
R_1	0.0288
wR_2	0.0702
R_1 (all data)	0.0401
wR_2 (all data)	0.0744
GOF	1.032
Maximum shift/error	0.002
Min & Max peak heights on final ΔF Map (e^-/Å)	-0.567, 1.536

Table D. 3 Summary of Crystal Data for **3**

Formula	$C_{34}H_{78}Cu_4P_2S_4$
Formula Weight (g/mol)	931.30
Crystal Dimensions (mm)	0.206 × 0.158 × 0.151
Crystal Color and Habit	colourless block
Crystal System	triclinic
Space Group	P -1
Temperature, K	150(2)
a, Å	9.468(3)
b, Å	10.869(4)
c, Å	12.157(5)
α,°	68.774(14)
β,°	78.351(10)
γ,°	82.542(12)
V, $Å^3$	1139.9(7)
Number of reflections to determine final unit cell	7723
Min and Max 2q for cell determination, °	5.58, 61.02
Z	1
F(000)	492
ρ (g/cm^3)	1.357
λ, Å, (MoKa)	0.71073
μ (mm^{-1})	2.115
Diffractometer Type	Bruker APEX-II CCD
Scan Type(s)	φ and ω scans
Max 2θ for data collection, °	71.81
Measured fraction of data	0.955
Number of reflections measured	25671
Unique reflections measured	8769
R_{merge}	0.0314
Number of reflections included in refinement	8769
Cut off Threshold Expression	$I > 2\sigma(I)$
Structure refined using	full matrix least-squares using F^2
Number of parameters in least-squares	208
R_1	0.0368
wR_2	0.0735
R_1 (all data)	0.0647
wR_2 (all data)	0.0821
GOF	1.005
Maximum shift/error	0.002
Min & Max peak heights on final DF Map ($e^-/Å$)	-0.451, 0.511

Table D. 4 Summary of Crystal Data for **4**

Formula	$C_{34}H_{78}Cu_4P_2S_4$
Formula Weight (*g/mol*)	931.30
Crystal Dimensions (*mm*)	0.612 × 0.233 × 0.223
Crystal Color and Habit	colourless needle
Crystal System	monoclinic
Space Group	P $2_1/c$
Temperature, K	110(2)
a, Å	10.2300(14)
b, Å	13.023(2)
c, Å	18.533(3)
α,°	90
β,°	114.317(4)
γ,°	90
V, $Å^3$	2250.0(6)
Number of reflections to determine final unit cell	4623
Min and Max 2θ for cell determination, °	5.74, 71.3
Z	2
F(000)	984
ρ (g/cm^3)	1.375
λ, Å, (MoKα)	0.71073
μ (mm^{-1})	2.143
Diffractometer Type	Bruker APEX-II CCD
Scan Type(s)	φ and ω scans
Max 2θ for data collection, °	78.722
Measured fraction of data	0.997
Number of reflections measured	19802
Unique reflections measured	19802
Number of reflections included in refinement	19802
Cut off Threshold Expression	$I > 2\sigma(I)$
Structure refined using	full matrix least-squares using F^2
Number of parameters in least-squares	212
R_1	0.0298
wR_2	0.0592
R_1 (all data)	0.0442
wR_2 (all data)	0.0625
GOF	1.016
Maximum shift/error	0.003
Min & Max peak heights on final ΔF Map (e^-/Å)	-0.477, 0.465

Table D. 5 Summary of Crystal Data for **5**

Formula	$C_{98}H_{160}Ag_8N_8S_8$
Formula Weight (*g/mol*)	2569.77
Crystal Dimensions (*mm*)	0.138 × 0.083 × 0.076
Crystal Color and Habit	colourless prism
Crystal System	triclinic
Space Group	P -1
Temperature, K	111(2)
a, Å	9.990(3)
b, Å	12.648(4)
c, Å	23.429(9)
α,°	78.597(13)
β,°	78.069(9)
γ,°	80.553(12)
V, $Å^3$	2815.7(17)
Number of reflections to determine final unit cell	9986
Min and Max 2θ for cell determination, °	4.86, 53.48
Z	1
F(000)	1308
ρ (g/cm^3)	1.516
λ, Å, (MoKα)	0.71073
μ (mm^{-1})	1.553
Diffractometer Type	Bruker APEX-II CCD
Scan Type(s)	φ and ω scans
Max 2θ for data collection, °	56.574
Measured fraction of data	0.999
Number of reflections measured	52327
Unique reflections measured	13901
R_{merge}	0.0362
Number of reflections included in refinement	13901
Cut off Threshold Expression	$I > 2\sigma(I)$
Structure refined using	full matrix least-squares using F^2
Number of parameters in least-squares	616
R_1	0.0464
wR_2	0.1068
R_1 (all data)	0.0778
wR_2 (all data)	0.1234
GOF	1.051
Maximum shift/error	0.002
Min & Max peak heights on final ΔF Map (e^-/Å)	-1.243, 1.728

Table D. 6 Summary of Crystal Data for **6**

Formula	$C_{47.38}H_{96.75}Ag_6N_4O_{0.34}S_6$
Formula Weight (g/mol)	1567.61
Crystal Dimensions (mm)	0.210 × 0.170 × 0.115
Crystal Color and Habit	colourless needle
Crystal System	monoclinic
Space Group	C 2
Temperature, K	150(2)
a, Å	29.293(11)
b, Å	12.976(5)
c, Å	19.198(8)
α,°	90
β,°	98.423(7)
γ,°	90
V, $Å^3$	7219(5)
Number of reflections to determine final unit cell	9974
Min and Max 2θ for cell determination, °	5.44, 43.96
Z	4
F(000)	3159
ρ (g/cm^3)	1.442
λ, Å, (MoKa)	0.71073
μ (mm^{-1})	1.798
Diffractometer Type	Nonius Kappa-CCD
Scan Type(s)	φ and ω scans
Max 2θ for data collection, °	57.698
Measured fraction of data	0.998
Number of reflections measured	101010
Unique reflections measured	18753
R_{merge}	0.0763
Number of reflections included in refinement	18753
Cut off Threshold Expression	$I > 2\sigma(I)$
Structure refined using	full matrix least-squares using F^2
Number of parameters in least-squares	638
R_1	0.0523
wR_2	0.1457
R_1 (all data)	0.0784
wR_2 (all data)	0.1648
GOF	1.043
Maximum shift/error	0.000
Min & Max peak heights on final DF Map ($e^-/Å$)	-0.896, 1.909

Table D. 7 Summary of Crystal Data for **7**

Formula	$C_{34}H_{78}Ag_4P_2S_4$
Formula Weight (g/mol)	1108.62
Crystal Dimensions (mm)	0.37 × 0.23 × 0.21
Crystal Color and Habit	colourless block
Crystal System	Triclinic
Space Group	P-1
Temperature, K	110(2)
a, Å	9.538(4)
b, Å	10.919(3)
c, Å	12.288(4)
α,°	69.848(19)
β,°	78.879(13)
γ,°	83.194(9)
V, Å^3	1177.0(7)
Number of reflections to determine final unit cell	9932
Min and Max 2θ for cell determination, °	5.16, 69.7
Z	1
F(000)	564
ρ (g/cm^3)	1.564
λ, Å, (MoKa)	0.71073
μ (mm^{-1})	1.905
Diffractometer Type	Bruker APEX-II CCD
Scan Type(s)	φ and ω scans
Max 2θ for data collection, °	71.16
Measured fraction of data	0.991
Number of reflections measured	26384
Unique reflections measured	8855
R_{merge}	0.0169
Number of reflections included in refinement	8855
Cut off Threshold Expression	>2σ(I)
Structure refined using	full matrix least-squares using F^2
Number of parameters in least-squares	208
R_1	0.0191
wR_2	0.0374
R_1 (all data)	0.0253
wR_2 (all data)	0.0396
GOF	1.024
Maximum shift/error	0.004
Min & Max peak heights on final DF Map (e-/Å)	-0.502, 0.470

Table D. 8 Summary of Crystal Data for **8**

Formula	$C_{42}H_{96}Ag_6P_2S_6$
Formula Weight (*g/mol*)	1502.70
Crystal Dimensions (*mm*)	0.066 × 0.052 × 0.039
Crystal Color and Habit	colourless tetragonal prism
Crystal System	orthorhombic
Space Group	P n n a
Temperature, K	110(2)
a, Å	24.641(9)
b, Å	15.066(5)
c, Å	16.081(5)
α,°	90
β,°	90
γ,°	90
V, $Å^3$	5970(4)
Number of reflections to determine final unit cell	9456
Min and Max 2θ for cell determination, °	6.06, 51.34
Z	4
F(000)	3024
ρ (g/cm^3)	1.672
λ, Å, (MoKα)	0.71073
μ (mm^{-1})	2.219
Diffractometer Type	Bruker APEX-II CCD
Scan Type(s)	φ and ω scans
Max 2θ for data collection, °	51.424
Measured fraction of data	0.998
Number of reflections measured	83082
Unique reflections measured	5693
R_{merge}	0.0927
Number of reflections included in refinement	5693
Cut off Threshold Expression	$I > 2\sigma(I)$
Structure refined using	full matrix least-squares using F^2
Number of parameters in least-squares	320
R_1	0.0411
wR_2	0.0878
R_1 (all data)	0.0792
wR_2 (all data)	0.1056
GOF	1.026
Maximum shift/error	0.001
Min & Max peak heights on final ΔF Map (e^-/Å)	-0.750, 0.850

Table D. 9 Summary of Crystal Data for **9**

Formula	$C_{40}H_{116}Cu_6OP_6Si_{12}$
Formula Weight (*g/mol*)	1517.46
Crystal Dimensions (*mm*)	0.270 × 0.210 × 0.200
Crystal Color and Habit	colourless prism
Crystal System	triclinic
Space Group	P -1
Temperature, K	150
a, Å	9.813(7)
b, Å	15.477(10)
c, Å	16.325(9)
α,°	62.453(15)
β,°	73.25(2)
γ,°	77.325(18)
V, $Å^3$	2094(2)
Number of reflections to determine final unit cell	9975
Min and Max 2θ for cell determination, °	4.68, 54.46
Z	1
F(000)	796
ρ (g/cm^3)	1.203
λ, Å, (MoKα)	0.71073
μ (mm^{-1})	1.806
Diffractometer Type	Bruker Kappa Axis Apex2
Scan Type(s)	φ and ω scans
Max 2θ for data collection, °	62.426
Measured fraction of data	0.999
Number of reflections measured	46231
Unique reflections measured	12781
R_{merge}	0.0465
Number of reflections included in refinement	12781
Cut off Threshold Expression	$I > 2\sigma(I)$
Structure refined using	full matrix least-squares using F^2
Number of parameters in least-squares	334
R_1	0.0585
wR_2	0.1510
R_1 (all data)	0.1119
wR_2 (all data)	0.1833
GOF	1.033
Maximum shift/error	0.023
Min & Max peak heights on final ΔF Map (e^-/Å)	-0.900, 1.969

Table D. 10 Summary of Crystal Data for **10**

Formula	$C_{40}H_{116}Ag_6OP_6Si_{12}$
Formula Weight (*g/mol*)	1783.44
Crystal Dimensions (*mm*)	0.200 × 0.150 × 0.020
Crystal Color and Habit	colourless block
Crystal System	triclinic
Space Group	P -1
Temperature, K	150(2)
a, Å	9.836(2)
b, Å	15.683(3)
c, Å	16.709(3)
α,°	63.81(3)
β,°	74.78(3)
γ,°	79.34(3)
V, $Å^3$	2224.6(10)
Number of reflections to determine final unit cell	9772
Min and Max 2θ for cell determination, °	4.08, 54.96
Z	1
F(000)	904
ρ (g/cm^3)	1.331
λ, Å, (MoKα)	0.71073
μ (mm^{-1})	1.587
Diffractometer Type	Bruker P4
Scan Type(s)	φ and ω scans
Max 2θ for data collection, °	55.05
Measured fraction of data	0.998
Number of reflections measured	18731
Unique reflections measured	10063
R_{merge}	0.0373
Number of reflections included in refinement	10063
Cut off Threshold Expression	$I > 2\sigma(I)$
Structure refined using	full matrix least-squares using F^2
Number of parameters in least-squares	326
R_1	0.0490
wR_2	0.1319
R_1 (all data)	0.0780
wR_2 (all data)	0.1489
GOF	1.048
Maximum shift/error	0.000
Min & Max peak heights on final ΔF Map (e^-/Å)	-1.062, 1.092

Table D. 11 Summary of Crystal Data for **11**

Formula	$C_{32}H_{54}CuN_4PSi_2$
Formula Weight (*g/mol*)	645.48
Crystal Dimensions (*mm*)	0.252 × 0.248 × 0.076
Crystal Color and Habit	colourless plate
Crystal System	triclinic
Space Group	P -1
Temperature, K	150(2)
a, Å	9.611(4)
b, Å	20.206(8)
c, Å	20.631(6)
α,°	102.042(13)
β,°	89.995(9)
γ,°	96.848(8)
V, Å^3	3889(2)
Number of reflections to determine final unit cell	4842
Min and Max 2θ for cell determination, °	4.52, 49.42
Z	4
F(000)	1384
ρ (*g/cm*^{3})	1.102
λ, Å, (MoKα)	0.71073
μ (*mm*$^{-1}$)	0.688
Diffractometer Type	Bruker Kappa Axis Apex2
Scan Type(s)	φ and ω scans
Max 2θ for data collection, °	51.186
Measured fraction of data	0.607
Number of reflections measured	9151
Unique reflections measured	9151
Number of reflections included in refinement	9151
Cut off Threshold Expression	I > 2σ(I)
Structure refined using	full matrix least-squares using F^2
Number of parameters in least-squares	755
R_1	0.1280
wR_2	0.3310
R_1 (all data)	0.1476
wR_2 (all data)	0.3411
GOF	1.323
Maximum shift/error	0.001
Min & Max peak heights on final ΔF Map (*e*$^-$/Å)	-1.933, 1.077

Table D. 12 Summary of Crystal Data for **12**

Formula	$C_{40}H_{62}CuN_2PSi_2$
Formula Weight (*g/mol*)	721.60
Crystal Dimensions (*mm*)	0.441 × 0.423 × 0.151
Crystal Color and Habit	colourless plate
Crystal System	monoclinic
Space Group	P $2_1/c$
Temperature, K	110
a, Å	22.988(7)
b, Å	10.325(3)
c, Å	18.132(4)
α,°	90
β,°	94.917(8)
γ,°	90
V, $Å^3$	4288(2)
Number of reflections to determine final unit cell	9967
Min and Max 2θ for cell determination, °	5.32, 53.9
Z	4
F(000)	1552
ρ (g/cm^3)	1.118
λ, Å, (MoKα)	0.71073
μ (mm^{-1})	0.629
Diffractometer Type	Bruker Kappa Axis Apex2
Scan Type(s)	φ and ω scans
Max 2θ for data collection, °	56.73
Measured fraction of data	0.996
Number of reflections measured	57174
Unique reflections measured	10642
R_{merge}	0.0538
Number of reflections included in refinement	10642
Cut off Threshold Expression	$I > 2\sigma(I)$
Structure refined using	full matrix least-squares using F^2
Number of parameters in least-squares	430
R_1	0.0925
wR_2	0.2521
R_1 (all data)	0.1145
wR_2 (all data)	0.2631
GOF	1.110
Maximum shift/error	0.000
Min & Max peak heights on final ΔF Map (e^-/Å)	-0.891, 1.200

Table D. 13 Summary of Crystal Data for **13**

Formula	$C_{98}H_{167}Ag_{12}N_{12}O_{0.50}P_6Si_6$
Formula Weight (*g/mol*)	3170.23
Crystal Dimensions (*mm*)	0.154 × 0.117 × 0.040
Crystal Color and Habit	orange plate
Crystal System	monoclinic
Space Group	P 2_1
Temperature, K	110(2)
a, Å	15.889(8)
b, Å	18.207(12)
c, Å	23.994(15)
α,°	90
β,°	95.206(15)
γ,°	90
V, $Å^3$	6913(7)
Number of reflections to determine final unit cell	9878
Min and Max 2θ for cell determination, °	4.66, 39.56
Z	2
F(000)	3162
ρ (g/cm^3)	1.523
λ, Å, (MoKα)	0.71073
μ (mm^{-1})	1.821
Diffractometer Type	Bruker APEX-II CCD
Scan Type(s)	φ and ω scans
Max 2θ for data collection, °	51.414
Measured fraction of data	0.932
Number of reflections measured	64639
Unique reflections measured	22050
R_{merge}	0.0616
Number of reflections included in refinement	22050
Cut off Threshold Expression	I > 2σ(I)
Structure refined using	full matrix least-squares using F^2
Number of parameters in least-squares	1245
R_1	0.0572
wR_2	0.1149
R_1 (all data)	0.1165
wR_2 (all data)	0.1359
GOF	1.024
Maximum shift/error	0.041
Min & Max peak heights on final ΔF Map (e^-/Å)	-0.996, 1.259

Table D. 14 Summary of Crystal Data for **14**

Formula	$C_{141}H_{250.80}Ag_{26}N_{16}P_{12}Si_{10}$
Formula Weight (*g/mol*)	5627.52
Crystal Dimensions (*mm*)	0.119 × 0.113 × 0.005
Crystal Color and Habit	orange plate
Crystal System	triclinic
Space Group	P -1
Temperature, K	293(2)
a, Å	17.285(4)
b, Å	20.433(5)
c, Å	29.512(8)
α,°	95.465(12)
β,°	91.603(9)
γ,°	90.317(19)
V, $Å^3$	10371(4)
Number of reflections to determine final unit cell	9762
Min and Max 2θ for cell determination, °	5.08, 49.24
Z	2
F(000)	5502
ρ (g/cm^3)	1.802
λ, Å, (MoKα)	0.71073
μ (mm^{-1})	2.582
Diffractometer Type	Bruker APEX-II CCD
Scan Type(s)	φ and ω scans
Max 2θ for data collection, °	49.556
Measured fraction of data	0.933
Number of reflections measured	128323
Unique reflections measured	35023
R_{merge}	0.0846
Number of reflections included in refinement	35023
Cut off Threshold Expression	$I > 2\sigma(I)$
Structure refined using	full matrix least-squares using F^2
Number of parameters in least-squares	1940
R_1	0.0555
wR_2	0.1142
R_1 (all data)	0.1234
wR_2 (all data)	0.1372
GOF	1.016
Maximum shift/error	0.001
Min & Max peak heights on final ΔF Map (e^-/Å)	-0.866, 2.185

Table D. 15 Summary of Crystal Data for **15**

Formula	$C_{36}H_{50}AuN_2PSi$
Formula Weight (*g/mol*)	766.80
Crystal Dimensions (*mm*)	0.235 × 0.182 × 0.171
Crystal Color and Habit	colourless block
Crystal System	triclinic
Space Group	P -1
Temperature, K	110
a, Å	13.049(3)
b, Å	16.047(5)
c, Å	17.969(5)
α,°	77.745(14)
β,°	89.241(10)
γ,°	86.737(10)
V, $Å^3$	3671.1(17)
Number of reflections to determine final unit cell	9622
Min and Max 2θ for cell determination, °	5.94, 73.34
Z	4
F(000)	1552
ρ (g/cm^3)	1.387
λ, Å, (MoKα)	0.71073
μ (mm^{-1})	4.108
Diffractometer Type	Bruker Kappa Axis Apex2
Scan Type(s)	φ and ω scans
Max 2θ for data collection, °	85.082
Measured fraction of data	0.996
Number of reflections measured	229426
Unique reflections measured	52085
R_{merge}	0.0603
Number of reflections included in refinement	52085
Cut off Threshold Expression	$I > 2\sigma(I)$
Structure refined using	full matrix least-squares using F^2
Number of parameters in least-squares	761
R_1	0.0367
wR_2	0.0657
R_1 (all data)	0.0765
wR_2 (all data)	0.0744
GOF	0.985
Maximum shift/error	0.004
Min & Max peak heights on final ΔF Map (e^-/Å)	-1.129, 1.511

Table D. 16 Summary of Crystal Data for **16**

Formula	$C_{34.25}H_{56.75}AuN_2PSi_2$
Formula Weight (*g/mol*)	780.68
Crystal Dimensions (*mm*)	0.345 × 0.315 × 0.223
Crystal Color and Habit	yellow block
Crystal System	triclinic
Space Group	P -1
Temperature, K	110
a, Å	12.547(3)
b, Å	16.043(4)
c, Å	20.509(5)
α,°	89.721(9)
β,°	78.309(12)
γ,°	77.757(15)
V, $Å^3$	3947.8(16)
Number of reflections to determine final unit cell	9181
Min and Max 2θ for cell determination, °	5.66, 68.1
Z	4
F(000)	1593
ρ (g/cm^3)	1.313
λ, Å, (MoKα)	0.71073
μ (mm^{-1})	3.850
Diffractometer Type	Bruker Kappa Axis Apex2
Scan Type(s)	φ and ω scans
Max 2θ for data collection, °	86.164
Measured fraction of data	0.997
Number of reflections measured	252467
Unique reflections measured	57841
R_{merge}	0.0407
Number of reflections included in refinement	57841
Cut off Threshold Expression	$I > 2\sigma(I)$
Structure refined using	full matrix least-squares using F^2
Number of parameters in least-squares	759
R_1	0.0326
wR_2	0.0613
R_1 (all data)	0.0727
wR_2 (all data)	0.0697
GOF	0.995
Maximum shift/error	0.007
Min & Max peak heights on final ΔF Map (e^-/Å)	-1.266, 2.303

Table D. 17 Summary of Crystal Data for **19**

Formula	$C_{75}H_{98}Au_3Cl_2N_4O_3P$
Formula Weight (*g/mol*)	1796.34
Crystal Dimensions (*mm*)	0.387 × 0.202 × 0.106
Crystal Color and Habit	colourless plate
Crystal System	orthorhombic
Space Group	P c a 2_1
Temperature, K	110
a, Å	20.843(4)
b, Å	14.477(3)
c, Å	24.559(5)
α,°	90
β,°	90
γ,°	90
V, $Å^3$	7411(2)
Number of reflections to determine final unit cell	9935
Min and Max 2θ for cell determination, °	8.26, 133.52
Z	4
F(000)	3544
ρ (g/cm^3)	1.610
λ, Å, (CuKα)	1.54178
μ (mm^{-1})	12.170
Diffractometer Type	Bruker Kappa Axis Apex2
Scan Type(s)	φ and ω scans
Max 2θ for data collection, °	133.59
Measured fraction of data	0.994
Number of reflections measured	70093
Unique reflections measured	12940
R_{merge}	0.0511
Number of reflections included in refinement	12940
Cut off Threshold Expression	I > 2σ(I)
Structure refined using	full matrix least-squares using F^2
Number of parameters in least-squares	822
R_1	0.0540
wR_2	0.1546
R_1 (all data)	0.0553
wR_2 (all data)	0.1562
GOF	1.047
Maximum shift/error	0.348
Min & Max peak heights on final ΔF Map (e^-/Å)	-5.905, 2.385

Table D. 18 Summary of Crystal Data for **20**

Formula	$C_{20}H_{15}O_2P$
Formula Weight (*g/mol*)	318.29
Crystal Dimensions (*mm*)	0.719 × 0.263 × 0.114
Crystal Color and Habit	yellow needle
Crystal System	triclinic
Space Group	P -1
Temperature, K	296
a, Å	5.9715(6)
b, Å	8.3046(9)
c, Å	16.379(2)
α,°	79.725(5)
β,°	87.641(4)
γ,°	78.852(5)
V, $Å^3$	784.11(15)
Number of reflections to determine final unit cell	9986
Min and Max 2θ for cell determination, °	5.48, 133.88
Z	2
F(000)	332
ρ (g/cm^3)	1.348
λ, Å, (CuKα)	1.54178
μ (mm^{-1})	1.606
Diffractometer Type	Bruker Kappa Axis Apex2
Scan Type(s)	φ and ω scans
Max 2θ for data collection, °	134.824
Measured fraction of data	0.960
Number of reflections measured	4094
Unique reflections measured	2705
R_{merge}	0.0248
Number of reflections included in refinement	2705
Cut off Threshold Expression	$I > 2\sigma(I)$
Structure refined using	full matrix least-squares using F^2
Number of parameters in least-squares	208
R_1	0.0330
wR_2	0.0868
R_1 (all data)	0.0367
wR_2 (all data)	0.0895
GOF	1.072
Maximum shift/error	0.000
Min & Max peak heights on final ΔF Map (e^-/Å)	-0.223, 0.446

E. Curriculum Vitæ

Bahareh Khalili Najafabadi

Education:

Ph.D. in Chemistry, The University of Western Ontario, Canada 2011–2015

- Thesis: Coinage Metal Silylphosphido Complexes Stabilized by N-Heterocyclic Carbene Ligands
- Advisor: Professor John F. Corrigan

M.Sc. in Chemistry, The University of Western Ontario, Canada 2009–2011

- Thesis: New Ferrocene Based Dithiolate Ligands
- Advisor: Professor John F. Corrigan

B.Sc. in Chemistry, Sharif University of Technology, Tehran, Iran 2004–2008

- Thesis: New Macrocyclic Ligands and their Ligation to Fullerene
- Advisor: Professor Bahram Ghanbari

Honours and Awards:

- Robert and Ruth Lumsden Fellowship in Science, UWO, $1,000 — 2015
- Ontario Graduate Scholarship (OGS), Government of Ontario, $15,000 — 2014–2015
- Ludo Frevel Crystallography Scholarship Award, The international Centre for Diffraction Data (ICDD), $2,500 — 2014
- 1st place in Materials stream, Industry Problem Solving Week (IPSW), UWO — 2014
- CSC travel award, UWO, $520 — 2013
- A Special International Research Experience (ASPIRE) award, Worked under supervision of Prof. Stefanie Dehnen at the Philipps-Universität Marburg, Marburg, Germany, $670 — 2013
- Western Graduate Research Scholarship (WGRS), UWO — 2009–2013
- Bronze medal in National Chemistry Olympiad in Iran — 2003

Publications:

1. **B. Khalili Najafabadi**, J. F. Corrigan, "Enhanced Thermal Stability of Cu-Silylphosphido Complexes via NHC Ligation", *Dalton Trans*., **2015**, 44, 14235.

2. M. Madadi, **B. Khalili Najafabadi**, M. Azizpoor Fard, J. F. Corrigan, ". NHC Stabilized Bis(trimethylsilyl)phosphido Complexes of Ni(II) and Pd(II)", *Eur. J. Inorg. Chem*. **2015**, 3094.

3. **B. Khalili Najafabadi**, J. F. Corrigan, "NHC Stabilized Ag-P Nanoclusters", *Chem. Commun*. **2015**, 665.

4. T. I. Levchenko, C. Kübel, D. Wang, **B. Khalili Najafabadi**, Y. Huang, J. F. Corrigan, "Controlled Solvothermal Routes to Hierarchical 3D Superparticles of Nanoscopic CdS", *Chem. Mater*. **2015**, *27*, 3666.

5. M. Azizpoor. Fard, M. Willans, **B. Khalili Najafabadi**, T. I. Levchenko, J. F. Corrigan, "Bidentate Silylchalcogen Reagents for the Generation of Novel Pd_2- and Pd_4-Chalcogenolate Complexes", *Dalton Trans*. **2015**, *44*, 8267.

6. Y. Liu, **B. Khalili Najafabadi**, M. Azizpoor Fard, J. F. Corrigan, "A Functionalized Ag_2S Molecular Architecture: Facile Assembly of the Atomically Precise Ferrocene Decorated Nanocluster $[Ag_{74}S_{19}(dppp)_6(fc(C\{O\}OCH_2CH_2S)_2)_{18}]$", *Angew. Chem*. **2015**, *54*, 4832.

7. M. Azizpoor Fard, **B. Khalili Najafabadi**, M. Hesari, M. S. Workentin, J. F. Corrigan, "New Polydentate Trimethylsilyl Chalcogenide Reagents for the Assembly of Polyferrocenyl Architectures", *Chem. Eur. J*. **2014**, *20*, 7037.

8. **B. Khalili Najafabadi**, J. F. Corrigan, "N-Heterocyclic Carbenes as Effective Ligands for the Preparation of Stabilized Copper- and Silver-*t*-Butylthiolate Clusters", *Dalton Trans*. **2014**, *43*, 2104.

9. C. B. Khadka, **B. Khalili Najafabadi**, M. Hesari, M. S. Workentin, J. F. Corrigan, "Copper Chalcogenide Clusters Stabilized with Ferrocene Based Diphosphine Ligands", *Inorg. Chem*. **2013**, *52*, 6798.

10. **B. Khalili Najafabadi**, M. Hesari, M. S. Workentin, J. F. Corrigan, "New Ferrocene Based Dithiolate Ligands", *J. Organomet. Chem*. **2012**, *703*, 16.

11. W. J. Humenny, S. Mitzinger, C. B. Khadka, **B. Khalili Najafabadi**, I. Vieira, J. F. Corrigan, "N-Heterocyclic Carbene Stabilized Copper- and Silver-Phenylchalcogenolate Ring Complexes", *Dalton Trans*. **2012**, *41*, 4413.

Oral Presentations:

1. **B. Khalili Najafabadi**, J. F. Corrigan, "New Metal-Phosphido Precursors for Metal-Phosphide Nanocluster Assembly", *96th Canadian Society for Chemistry Conference*, Quebec, QC, Canada, **2013**.
2. **B. Khalili Najafabadi**, J. F. Corrigan, "Ferrocene Based Dithiolate Ligands for Nanocluster Assembly", *94th Canadian Society for Chemistry Conference*, Montreal, QC, Canada, **2011**.
3. **B. Khalili Najafabadi**, J. F. Corrigan, "Ferrocene Based Dithiolate Ligands for Nanocluster Assembly", *43rd Annual Inorganic Discussion Weekend*, Windsor, ON, Canada, **2010**.
4. **B. Khalili Najafabadi**, B. Ghanbari, "Designing new Ligands", *Sharif University of Technology,* Tehran, Iran, **2008**.
5. **B. Khalili Najafabadi**, "A Chemistry Software", *First Chemistry Festival of Students of Iran*, Abadan, Iran, **2003**.

Poster Presentations:

1. **B. Khalili Najafabadi**, J. F. Corrigan, "New Metal-Phosphido Precursors for Metal-Phosphide Nanocluster Assembly", *45th Annual Inorganic Discussion Weekend*, Ottawa, ON, Canada, **2012**.
2. **B. Khalili Najafabadi**, J. F. Corrigan, "New Metal-Phosphido Precursors for Metal-Phosphide Nanocluster Assembly", *2nd CAMBR Distinguished Lecturer and Research Day*, London, ON, Canada, **2012**.
3. **B. Khalili Najafabadi**, J. F. Corrigan, "Ferrocene Based Dithiolate Ligands for Nanocluster Assembly", *93rd Canadian Society for Chemistry Conference*, Toronto, ON, Canada, **2009**.

Teaching Experience:

The University of Western Ontario		London, ON
Inorganic Chemistry	Chem 3371	2009, 2010, 2011
Inorganic Chemistry	Chem 2271	2011, 2014
Inorganic Chemistry	Chem 2281	2012, 2014
General Chemistry	Chem 1301, 1302	2010, 2011, 2012
Organic Chemistry	Chem 2223	2015
X-ray Crystallography Assistant		2010
NMR Assistant		2013

Workshops and Certificates:

- The American Crystallographic Association (ACA) Summer Course in Chemical Crystallography (2014)
- Mitacs' Workshop on "Skills of Communication", The University of Western Ontario (2014)
- Mitacs' Workshop on "Foundations of Project Management I & II", The University of Western Ontario (2014)
- Western University certificate in Academic Engagement (2013)
- The Language of Conference Presentations certificate, University of Western Ontario (2013)
- Teaching Master Class Program: Lecture in Chemistry (2013)
- Future Professor Workshop Series (2013)
- Western University certificate in Teaching Assistant Training Program (2009)
- Graduate Student Conference on Teaching (2009)
- Iran Mountaineering Federation & Sport Climbing certificate in Mountain Climbing (2006)

Community Involvement:

1. A steward for chemistry department in the GTA union, the University of Western Ontario (2010−2014)
2. Graduate representative on the Social Committee of the Department of Chemistry, University of Western Ontario (2013−present)
3. Volunteer student for administrative work in 1st and 2nd CAMBR Distinguished Lecturer and Research Day, University of Western Ontario (2011−2012)
4. Volunteer student host in "porch light" program in international center of the University of Western Ontario (2010)
5. Volunteer host and program producer in Radio Andisheh, a weekly radio, founded in London, ON as of January 2010, by a group of interested Iranian individuals.
6. Organizing annual bake sales to help Children's Aid Society of London, Department of Chemistry, The University of Western Ontario (2012−2014)

7. Volunteer with Friends of Gardens at the University of Western Ontario (FOGS) for planting seeds and organizing a plant sale (2014)
8. Active member (2005−2008) and chief director (2007) of the Sharif University Mountain Club.

Coursework:

Chem 9541	Crystallography I	82
Chem 9651	Organometallic chemistry I	81
Chem 9658	Seminar	87
Chem 9754A	Structural chemistry of solid materials	93
Chem 9503S	Advanced NMR spectroscopy	81
Chem 9555R	Organic photochemistry	99
Chem 9631Q	Bioinorganic chemistry	88
Chem 9551R	Clusters and colloids	94

Computer Skills:

- **Operating Systems:** Windows, Mac OS X
- **Software Programs:** Pascal, Delphi, Visual Basic, Microsoft Office
- **Visualization Tools:** Mercury, SCHAKAL, Adobe Photoshop, ChemDraw
- **Chemistry Packages:** SHELX, APEX II, ACD/Labs, VnmrJ, Gaussian, Olex2, Sir2014